268
3/6/68
Pea

SNAP-21 PROGRAM, PHASE II

DEEP SEA RADIOISOTOPE-FUELED THERMOELECTRIC GENERATOR POWER SUPPLY SYSTEM

QUARTERLY REPORT NO. 6

Space and Defense Products
ELECTRICAL PRODUCTS GROUP
3-M CENTER, ST. PAUL, MINN. 55101, PH 633-9400
3M COMPANY

DISCLAIMER

Report No. MMM 3691-26

AEC RESEARCH AND DEVELOPMENT REPORT

This report has been prepared under Contract AT(30-1)3691
with the U.S. Atomic Energy Commission

SNAP-21 PROGRAM, PHASE II

DEEP SEA RADIOISOTOPE-FUELED THERMOELECTRIC GENERATOR POWER SUPPLY SYSTEM

QUARTERLY REPORT NO. 6

FEBRUARY 1968

Period Covered
October 1, 1967 to December 31, 1967

Prepared by:
F. Fox

Approved by:
J. Brandt
Program Manager
SNAP-21 Program

Issued by

Space and Defense Products

MINNESOTA MINING AND MANUFACTURING COMPANY

ST. PAUL, MINNESOTA 55101

BLANK

LEGAL NOTICE

~~THIS DOCUMENT FOR OFFICIAL USE ONLY PENDING PATENT CLEARANCE~~

DISTRIBUTION

Distribution of this document is in accordance with TID-4500 (50th Edition) category UC33.

BLANK

TABLE OF CONTENTS

TABLE OF CONTENTS (Continued)

TABLE OF CONTENTS (Continued)

BLANK

LIST OF FIGURES

LIST OF FIGURES (Continued)

LIST OF TABLES

BLANK

1.0 SUMMARY

Significant highlights which occurred during this report period are summarized below.

- Completed computer program for analyzing the thermal characteristics of the SNAP-21 system.
- Shields 3 and 4 were received and examined.
- Selected compatibility barrier material for use between the biological shield, spider and inner liner. The material selected was plasma sprayed aluminum oxide (Al_2O_3).
- The shield plug design was completed and the drawings released.
- Insulation system shipping containers were completed.
- Insulation system 10D1 was instrumented, its thermal performance was evaluated, and dynamically tested to specification levels.
- Insulation system 10D2 was assembled, instrumented, thermal performance testing was completed.
- The redesigned segmented retaining ring was dynamically tested to specification levels.
- The pressure vessel design was completed.
- In-line generator design was completed.
- Generator A10D5 was assembled, processed, and tested.

- Generator A10D6 was assembled.
- Power conditioner design was completed and component vendors were selected.
- Four prototype fuel capsules were assembled, welded and hydrotested.
- Short term isothermal testing of compatibility barrier materials was completed.
- The getter evaluation test data was analyzed and the static proof test evaluation was performed.
- Ball and socket generators A10D1, A10D2 and A10D4 have completed short term and dynamic testing.
- Phase II System S10D1 was assembled and testing was started.
- Fabricated parts for ten electrically heated fuel capsules.

2.0 TASK I

2.1 INTEGRATED SYSTEM DESIGN AND ANALYSIS

2.1.1 SYSTEM HEAT TRANSFER ANALYSIS

The computer program for analyzing the thermal characteristics of the SNAP-21 system has been completed. The method of analysis used is that of a system of equations which describes the heat flow at various nodes within the system. Initially it was assumed that a three dimensional heat transfer analysis would be necessary; however, it was found that the symmetry of the system lent itself to two dimensional heat transfer analysis rather than three dimensional analysis. This has decreased the complexity of the program considerably.

The program has been optimized insofar as possible, and, to increase flexibility, has been written to permit varying inputs and parameters. Initial computer runs have been made and the program is now in the "debugging" state.

Preliminary results show that the temperature distribution and the heat balance throughout the system for a given fuel loading compares closely to the experimental values. Actual comparisons of experimental to computer data will be included in the next quarterly report.

The method used in this thermal analysis is the well known relaxation method. An analytical model of the system was established by dividing it axially into three equal segments and then assuming radial isotherms within these three segments. The system configuration lends itself well to this approach because it is symmetrical about its center line except for the three shield support tie rods in

the insulation system. Thus, by dividing the system into three equal segments with a tie rod in each segment, the temperature distribution in each segment should be equal.

The application of the relaxation method to heat transfer problems can be found in many standard heat transfer texts such as, Kreith, Principles of Heat Transfer, 2nd Edition, pages 96-115. However, the method consists basically of subdividing the system into a number of small but finite subvolumes. Each subvolume is then assumed to be at a temperature corresponding to its center, which is called a nodal point. The nodal point of each subvolume is then connected to adjacent nodal points by a network of fictitious heat conducting rods that have a thermal conductance corresponding to the conductance of the actual material between nodal points. In the absence of heat sources or sinks within the system, the rate of heat flow toward a nodal point must equal the rate of flow away from it.

A schematic of the SNAP-21 system showing the nodal point locations is shown in Figure 2-1.

A set of heat balances is then set up for all nodal points and the relaxation method is used to solve the resulting set of algebraic equations. To expedite the mechanical analysis involved in solving the equations with the relaxation method, a fortran computer program was written for use with the time share computer. This program solves all the nodal equations simultaneously. The number of iterations required for a solution of the heat flow to each nodal point depends upon the accuracy desired. By using the solved-for temperatures, the total heat flow throughout the system is obtained.

An obvious shortcoming of this analysis, and of any analysis, is that the solution will only be as accurate as the data input. Some of the inputs to the system that are difficult to estimate are: the thermal conductance across interfaces that are clamped or pressed together, the surface coefficients for water and air, the conductance across air gaps and, since thermal conductivity is a function of temperature and the temperature gradient is very steep in the legs, the conduction through the thermoelectric legs. For these reasons, the analytical solution must be compared with experimental results and appropriate adjustments made to the data input.

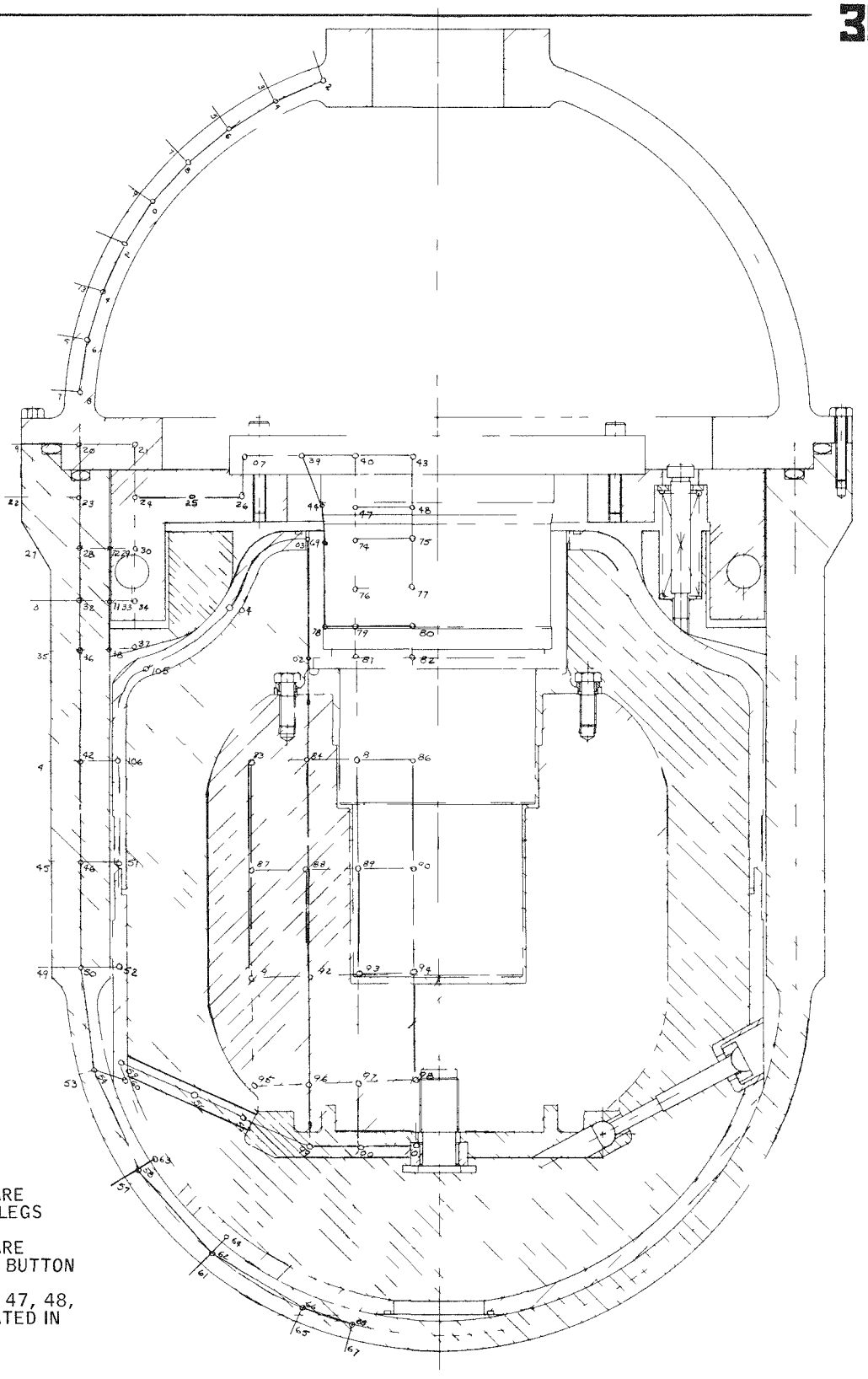

NOTES:

1. NODAL POINTS 76 AND 77 ARE LOCATED AT COLD CAP OF LEGS
2. NODAL POINTS 79 AND 80 ARE LOCATED AT HOT JUNCTION BUTTON
3. NODAL POINTS 39, 40, 43, 47, 48, 74, 75, AND 107 ARE LOCATED IN GENERATOR COLD FRAME

Figure 2-1. Nodal Point Locations - System Heat Transfer Analysis

2.1.2 SYSTEM ASSEMBLY ANALYSIS

During this report period, the problems involved in system wiring during assembly were reviewed. This review was made to determine what method of internal wiring would be best from overall system considerations.

Based on the findings of this review it was decided that the best wiring method would be to terminate all instrumentation and power leads from the lower half of the system (insulation system, pressure vessel body, thermoelectric generator and segmented retaining ring) in panel connectors mounted on the segmented retaining ring. The continuation of these leads to the upper half of the system (power conditioner, pressure vessel cover and electrical receptacle) would be from connectors mounted on the pressure vessel cover that mate with the connectors on the segmented retaining ring. These mating connectors would engage when mating the cover assembly to the lower assembly. This wiring arrangement permits "hard wiring" the lower and upper halves of the system independently prior to final assembly, and simplifies the assembly process and electrical checkout of both halves.

The final electrical connection is to be made when the upper portions of the panel connectors mounted on the pressure vessel cover are mated to the lower halves mounted on the segmented retaining ring. Because of the configuration of the system components the mating process is not visible. Consequently the upper and lower halves of the system must be accurately indexed and aligned. The indexing will be provided by dowel pin holes in the pressure vessel cover and body bolt circles. Alignment will be achieved by assembly jigs located by the dowel pin holes. A small amount of misalignment is acceptable since the panel connectors are mounted on a "floating" base and have guide pins of their own.

The panel connector selected for this application is an Amphenol Series 26 with guide pins. This connector has gold-plated contacts and provide the lowest contact resistance of commercially available units. In the electrically heated systems, several of these contacts can be wired in parallel to reduce the power losses in circuits with large current loads.

An added advantage of this method of wiring is that electronic gear placed in the pressure vessel cover by a customer can be assembled and checked out in the cover by the customer, at his facility, without affecting the assembly of the lower portion of the system.

2.2 COMPONENT DESIGN AND DEVELOPMENT

2.2.1 FUEL CAPSULE DESIGN

Two minor changes were incorporated in the SNAP-21 fuel capsule design. It was found that the diametrical clearance between the inner liner and primary capsule should be increased by approximately 0.010 inch to make assembly easier. The clearance was obtained by reducing the liner wall thickness from 0.030 inch to 0.025 inch.

The second change consisted of specifying an increase in the electron beam weld penetration from 0.170 inch to 0.205 inch. This was done to insure that the slight weld root porosity which occurred during weld development tests will not occur in a critical portion of the weld. Figure 2-2 shows a comparison of a 0.170 inch deep and a 0.205 inch deep weld.

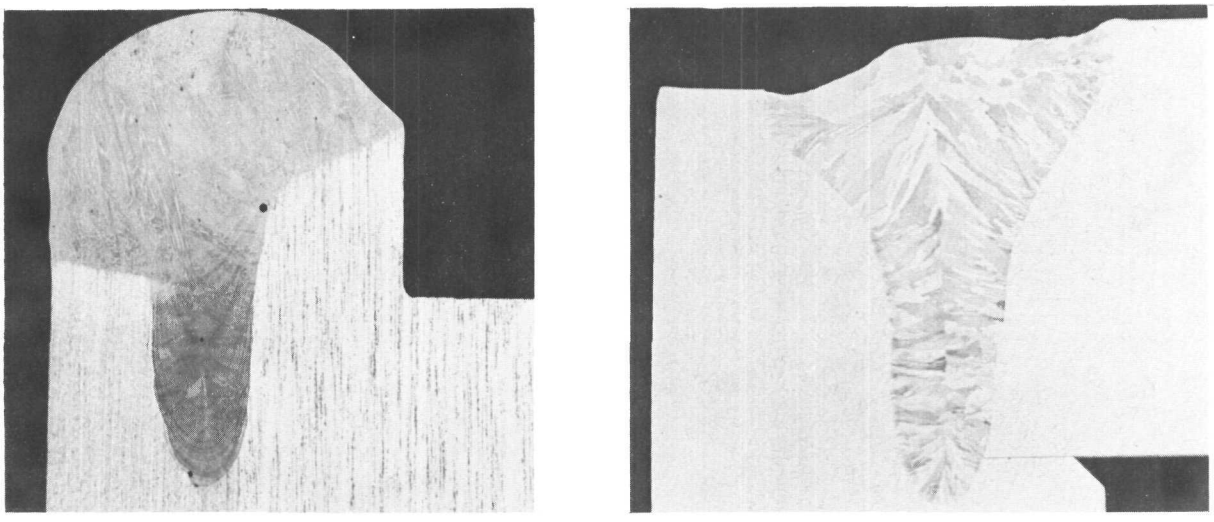

a) Root Porosity in 0.170 in. deep Weld

b) Root Porosity in 0.205 in. deep Weld

Figure 2-2. Comparison of Electron Beam Welds 0.170 and 0.205 inch Deep.

2.2.2 BIOLOGICAL SHIELD, SPIDER AND PLUG

2.2.2.1 Biological Shield

Shield Nos. 3 and 4 were received and the dimensions of the interface mating with the inner liner and the spider shield support were examined for adherence to specification tolerances. No discrepancies were noted.

2.2.2.2 Spider

During this report period, the compatibility barrier material between the biological shield, spider, and inner liner was selected. The selected material is plasma-sprayed aluminum oxide (Al_2O_3). This selection was based on the results of the isothermal compatibility tests, the ease of application, and the widespread use of this material. (The isothermal compatibility test results are given in SNAP-21 Quarterly Report No. 5, MMM 3691-23.)

On the first spider to be sprayed with aluminum oxide, some chipping occurred on the corner of the 4.50 inch diameter ring. This problem was solved by putting a 0.10 radius on the corner as shown in Figure 2-3.

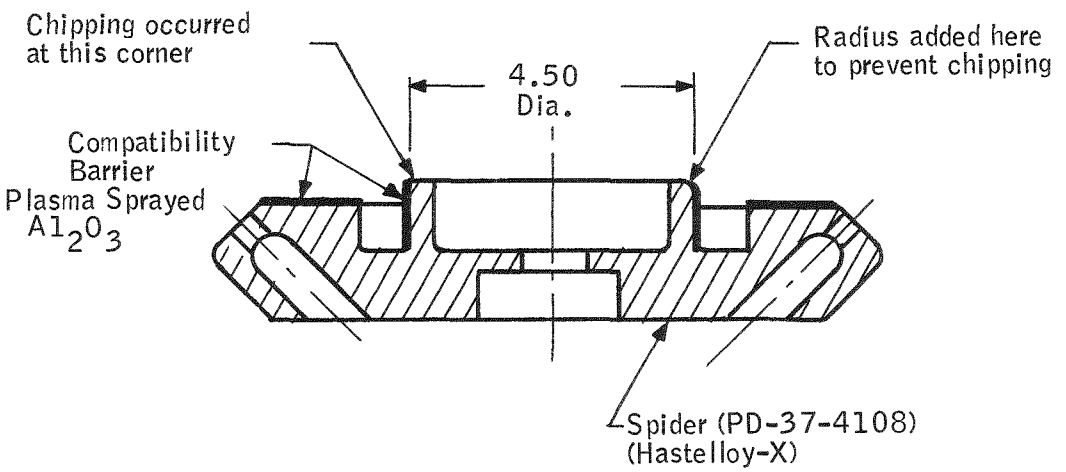

Figure 2-3. Shield Support Spider

2.2.2.3 Shield Plug

The shield plug design was completed and the drawings released. The U-8Mo plug is encapsulated in a stainless steel container with an integral radiation disk (see Figure 2-4). The encapsulation is required to prevent oxidation of the radiation plug. To prevent eutectic formation between the plug and the encapsulating body, an alumina (Al_2O_3) compatibility barrier is plasma sprayed on the body of the shield plug. This is the same compatibility barrier material as used on the neck tube and the spider.

2.2.3 INSULATION SYSTEM

Linde has continued work under subcontract AT(30-1)3691-5511. Work has progressed on fabrication of development insulation systems 10D1, 10D2, 10D3, and 10D4. The unit shipping containers were completed and additional tooling and fixtures were fabricated.

2.2.3.1 Development Insulation System 10D1

a) Unit Insulation

A total of 165 insulation layers were applied to the unit during this report period. The composition, thickness and layer density is presented in Table 1.

Table 1. Insulation Composition Unit 10D1

Number of Layers	Layer Composition	Total Thickness (Inch)	Layers per Inch
2	Quartz Cloth		
45	Nickel Foil Quartz Paper	0.422	106
60	Copper Foil Quartz Paper	0.625	96
60	Aluminum Foil 106 Paper	0.406	148

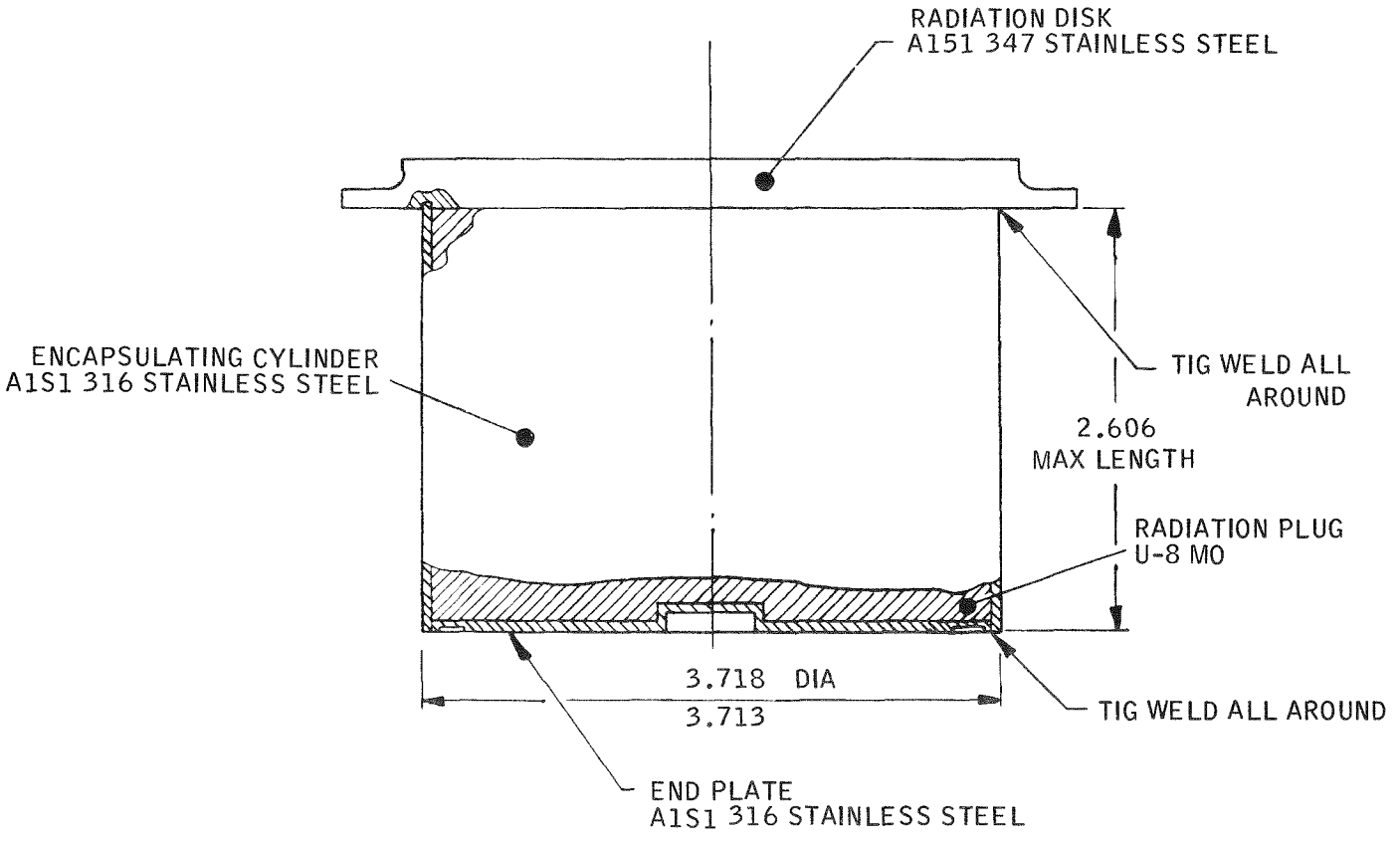

Figure 2-4. Shield Plug Assembly

Upon completion of the insulation application, two layers of nickel foil were applied over the insulation to provide protection during the unit closure. Figure 2-5 shows the completely insulated unit looking at the inner liner end of the unit; Figure 2-6 shows the insulated unit looking at the spider end.

b) Unit Closure

After applying the nickel foil, the enclosure support rod receptacles were aligned and, using the receptacle welding fixture, tack welded to the bottom outer enclosure shell. After tack welding, the receptacles were manually welded to the head using the weld parameters developed in the weld development program. For this unit, which does not use a getter, a circular stainless steel disk was edge welded to the bottom outer enclosure shell to seal the hole provided for the seal-off device to be used on subsequent units. After welding the bottom was again leak checked. The leak rate of the receptacle welds was acceptable.

One strain gauge (type SR-4) was attached to the long side of each receptacle to measure the axial strain in the receptacle. These strain gauges were used to determine the pretension to be applied to the tension rods during the final assembly.

The upper outer enclosure shell was installed over the assembly fixture shaft to mate with the top edge of the inner liner. The head was aligned on, and tack welded to, the inner liner using the tension rod alignment fixture. The alignment fixture was then partially disassembled to provide the clearance required to make the semi-automatic neck tube edge weld. This weld was made by rotating the unit in the assembly fixture while welding with a hand-held heliarc torch. The weld parameters recorded for this neck tube edge weld were: 68-70 amps, 9-11 volts, 10 IPM speed, 25 cfh argon shield gas.

Following the inner liner edge weld, the assembly fixture was reassembled for installation of the bottom head on the unit. The bottom head was aligned as shown in Figure 2-7. Pins inserted through the alignment fixture bars into the receptacles provided the angular line-up of the receptacle to the spherical tension rod seat of the spider so that the tension rod was located in the plane of the unit

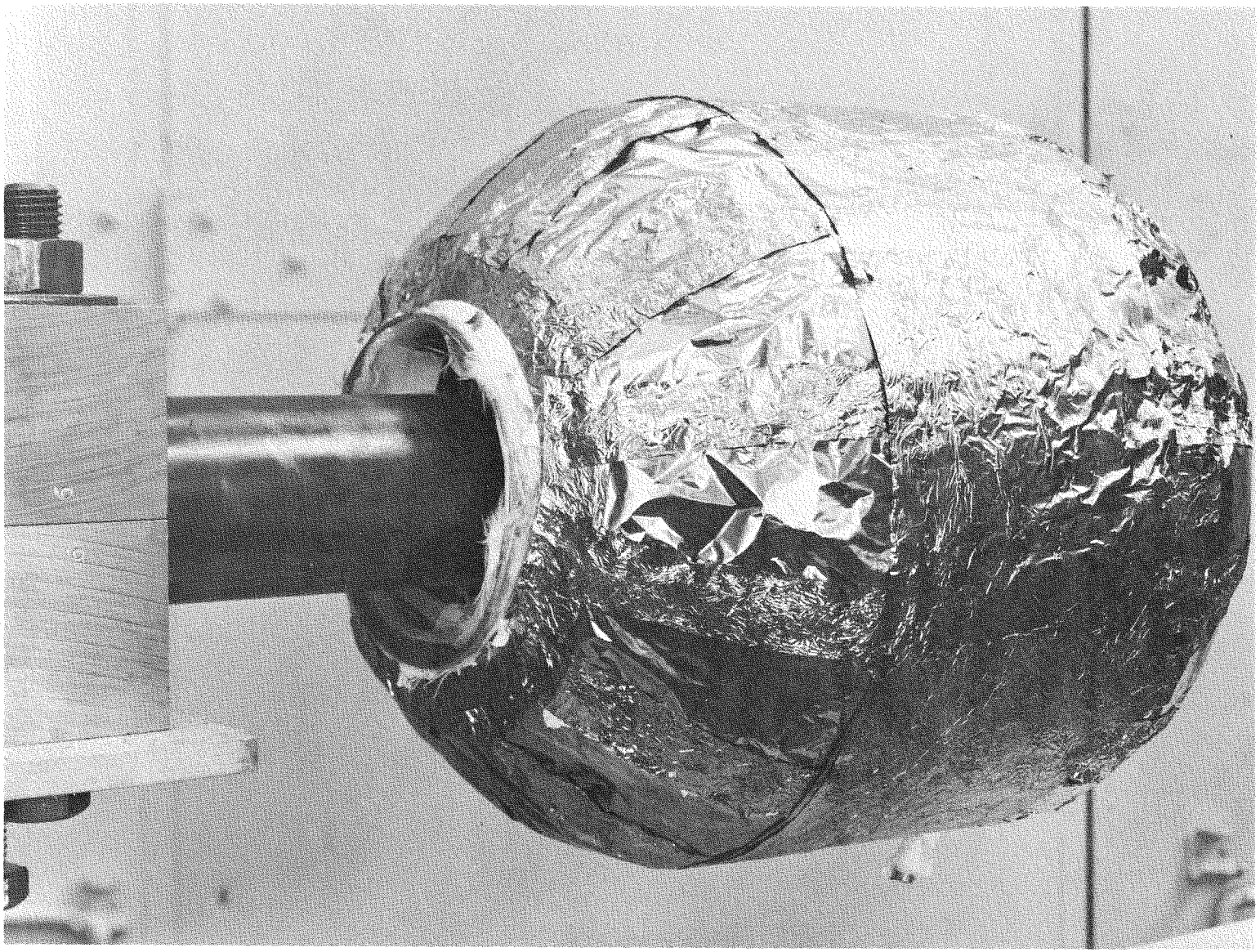

Figure 2-5. Insulated Unit 10D1 — Top View

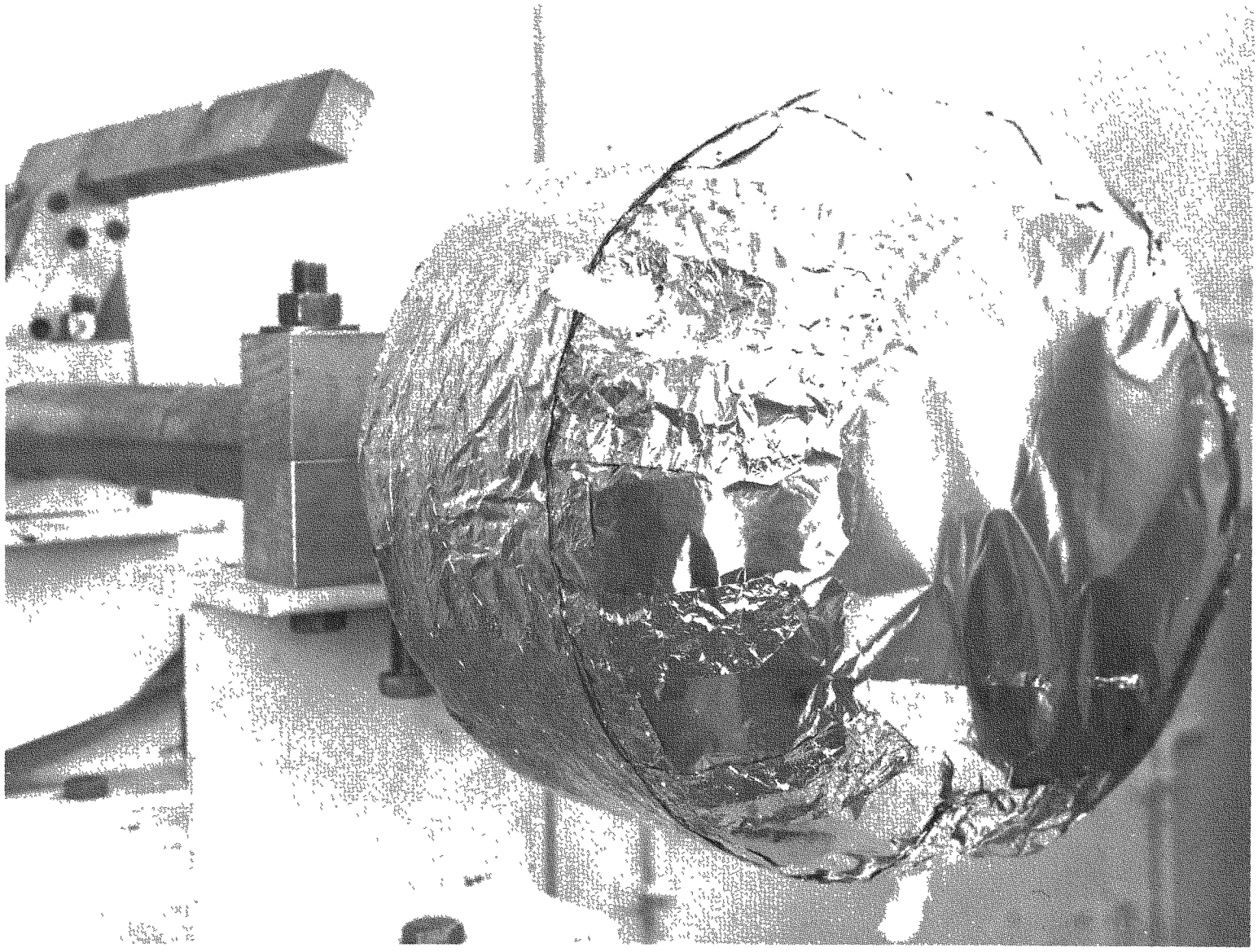

Figure 2-6. Insulated Unit 10D1 – Bottom View

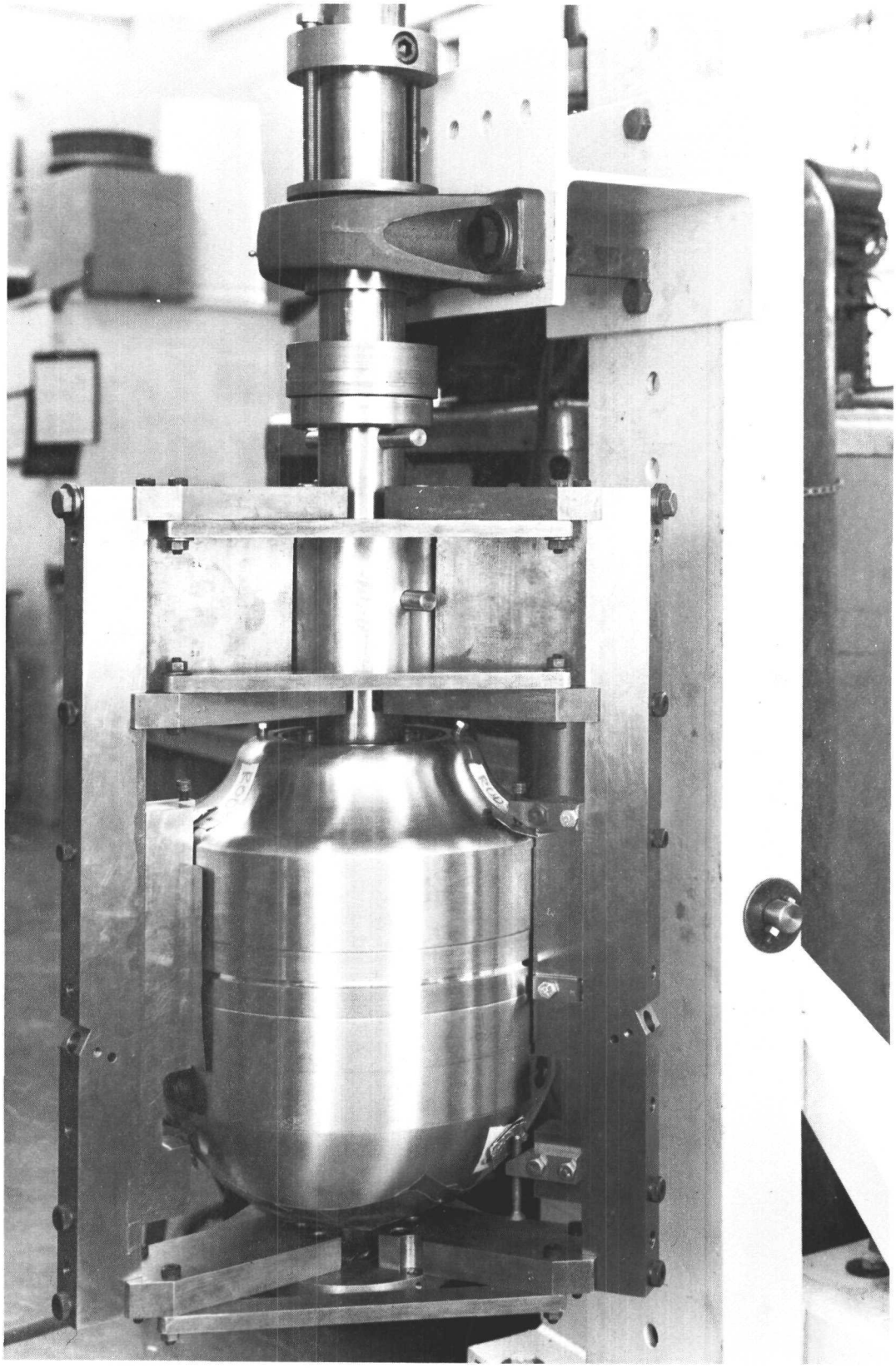

Figure 2-7. Alginment of Bottom Head, Unit 10D1

axis. The bottom outer enclosure shell was tack welded to the upper outer enclosure shell. The unit was oriented to the horizontal position in the assembly fixture and moved to the welding area to perform the automatic girth weld. Prior to welding the unit, several automatic welds were made on 6 inch O. D. stainless steel pipe to check out the automatic welding machine and set the desired weld parameters. The girth weld was made in two passes with the following parameters recorded:

Pass	Amps	Volts	Wire Feed IPM	Travel IPM	Shield Gas CFH
1	288 – 290	11.5 – 13.5	80	15	25 argon 75 helium
2	292 – 296	15.0 – 15.5	100	15	25 argon 75 helium

The filler wire was 0.045 inch diameter, 308 ELC. The first pass filled the weld joint to approximately 0.020 under flush. The second pass provided a slight crown on the weld joint which was smaller than the outside diameter of the unit.

Using the assembly fixture, the tension rods were located and torqued to 40 in lb. to temporarily secure the spherical washer to the receptacle. The adjusting pins were then installed between the spherical washer and the receptacle and tack welded as shown in Figure 2-8 for rod No. 1.

Following the tack welding of the spherical washers, the tension rods were loosened and then sequentially torqued in 5 in lb. increments to 22.5 in lb. The rod anti-rotation devices were then installed and tack welded to the spherical washers as shown in Figure 2-9 for rod No. 1 to prevent loosening of the tension rods. The receptacle seal-off plugs were tack welded to the receptacles and the vacuum seal for this unit was made with an epoxy. Epoxy was used so the plugs could be removed after the unit failure dynamic test to examine the tension rods for damage.

After closure, the unit was evacuated through the Hooke vacuum valve with a Veeco MS-9 helium leak detector. When the unit pressure was slightly greater than 100 microns, the unit was enclosed in a plastic bag and the bag was filled

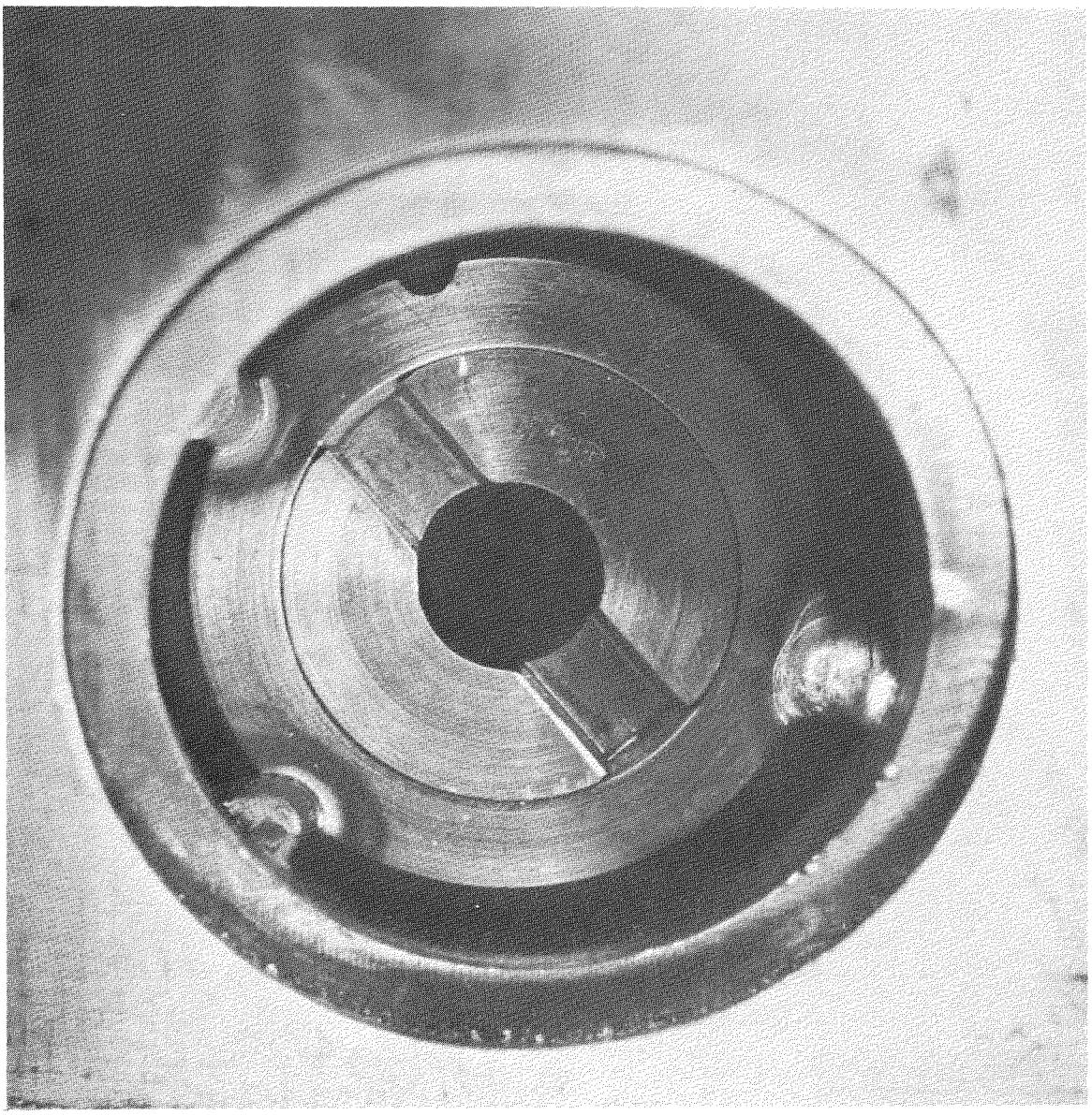

Figure 2-8. Spherical Washer Tacked to Receptacle, Unit 10D1, Rod No. 1

Figure 2-9. Rod Anti-Rotation Device Tacked to Spherical Washer, Unit 10D1, Rod No. 1

with helium gas to conduct a unit leak check as per the standard leak detection procedure. The unit leak rate was determined to be 9.9×10^{-11} std-cc/sec-air.

c) Unit Thermal Performance

Following the leak check, the unit was instrumented for conditioning and thermal performance evaluation. Four heaters were installed in the heater block and two chromel-alumel thermocouples were welded to the top of the heater block near the edge and 180° apart. The heater block was then installed in the inner liner.

The neck tube volume above the heater block was filled with inch-thick disks of Min-K 2000 insulation with the ceramic beaded heater wires and ceramic beaded thermocouple wires passing through the insulation. Voids around the wires and the edge of the insulation disks were filled with powdered Min-K 2000 tightly packed in place. A stainless steel cover plate was installed over the Min-K insulation to reduce convection. This plate was sealed to the upper head with silicone rubber. Figure 2-10 shows the unit instrumented for the thermal test.

All four heaters were connected in parallel and wired through a watt-meter, recording ammeter, variac, constant voltage power supply, and isolation transformer to the line power. Chromel-alumel thermocouples were installed in the following locations on the unit: cover plate (1), upper unit head (1), cylindrical portion of the unit near girth weld (2), near flat on bottom head (1). All thermocouples were connected to a temperature recorder. The unit was continuously evacuated throughout the unit heat-up, conditioning and thermal test period.

Power was supplied to the heaters initially at 50 watts for 24 hours (365° F), then increased to 70 watts. The 70-watt power input was continued until the total accumulated time was 95 hours (1060°F) when the power was increased to 90 watts. Ninety watts power input was continued until 222 hours was reached and the unit temperature was 1470° F. The power was then turned off. Because this unit is not permanently sealed, it was not fully conditioned at 1550°F, but conditioned only enough to achieve acceptable pressures at operating temperature.

When the unit had cooled to 1300°F, the power was switched on at 20 watts to get the heaters operating. As the unit cooled, the power was increased to achieve a steady 1285°F temperature. Maintaining this temperature required

Figure 2-10. Unit 10D1 Instrumented for Thermal Test

65 watts, as read on the wattmeter. The insulation pressure was at 3 microns during the determination of the thermal performance.

Thermal Performance Evaluation

To determine the actual thermal performance of the unit, the input power must be corrected as follows:

Measured power on wattmeter	65.0 watts
Power wire I^2R loss	0.9 watt
Wattmeter calibration correction	3.0 watts
Corrected power to unit	61.1 watts
Min-K neck tube insulation loss	4.7 watts
Thermocouple wires loss	0.8 watt
Heater lead wire loss	9.3 watts
Total chargeable unit heat loss	46.3 watts

For the operating conditions of the thermal test, the calculated heat loss to obtain a 45-watt unit at operating conditions is as follows:

Neck tube heat loss	20.8 watts
Tension rod heat loss	10.5 watts
Insulation heat loss	11.1 watts
Calculated unit heat loss for test condition	42.4 watts

A comparison of the measured heat loss (46.3 watts) and the calculated heat loss (42.4 watts) shows that this unit is over specified heat loss by 3.9 watts.

Following the thermal performance test, the power was turned off and the unit allowed to cool.

The following steps will be taken on Unit 10D3 to increase the unit efficiency:

- Eliminate the pilot rod between the male and female portions of the tension tie rods.
- Install insulation in the hole in the female portion of the tension tie rod.
- Quartz cloth on the neck tube will be replaced by quartz paper.
- The method of wrapping insulation materials on the unit will be altered.
- The density of the aluminum foils will be changed from 146 layers per inch to 100 layers per inch.

2.2.3.2 Development Insulation System 10D2

a) Unit Assembly

Upon inspection of the inner liner, spider and biological shield, it was found that the diametral fit between the inner liner and the biological shield ranged from 0.0002 inch clearance to 0.0002 inch interference while the diametrical fit between the spider and the biological shield ranged from 0.0003 inch to 0.0014 inch clearance. The inner liner was chilled with liquid nitrogen and assembled onto the shield the same as was done with Unit 10D1. The eight molybdenum washers were located in the inner liner flange and the U8-Mo bolts were installed. The bolts were torqued to the specified 38 in lb. and a molybdenum safety wire was installed.

The male support rods were lapped into the spherical seats in the spider. The spider was then cooled in liquid nitrogen and assembled to the biological shield. The molybdenum spider washer was put on the spider and the U8-Mo spider bolt was threaded into the shield. The spider bolt was torqued to the specified 60 ft lb. torque and a double molybdenum safety wire anchored the bolt to the spider. The male support rod was installed in the spider after coating the ball with Molykote Type Z dry powder lubricant and the rod antirotation device was installed in the spider through a hole in the rod ball.

b) Unit Insulation

During this reporting period, the insulation of Unit 10D2 was completed. A total of 165 insulation layers were applied to the unit. The layer composition, thickness, and layer density is shown in Table 2.

Table 2. Insulation Composition, Unit 10D2

Number of Layers	Layer Composition	Total Thickness (Inch)	Layers per Inch
2	Quartz Cloth	--	--
45	Nickel Foil Quartz Paper	0.493	91
60	Copper Foil Quartz Paper	0.641	94
60	Aluminum Foil 106 Paper	0.359	167

c) Unit Closure

The attachment of the outer shell sections on this unit was essentially the same as on Unit 10D1, except that strain gauges were not used on the tension rod receptacles. A getter enclosure and a seal-off device were used on this unit.

The weld parameters recorded for the neck tube weld were as follows: 71-73 amps, 10.5-11.0 volts, 10 IPM, and 25 cfh argon.

The bottom enclosure shell was prepared for assembly on the top shell by welding on the following components: enclosure support rod receptacle (3), getter seal-off device female end (1), hydrocarbon getter enclosure assembly (1), and getter retainer assembly (1).

The receptacles were aligned in the bottom enclosure shell. Each receptacle was tack welded in three places and manually welded with 0.045 inch 308L filler wire and 25 cfh argon. Weld parameters were: No. 1 – 78-82 amps, 9.5-11.0 volts; No. 2 – 72-84 amps, 9.0-11.5 volts; and No. 3 – 72-88 amps, 9.0-11.0 volts.

The female end of the getter seal-off device was aligned in the bottom head to be flush with the flat on the head. Four tack welds were made 90° apart. The edge weld was done manually with the following parameters recorded: 48-50 amps, 8.5-10.0 volts, 25 cfh argon, 6 IPM torch travel, no filler wire added.

The hydrocarbon getter enclosure, which contained 1.068 grams of getter, was centered on the female end of the seal-off device, and the attachment lugs were welded to the head using 60-64 amps, 9-10 volts, 25 cfh argon, 0.045 inch 308L filler wire.

The getter retainer assembly was aligned in the bottom head and tack welded in eight places around the circumference. The seal weld was manually performed using 72-84 amps, 8.5-10.5 volts, 2-3 IPM, 0.045 inch 308L filler wire, 25 cfh argon. This weld was not continuous. Approximately two inches were welded before skipping across the diameter to weld the next two inches. This procedure was employed to keep the shrinkage to a minimum.

The bottom head, with all components installed, was cleaned and leak checked again. The leak rate was acceptable. The bottom shell was then mated with the top enclosure shell and the weld joint closed until there was no gap. The top shell was then tack welded to the bottom shell with 9 tacks equally spaced on the circumference. The girth weld was done in two passes. The following parameters were recorded:

Pass	Amps	Volts	Wire Feed IPM	Travel IPM	Shield Gas cfh
1	292 – 295	12.0 – 12.5	80	15	25 argon
2	290 – 292	15.0 – 15.5	100	15	75 helium

The filler wire was 0.045 inch diameter 308L.

d) Unit Thermal Performance

The unit was instrumented for the thermal performance test much the same as Unit 10D1. Unit 10D2, which includes a getter, was evacuated from the bottom,

while Unit 10D1 was evacuated from the top through a small tube. To decrease the time required for conditioning, more power was supplied to the heaters of this unit than to those of Unit 10D1. The unit was conditioned and the thermal performance test completed. The results of the thermal performance test have not yet been evaluated; the report for the next period will include the evaluation. After cooling, the getter was installed and the seal-off was effected. The unit was placed in its shipping container and is awaiting shipment.

2.2.3.3 Development Insulation System 10D3

a) Unit Assembly

Linde received the inner liner, spider and biological shield and after inspection, assembled the inner liner to the biological shield as described in paragraph 2.2.3.2.

Upon receipt of the spider it was noted that some of the aluminum oxide compatibility barrier had chipped off the interference fit diameter. This spider was resprayed and reground, found to be satisfactory and assembled to the biological shield as described in paragraph 2.2.3.2.

b) Unit Insulation

Wrapping of insulation material on Unit 10D3 was started and, at the end of this report period, wrapping was 40 percent complete.

2.2.3.4 Development Insulation System 10D4

a) Unit Assembly

The inner liner spider and biological shield were received by Linde and inspected. The parts were then assembled as described in paragraph 2.2.3.3.

2.2.3.5 Tooling and Fixtures

The following fixtures were fabricated during this period: unit handling fixture, receptacle welding fixture and bottom enclosure head inspection fixture.

The unit handling fixture shown in Figure 2-11 allows rapid manipulation of the unit from the vertical to the horizontal position. The fixture has provision for three sets of shaft supporting bearings which allows removal of the assembly fixture from the shaft and installing the top head without removing the unit from the handling fixture. This fixture is also used to rotate the unit while making the inner liner and girth welds.

The receptacle welding fixture provides the correct angular alignment and depth while welding the receptacles to the bottom outer enclosure shell.

The bottom outer enclosure shell inspection fixture permits accurate inspection of the location and angle of the tension rod receptacle holes.

2.2.4 SEGMENTED RETAINING RING

The redesigned segmented retaining ring was dynamically tested to the increased dynamic criteria of 6 g shock and found satisfactory. Details of this test are discussed in Section 2.3.4 of this report.

2.2.5 PRESSURE VESSEL

Design of the pressure vessel was finalized during this report period. This final design is based on actual material tests conducted by the Beryllium Corporation of America and the 3M Company. A summary of the pertinent design information is presented below. Methods of analysis used in the design were related in considerable detail in Quarterly Report No. 5 (MMM 3691-23), and are not included here.

a) Material:

The pressure vessel will be fabricated from forged Berylco 165 annealed and heat-treated to produce tension yield strengths (at 0.20 percent offset) of 130,000 to 160,000 psi. Since compression data on Berylco 165 has been lacking in the past, additional tests were conducted to characterize the material.

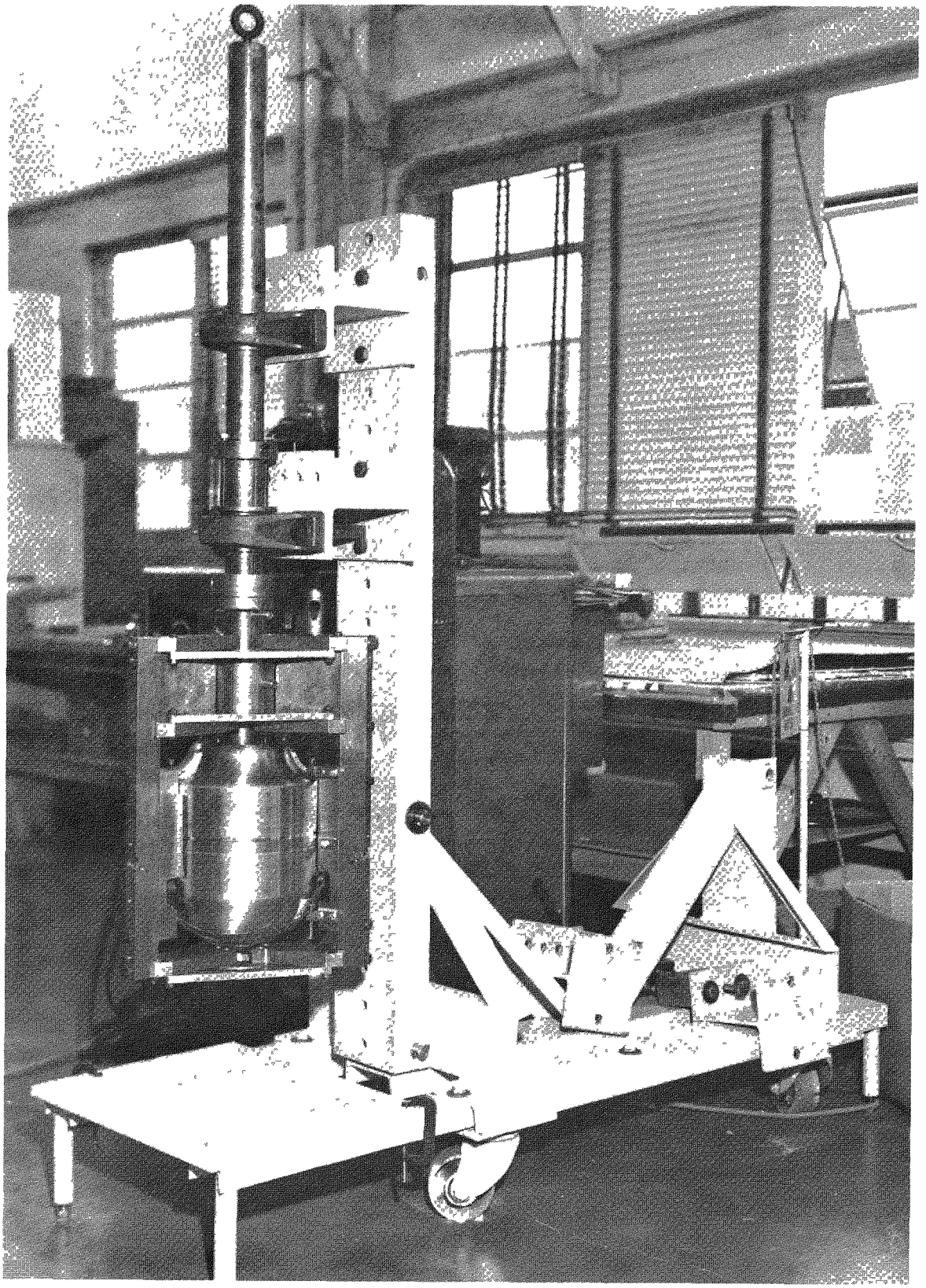

Figure 2-11. Unit Handling Fixture

Independent compression tests were conducted; two tests by the Beryllium Corporation of America and five by the 3M Company, so that a cross check of the data could be made. The data from these tests were combined and used to formulate design curves of compression stress versus strain and secant and tangent modulus. Since a limited number of tests were used to establish these design curves, the actual test data was appropriately reduced to allow for normal deviations in test data and heat-to-heat variations in the material.

Typical results from these tests showed a yield strength of 172,000 psi at 0.20 percent offset in tension and 190,000 psi in compression. The ratio of yield strength is thus:

$$\frac{190,000}{172,000} = 1.105$$

To specify the material requirements on the pressure vessel drawings, the requirements of AMS 4650E were used with several exceptions. One of these exceptions is a change in the 0.20 percent offset tension yield strength from a minimum of 145,000 psi to a range of 130,000 to 160,000 psi. The reasoning used as a basis for this change is that the minimum elongation of 3 percent called for by the specification will be somewhat greater at the lower yield strengths. Our design values must reflect this possibility of a minimum strength material. Using the factor obtained above, a new minimum compression yield strength at 0.20 percent offset is obtained as 1.105 x 130,000 = 143,650. This number was further rounded off to 140,000 psi (conservative) The actual mechanics of the operation consisted of using the shape of the stress-strain curve and modulus of elasticity as determined from the actual compression tests. This curve was then adjusted to pass through the 0.20 percent offset yield of 140,000 psi by drawing the design curve affine to the test curve and passing through the desired yield point. Compression characteristics from these tests are shown in Figures 2-12 and 2-13.

b) Dimensions:

For the body and the long cover, the cylindrical portion of the inner diameter is 12.540 inches and the wall thickness is 0.975 inch.

The hemispherical portions of all parts (body, short cover, and long cover) have an inner radius of 6.540 inches, and wall thickness of 0.450 inch. These

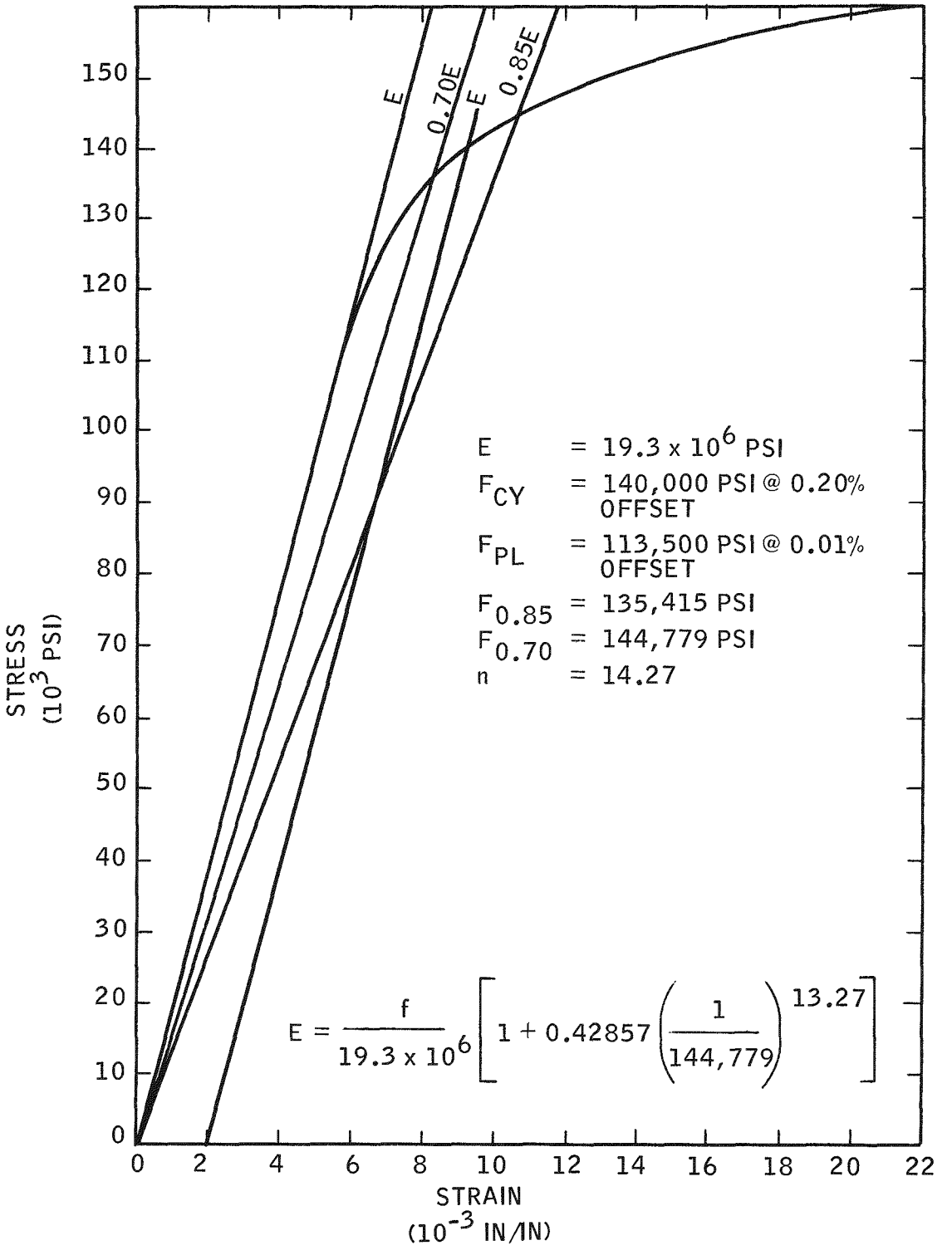

Figure 2-12. Berylco-165 (AT) Stress vs. Strain in Compression. Minimum Design Properties for SNAP-21 Pressure Vessel

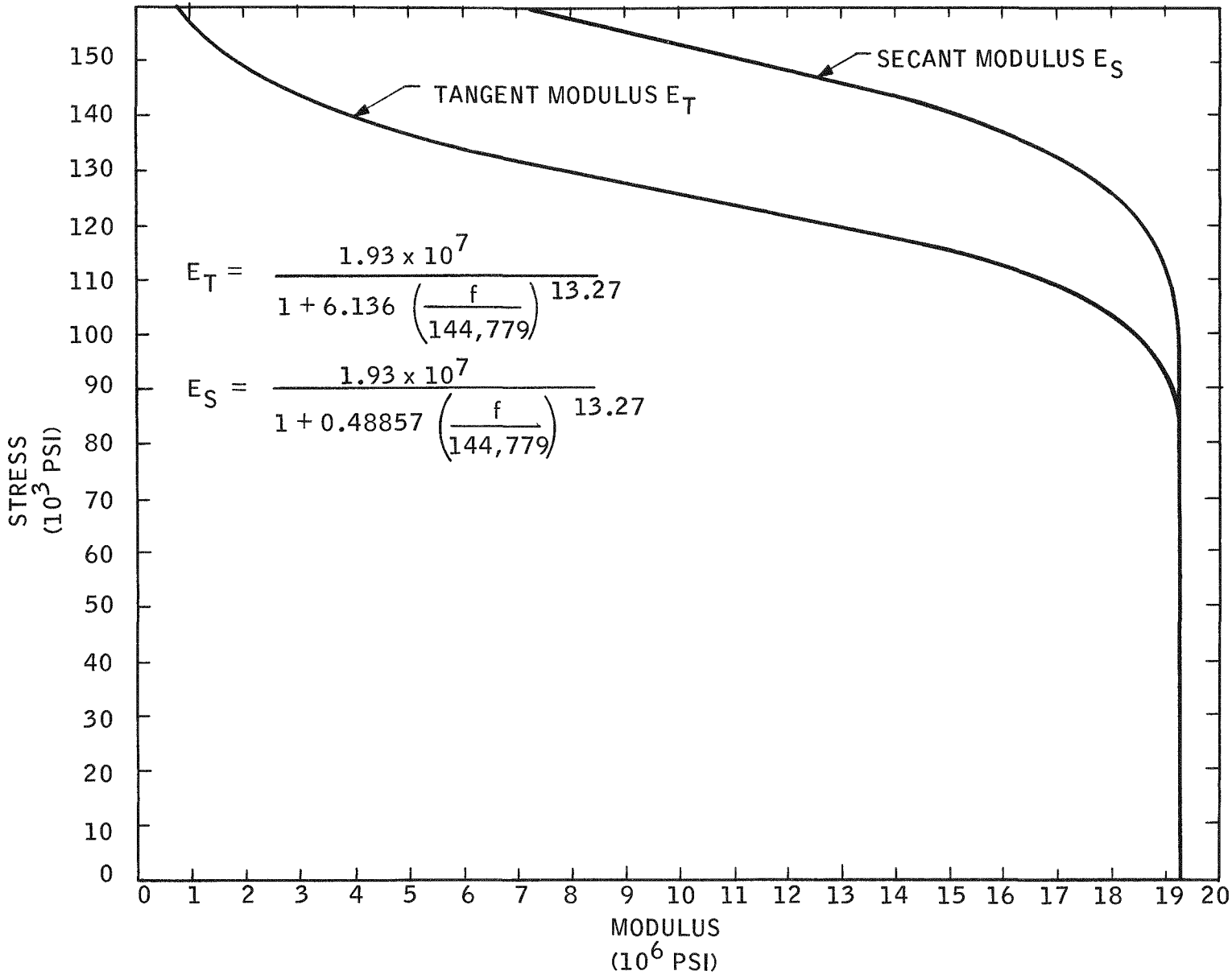

Figure 2-13. Berylco-165 (AT) in Compression. Tangent Modulus and Secant Modulus vs. Stress Level Based on Design Compression Curve

dimensions are all nominal values. Complete dimensional details of the pressure vessel components are shown on 3M Company drawings PD-37-4220 (body), PD-37-4222 (short cover) and PD-37-4221 (long cover). These drawings are shown in Figures 2-14, 2-15 and 2-16, respectively.

c) Pressures:

Working pressure = 10,000 psi

Design pressure = 16,500 psi

Proof pressure = 11,000 psi

The design pressure was established as follows:

Design Pressure = working pressure x 1.5 safety factor + 10% factor for variations in materials and heat treatment.

The 16,500 psi external pressure was used to determine wall thicknesses such that material yield stress would not be exceeded, and failure by buckling instability would not occur.

d) Maximum calculated stress at 11,000 psi proof pressure:

For cylindrical portion	77,850 psi
For hemispheres	91,200 psi
For hemisphere penetration boss through the cover	94,950 psi

Minimum safety factor based on yield strength is, therefore:

$$\frac{140,000}{94,950} = 1.48$$

e) Pressure vessel dimensional changes at 11,000 psi external pressure:

For the hemispheres in the radial direction	0.0216 inch
For the cylindrical portions in the radial direction	0.0242 inch
For the cylindrical portions in the longitudinal direction	0.00885 inch

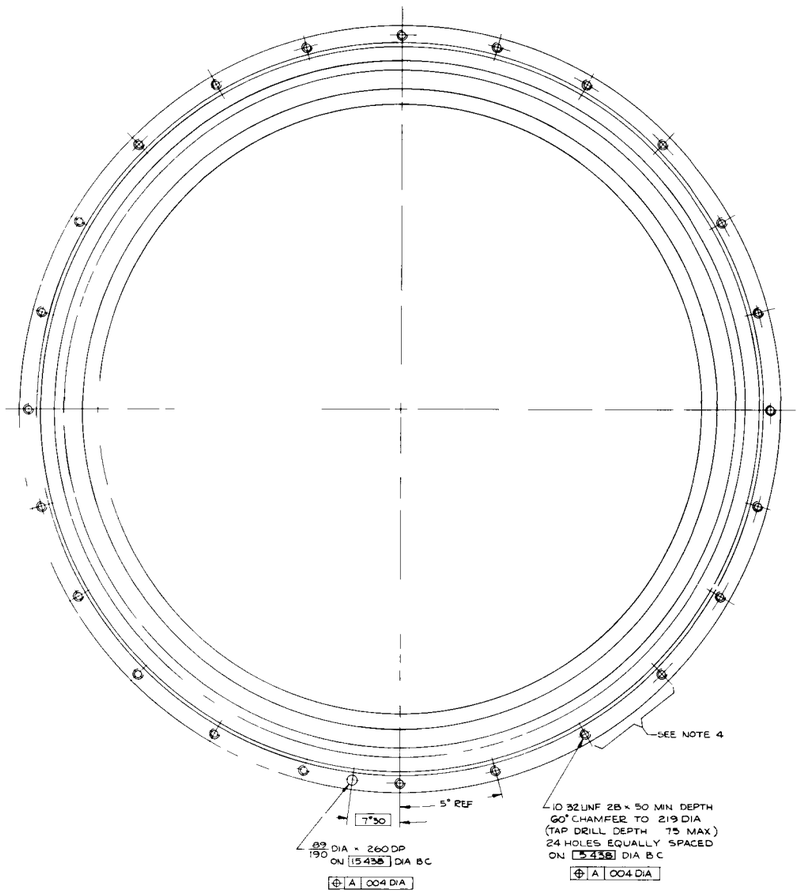

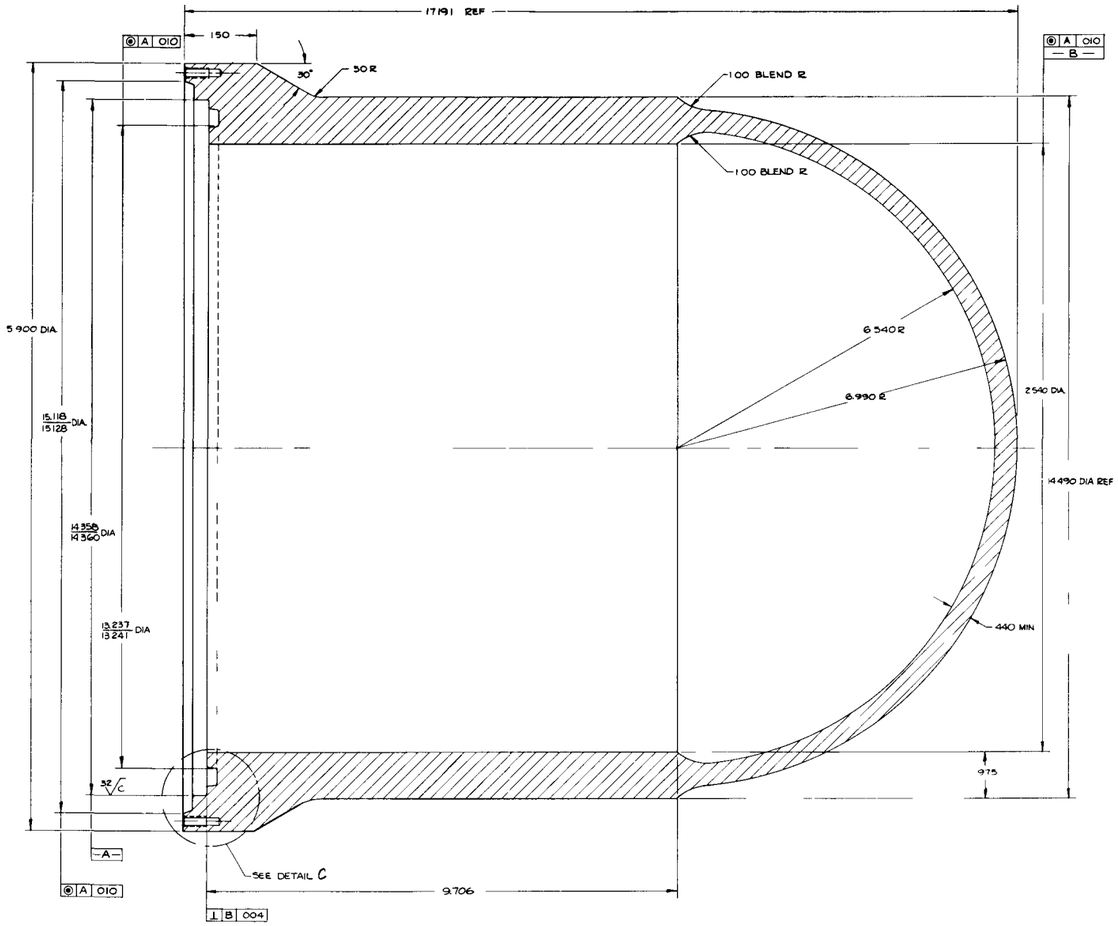

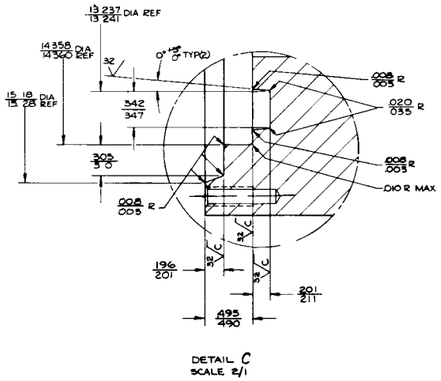

DETAIL C
SCALE 2/1

7 REMOVE BURRS AND BREAK SHARP EDGES

6 THREAD FORM IN ACCORDANCE TO MIL S 7742

5 EACH FINISHED PART TO BE HYDROTESTED TO EXTERNAL PROOF PRESSURE OF 1 000 ± 200 PSI FOR FOUR (4) HOURES MIN TESTS TO BE PERFORMED ON BODY PD 37-4220) PLUS EITHER LONG COVER (PD 37 4221) OR SHORT COVER (PD 37-4222) AS AN ASSEMBLY

4 IDENTIFICATION IDENTIFY BY P/N AND APPLICABLE REVISION LEVEL PER AMS2800A PARA 4 2 2

3 100% PENETRANT INSPECTION PER MIL I 6866B (ASG) DATED 2 26-64 AMENDMENT 1 10 AUG 1964 PENETRANT METHOD OF INSPECTION TYPE I

2 100% RADIOGRAPHICALLY INSPECT PER MIL STD 453 CHANGE 1 4 SEPT 1963

1 MATERIAL BERYLCO 165 PER AMS 4650(E) EXCEPT AS FOLLOWS,
PARA 4 COMPOSITION BERYLLIUM -1.60% MIN -1.80% MAX
PARA 6.4 GRAIN SIZE 0.030 MM
PARA 6.5 PROPERTIES AFTER PRECIPITATION HEAT TREATMENT HEAT TREATMENT TEMPERATURE 600°F MIN
PARA 6.5.1 TENSILE PROPERTIES TENSILE STRENGTH 150 000 180 000 PSI
YIELD STRENGTH 130 000 160 000 PSI AT 0.2% OFFSET

NOTES

Figure 2-14 Pressure Vessel Body

BLANK

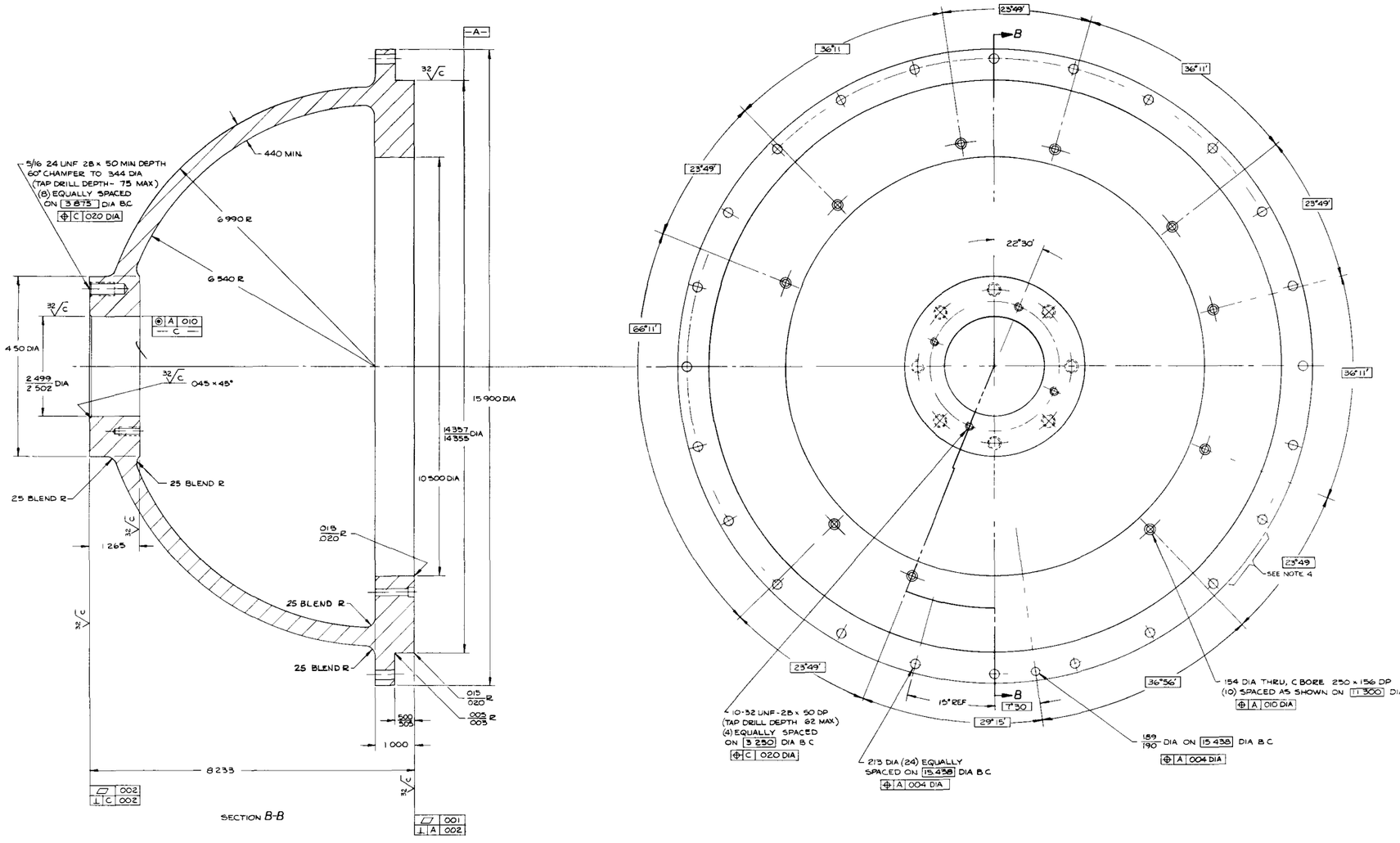

7 REMOVE BURRS AND BREAK SHARP EDGES

6 THREAD FORM IN ACCORDANCE TO MIL-S-7742

5 EACH FINISHED PART TO BE HYDROTESTED TO EXTERNAL PROOF PRESSURE OF 11,000 ± 200 PSI FOR FOUR (4) HOURS MIN. TESTS TO BE PERFORMED ON SHORT COVER (PD-37-4222) PLUS THE BODY (PD-37-4220) AS AN ASSEMBLY

4 IDENTIFICATION IDENTIFY BY P/N AND APPLICABLE REVISION LEVEL PER AMS 2800A PARA 4.2.2

3 100% PENETRANT INSPECTION PER MIL-I-6866B (ASG) DATED 2-26-64 AMENDMENT 1, 10 AUG 1964 PENETRANT METHOD OF INSPECTION TYPE I

2 100% RADIOGRAPHICALLY INSPECT PER MIL-STD-453, CHANGE 1, 4 SEPT 1965

1 MATERIAL BERYLCO 63 PER AMS 4650E EXCEPT AS FOLLOWS
PARA 4 COMPOSITION BERYLLIUM - 1.60% MIN - 1.80% MAX
PARA 6.4 GRAIN SIZE 0.050 MM
PARA 6.5 PROPERTIES AFTER PRECIPITATION HEAT TREATMENT HEAT TREATMENT TEMPERATURE 600°F MIN
PARA 6.5.1 TENSILE PROPERTIES TENSILE STRENGTH - 150,000 - 180,000 PSI
YIELD STRENGTH - 130,000 - 160,000 PSI AT 0.2% OFFSET.

Figure 2-15. Pressure Vessel Short Cover

BLANK

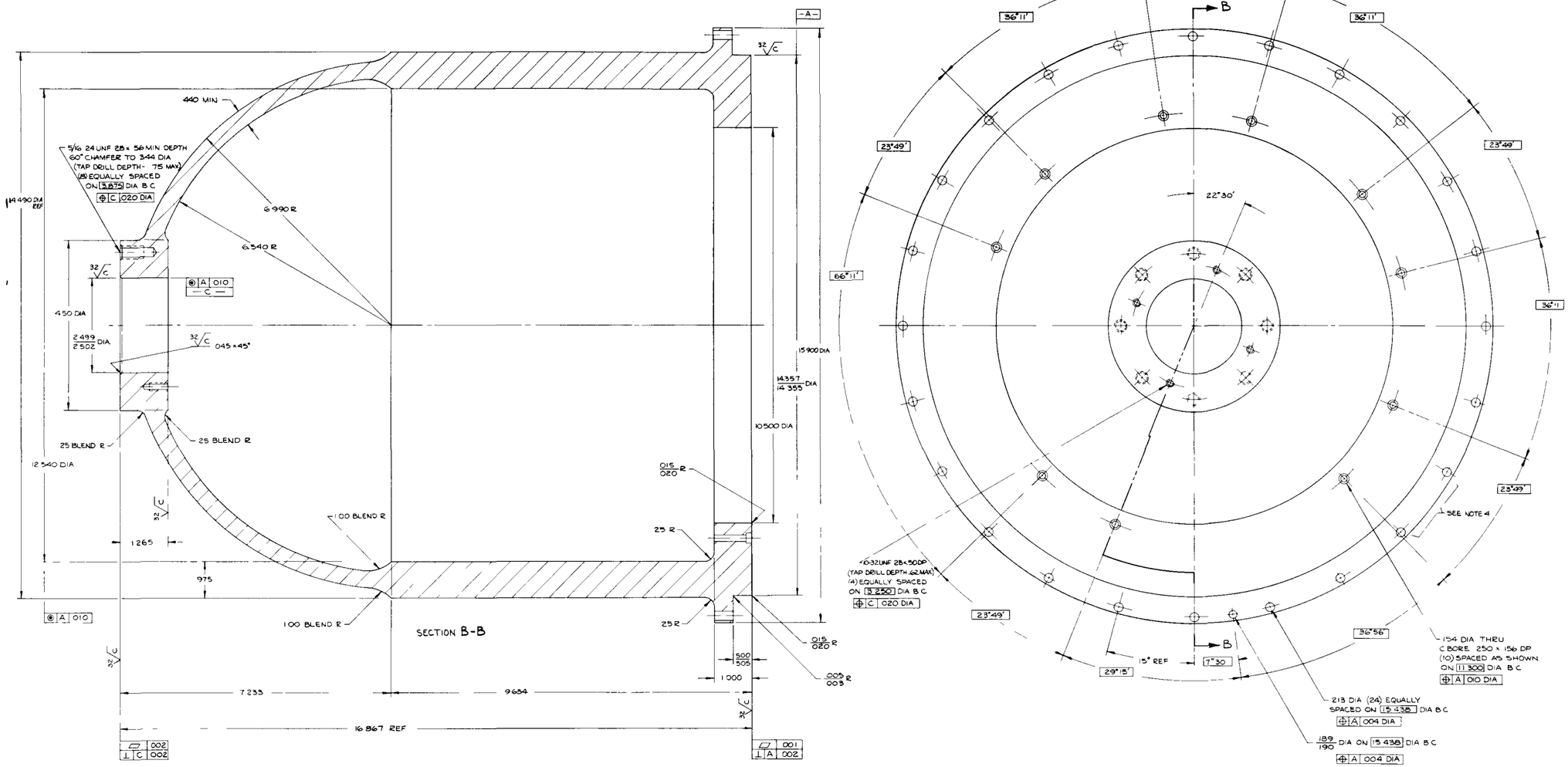

7 REMOVE BURRS AND BREAK SHARP EDGES

6 THREAD FORM IN ACCORDANCE TO MIL-S-7742

5 EACH FINISHED PART TO BE HYDROTESTED TO EXTERNAL PROOF PRESSURE OF 11 000 ± 200 PSI FOR FOUR (4) HOURS MIN TESTS TO BE PERFORMED ON LONG COVER (PD-37-4221) PLUS THE BODY (PD-37-4220) AS AN ASSEMBLY

4 IDENTIFICATION IDENTIFY BY P/N AND APPLICABLE REVISION LEVEL PER AMS 2800A PARA 4.2.2

3 100% PENETRANT INSPECTION PER MIL-I 6866B (ASG) DATED 2 26-64 AMENDMENT 1, 10 AUG 1964
PENETRANT METHOD OF INSPECTION TYPE I

2 100% RADIOGRAPHICALLY INSPECT PER MIL-STD-453, CHANGE 1, 4 SEPT 1963

1 MATERIAL BERYLCO 165 PER AMS 4650E EXCEPT AS FOLLOWS
PARA. 4 COMPOSITION BERYLLIUM - 1.60% MIN - 1.80% MAX
PARA 6.4 GRAIN SIZE: 0.050 MM
PARA 6.5. PROPERTIES AFTER PRECIPITATION HEAT TREATMENT. HEAT TREATMENT TEMPERATURE 600°F MIN
PARA 6.5.1 TENSILE PROPERTIES: TENSILE STRENGTH - 150,000-180,000 PSI
YIELD STRENGTH - 130,000-160,000 PSI AT 0.2% OFFSET

NOTES:

Figure 2-16. Pressure Vessel Long Cover

BLANK

2.2.6 THERMOELECTRIC GENERATOR

2.2.6.1 Design

During this report period, design of the in-line series of generators was completed. This included the release of all drawings necessary for the building and operation of generators A10D5, A10D6, and A10D7. This series of generators will incorporate three different insulation materials.

Initially, the thermal insulating material for all three generators was to be shredded Microquartz; however, further analysis of the test matrix revealed that this could lead to data interpretation problems in the event of probable failure modes. The final insulation specification for each generator is as follows:

Generator A10D5	Microquartz (shredded)	All generators will be back-filled with xenon.
Generator A10D6	Min-K 1301 (powdered)	
Generator A10D7	Min-K 1999 (powdered)	

Note: Microquartz, Min-K 1301 and Min-K 1999 are product designations of the Johns-Manville Company.

The basis for this assignment is as follows:

- Generator A10D5 – Microquartz was selected as a candidate insulation material primarily to reduce cost. This reduction in cost is achieved because of the decrease in generator processing time (2 days versus 6 days for Min-K 1301). The thermal conductivity of Microquartz is, however, greater than that of Min-K 1301. The thermal conductivity, k, (BTU/Hr-ft-°F) for Microquartz is 0.026 and for Min-K 1301, 0.014. Consequently, an additional heat leak of approximately 7 watts through the generator is expected. All 3M commercial generators are insulated with Microquartz and its compatibility with thermoelectric materials is well known. Consequently, it is not considered necessary to have more than one generator insulated with it to provide backup data.

- Generator A10D6 – This generator will be insulated with Min-K 1301, the same material used in all previous SNAP-21 generators. This unit is

considered necessary to provide a baseline for comparing the in-line and the ball and socket generator. In the in-line generators, the most likely mode of poor performance is high internal resistance. This can be caused by micro-cracks in the legs (design induced) or oxidation of the legs (process or insulation induced). Without a baseline generator, a long and costly teardown and analysis would be necessary to pinpoint the cause if high internal resistance should be encountered.

- Generator A10D7 – Min-K 1999 was selected for this generator. This insulation was selected because currently available data indicates that it offers the same thermal insulating properties as Min-K 1301 but can be processed with a shorter cycle similar to Microquartz. The shorter cycle is possible because it does not have the hydrocarbon binder that Min-K 1301 does. Although this insulation appears to combine the advantages of both Min-K 1301 and Microquartz, it was not specified for all three generators because of the limited amount of experience with it in conjunction with thermoelectric materials.

2.2.6.2 Electrical Feedthrough Headers

Considerable leakage problems were encountered in the first development ceramic instrumentation headers used in Generators A10D5 and A10D6. The leaks all occurred at the instrumentation wire-to-Kovar tube joint. Although this joint was tested after manufacture and found acceptable, leaks developed after handling and assembly. The leaks were caused by the soft solder joint used to seal the wire to the tube. Soft solder was used rather than a high-temperature braze because the length of wire specified made it difficult to get it in a furnace and because the initial schedule did not permit time to solve a wetting problem between the Kovar tube and the constantan wires. A schematic of the feedthrough header is shown in Figure 2-17.

Discussions with the vendor resulted in the following design changes:

- The lead wire lengths were shortened to make it easier to get in a furnace.
- The length of the Kovar tube was shortened to reduce the bending moment and make it stiffer.

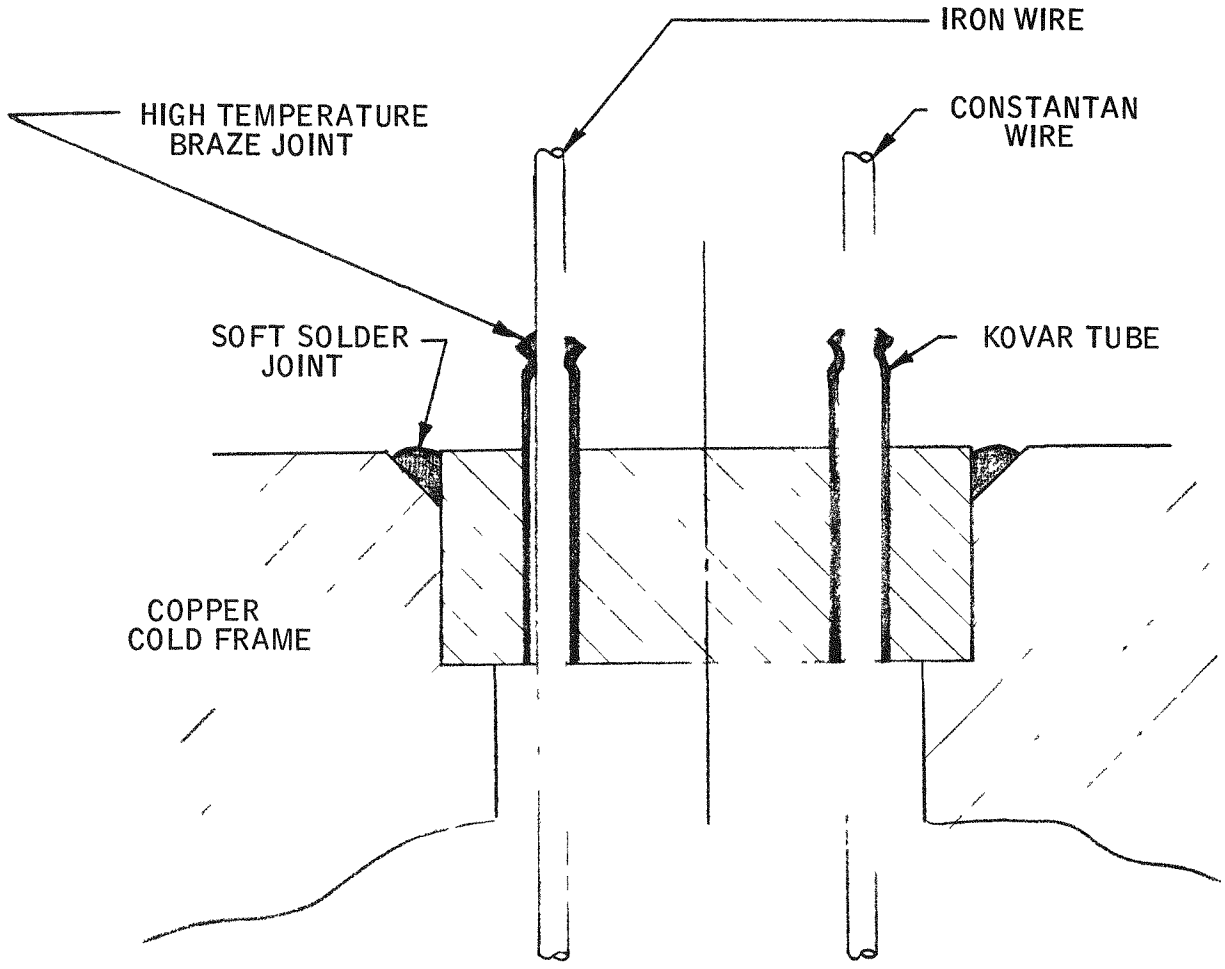

Figure 2-17. Schematic of Electrical Feedthrough Header

- A high melting point (1900°F) braze alloy was substituted for the soft solder.
- The braze joint was made in a hydrogen furnace to facilitate wetting.

Headers incorporating these design changes have been received and appear to be leak-tight. They were successfully incorporated in Generator A10D7.

2.2.6.3 Quality Control

a) Generator

Generator A10D5 was completed through assembly, processing, and testing. All departures and changes encountered were entered on process routing sheets and appropriate disposition was assigned. The generator is currently waiting for shock and vibration tests.

Generator A10D6 was completed through assembly and is currently on the processing station undergoing the remaining portion of the processing cycle. All departures and changes have been documented and dispositioned.

Beginning with Generator A10D6 the process routing sheets for assembly and processing were revised to eliminate inspection steps without jeopardizing product quality. The result is a reduction in the inspection manhours required to witness and verify manufacturing operations.

During the month of November 3M, working with the AEC site representative, performed a formal audit of 3M's traceability system on generator assemblies and components. By accurately tracing the total history of specific parts, from raw material through final assembly into the generator, the traceability system was shown to be valid for this check. Generators A10D2 and A10D4 were used.

Fluorescent penetrant inspection techniques were developed in-house to fulfill the penetrant inspection requirements, thereby eliminating the necessity for subcontracting parts for inspection.

b) Insulation System

Two trips to Linde Corporation at Tonawanda, New York were made in November by 3M Quality Assurance representatives. The first trip was to correlate inspection data on heater blocks, heaters, inner liners and biological shields. The Linde inspection was performed on the parts without allowing sufficient time for temperature stabilization. After the parts were allowed to stabilize, a re-inspection indicated proper correlation. The second trip was to review and survey Linde's total quality system. Two action items were assigned: 1) 3M accepted an action item to define the traceability requirements to be maintained by Linde, and 2) Linde accepted an action item to take the necessary steps for calibration of equipment.

Follow-up shows that Linde is taking the necessary steps to document and implement the needed controls for instrument calibration, traceable to National Bureau of Standards and Material Traceability, similar to and compatible with 3M's system.

c) Fuel Capsule

A meeting was held at Oak Ridge National Laboratory with personnel from Pacific Northwest Laboratory, Oak Ridge National Laboratory and 3M Company to discuss weld procedures, parameters and non-destructive inspection acceptance criteria of the fuel capsule welds for the SNAP-21 generators. The meeting resulted in establishment of tentative acceptance criteria for the fuel capsule.

2.2.7 POWER CONDITIONER

During this report period the power conditioner design was completed and vendors were selected for all components. In addition, the electronic components of the first development power conditioner, H10D1 were assembled. Figure 2-18 shows in-process views of the power conditioner base plate assembly. The electronic components are now in the process of a 240-hour burn-in period. The burn-in period consists of operating the power conditioner at rated EOL load conditions with all input power dissipated in the voltage regulator portion of the conditioner. This results in component operating temperatures of up to 135°F, which is

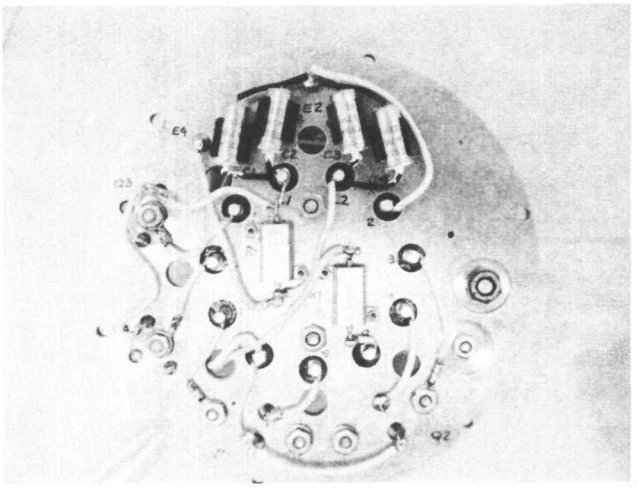

a. Bottom Side of Base

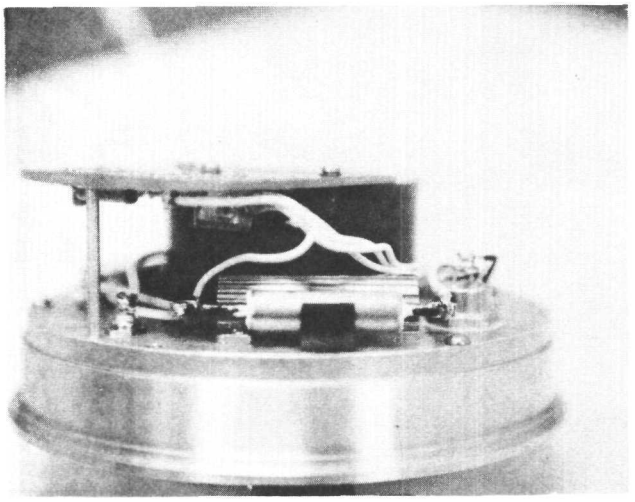

b. View Toward Resistor R20 Base Plate Mounted on the Container Base

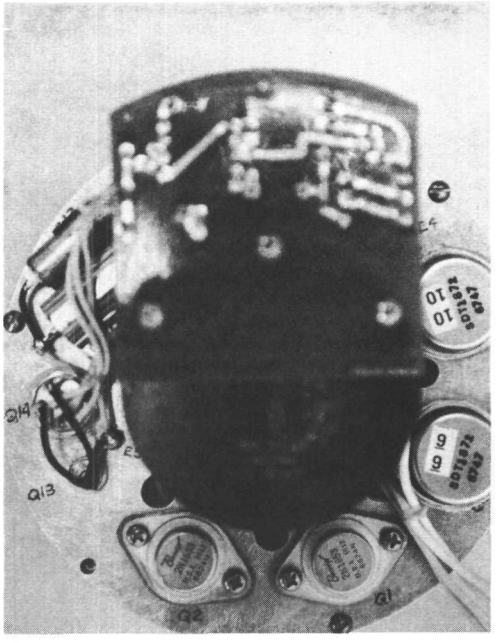

c. Top Side of Base Plate

Figure 2-18. Power Conditioner H10D1

approximately two times the normal operating temperature. This elevated temperature test is designed to detect failure in marginal components. After the burn-in the power conditioner will be sealed in its container.

Conversion efficiency measurements taken prior to the burn-in indicate an efficiency of 89 percent. This is somewhat lower than the 90 to 91 percent anticipated, however, it is above the minimum value of 87 percent established as a design goal. The components in the design will be monitored during operational tests during the next report period to determine the cause of the lower efficiency and to determine if it can be improved.

The present circuit configuration is shown in Figure 2-19; the overall assembly is shown in Figure 2-20.

Some of the design changes incorporated in this power conditioner which were not in the Phase I conditioners include:

- Circuit changes (defined in Quarterly Report No. 5) were incorporated to improve starting characteristics, filter efficiency, voltage regulator stability and to adjust the design to compensate for the non-availability of some components.

- A redesigned enclosure. The new power conditioner enclosure will be of welded aluminum construction in the form of a solid right cylinder with an outside diameter of approximately 6.5 inches and a height of approximately 3.5 inches. It will be threaded into a center attachment ring mounted below the receptacle in the penetration area of the pressure vessel. A plastic thread locking device will prevent the power conditioner from coming loose during shock and vibration tests.

- A printed circuit board will be used for the wiring assembly in the amplifier section of the voltage regulator. This will simplify assembly and improve reliability by reducing the possibility of error during wiring.

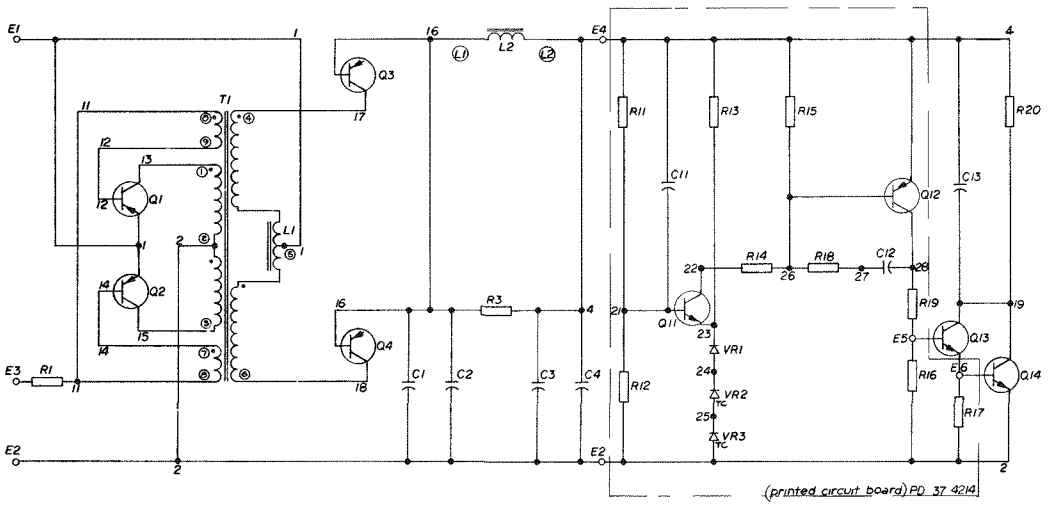

PARTS DEFINITION LIST

DEVICE DESIGN	3M DWG NUMBER	MANUFACTURER NAME	MANUFACTURER NUMBER	APPLICABLE MIL SPEC	MILITARY SPEC MIL SPEC DESIGN
Q Q2	20 2017	BENDIX CORP	USA 2N1653		
Q3 Q4	20 2068	SOLITRON DEVICES	ES 291(SDT 872)		
Q11	20 2021	FAIRCHILD SEMI CONDUCTORS	2N 2484		
Q12	20 2019	MOTOROLA	2N 2907A		
Q 3	20 2020	SOLITRON DEVICES	2N 2698 (SDT 4599)		
Q14	20 2016	SOLITRON DEVICES	2N 2814 (SDT 7158)		
VR1	20 2022	FAIRCHILD SEMI CONDUCTORS	USN N753A	MIL S 9509/127B	
VR2,VR3	20 2023	FAIRCHILD SEMI CONDUCTORS	1N4611A (MCR 2222)		
R	20 2009P6	DALE ELECT NC	ARH 10 10W 6 81Ω	MIL R 39009	RER65F6R81P
R3	20 2009P5	DALE ELECT INC	ARH 0 10 W 3 0Ω	MIL R 39009	RER65F3R00P
R20	20 2009P7	DALE ELECT NC	ARH 50 50W 309Ω	MIL R 39009	RER75F30R9S
R 1	20 2010 P	IRC NC	GEM 60 /8W 14 3K	MIL R 55182	RNR60E1432FP
R12	20-2010P2	IRC INC	GEM60 /8W	MIL R 55182	RNR60E3922FP
	20 2010P47	IRC NC	39 2K TO 130 3K		RNR60E1303FP
R13	20 2008P4	DALE ELECT INC	ARS 2 3090Ω 2W	MIL R 39007A	RWR71G3091FS
R 4	20 2008P3	DALE ELECT INC	AGS 3 2320Ω 2 25W	MIL R 39007A	RWR80G2321FS
R15 R18 R19	20 2008P2	DALE ELECT INC	AGS 3 1500Ω 2 25 W	MIL R 39007A	RWR80G1501FS
R 6	20 2008P5	DALE ELECT NC	ARS 2 5,110Ω 2W	MIL R 39007A	RWR71G5111FS
R17	20 2008P1	DALE ELECT INC	AGS 3 511Ω 2 25W	MIL R 39007A	RWR80G5110FS
C C4	20 2015P2	MALLORY CO	TS54476K035PD 47uf 35V	MIL-C 26655B (CASE ONLY & VALUE ONLY)	CS12BF476K
C11	20 2081P	CORNING ELECT	CYFR 0G101J 100 mmf 350	MIL C 23269A	CYR10C101JR
C12	20 2081P2	CORNING ELECT	CYFE20G202J 2000 mmf 300V	MIL C 23269A	CYR20C202JR
C13	20 2082P1	SPRAGUE ELECT	19551043252 .27uf 200V	MIL-C 14157C	CPV0BA1KC104KR
T1 L #L2	E PD 37 355	ADC CORP	3M T MP U XX	MIL T 39015	TFR5R03ZZR

3 REFERENCE DRAWINGS - PD 37 4217 ASSEMBLY BASE PLATE POWER CONDITIONER
PD-37-4218 POWER CONDITIONER ASSEMBLY

2 RESISTOR, R12 SELECTED AT ASSEMBLY FOR 24 5 VOLTS AT 0 4 AMP OUTPUT

1 NUMBERS APPEARING ON THE ELEMENTARY DIAGRAM INDICATE POINTS AT COMMON POTENTIAL NUMBERS WITHIN CIRCLES INDICATE COMPONENT TERMINAL IDENTIFICATIONS

NOTES

Figure 2-19. Elementary Diagram Power of Conditioner

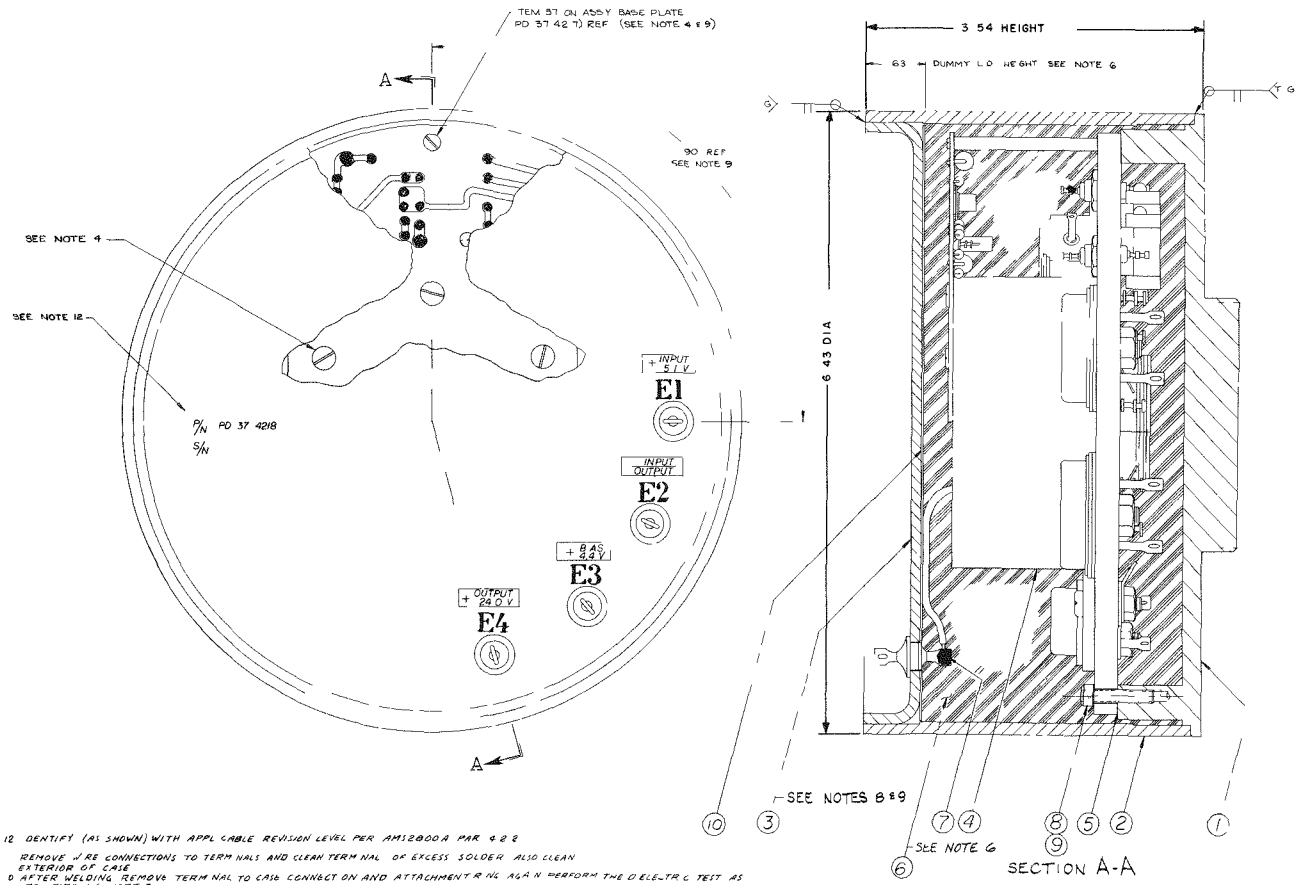

ITEM	LOC	QUAN	PARTS LIST PART NUMBER	DESCRIPTION
		1	PD 37 428	ASSY, POWER CONDITIONER
			PD 37 421	BASE CONTAINER, POWER CONDITIONER
2			PD 37 422	CYLINDER CONTAINER, POWER CONDITIONER
3			PD 37 426	ASSY LID, CONTAINER, POWER CONTAINER
4		1	PD 37 4217	ASSY BASE PLATE, POWER CONDITIONER
5		A/R	20 2078	HEAT SINK COMPOUND
6		A/R	20 219	ELECTRICAL INSULATING FOAM 3M XR 5017
7		A/R	20 2050	SOLDER, 60 40 RES N CORE
8		6	MS16995 9	SCR CAP SOC HD 6 32 UNC 2A x 5/8 LG
9		6	MS35333 71	WASHER LOCK INTERNAL TOOTH #6
10			PD 37 4228	INSULATION DISK MICA

12 IDENTIFY (AS SHOWN) WITH APPL CABLE REVISION LEVEL PER AMI2800A PAR 4.2.2

REMOVE WIRE CONNECTIONS TO TERMINALS AND CLEAN TERMINAL OF EXCESS SOLDER ALSO CLEAN EXTERIOR OF CASE

10 AFTER WELDING, REMOVE TERMINAL TO CASE CONNECTION AND ATTACHMENT RING AGAIN PERFORM THE DIELECTRIC TEST AS SPECIFIED IN NOTE 9

9 INSTALL THE LID ASSEMBLY (ITEM 3) ORIENTATED AS SHOWN SHORT THE FOUR ELECTRICAL TERMINALS TOGETHER AND PERFORM A DIELECTRIC TEST IN ACCORDANCE WITH MIL STD 202C METHOD 301. APPLY 300 VDC RELATIVE TO FOUR SHORTED TERMINALS TO CASE. THE LEAKAGE CURRENT SHOULD NOT EXCEED 5 MICROAMPS. AFTER THE DIELECTRIC TEST DISCONNECT THE TERMINALS TO THE CONTAINER BASE BY SOLDERING OR BOLTING #16 AWG JUMPERS TO THE TERMINALS AND TO THE POWER CONDITIONER ATTACHMENT RING (DWG PD 37 496). WELD THE LID ASSEMBLY TO THE CONTAINER BY MEANS OF INERT GAS SHIELDED ARC WELDING. THE MAXIMUM PERMITTED BASE TEMPERATURE IS 150°F. THE MAXIMUM LID TERMINAL TEMPERATURE PERMITTED IS 250°F

8 CLEAN MOUNTING SURFACES OF LID ASSEMBLY (ITEM 3) AND CONNECT LEADS FROM ASSEMBLY BASE PLATE (ITEM 4) TO LID ASSEMBLY TERMINALS CUT OUT FOAM AS REQUIRED TO CAPTIVATE LEADS BY COVER USE SOLDER (ITEM 7) AND A SOLDERING IRON WHICH HAS A MEANS OF AUTOMATICALLY CONTROLLING THE TIP TEMPERATURE TO 600±60°F

7 AFTER CURING, REMOVE DUMMY LID AND ALLOW FOAM SURFACE TO BE EXPOSED TO AMBIENT AIR FOR 96 HOURS TO ALLOW ENTRAPPED FOAMING GAS TO DIFFUSE

6 THOROUGHLY CLEAN INTERIOR OF ASSEMBLY AND PREPARE UNIT FOR INSULATING FOAM (ITEM 6) BY HEATING ASSEMBLY TO 150°F APPLY FOAM (ITEM 6) IN ACCORDANCE WITH MANUFACTURERS INSTRUCTIONS CONFINE FOAM TO DESIRED VOLUME BY DUMMY LID COATED WITH A PARTING AGENT USE DUMMY LID TO HOLD LEADS FROM ASSEMBLY BASE PLATE (ITEM 4) IN PLACE CURE FOAM FOR 3 HOURS AT 50°F

5 ARRANGE LEADS FROM ASSEMBLY BASE PLATE (ITEM 4) FOR MINIMUM LENGTH CONSISTANT WITH CONNECTION TO TERMINALS OF ASSEMBLY LID CONTAINER (ITEM 3)

REMOVE (4) HOLDING SCREWS OF PRINTED CIRCUIT BOARD ASSEMBLY AND MOVE IT BACK TO PERMIT INSTALLATION OF BASE PLATE SCREWS & WASHERS (ITEMS 8&9) TIGHTEN ALL BASEPLATE SCREWS TO 0.2 N LBS REINSTALL PRINTED CIRCUIT BOARD ASSEMBLY & REINSTALL HOLDING SCREWS TO 5.6 LBS

3 APPLY A THIN FILM OF HEAT SINK COMPOUND (ITEM 5) TO THE MOUNTING SURFACE OF THE ASSY BASE PLATE (ITEM 4)

2 THOROUGHLY CLEAN ALL PARTS OF ALL FOREIGN MATTER ESPECIALLY SMALL METAL PARTICLES & FILLINGS INSIDE OF HOLES BY BRUSHING COMPRESSED AIR OR SELECTIVE AREA SOLVENT APPLICATION

WELD THE CYLINDER (ITEM 2) TO THE BASE (ITEM) BY MEANS OF INERT GAS SHIELDED ARC WELDING PERFORM HERMETIC SEAL MAXIMUM ACTUAL LEAK RATE SHOULD NOT EXCEED 5.2 X 10⁻⁷ CC HELIUM PER SEC AT 25±5°C

NOTES:

Figure 2-20. Power Conditioner Assembly

- Scotchcast Brand resin number XR-5017, a two-part silicone rubber electrical insulating foam, has been selected to fill the power conditioner enclosure. Tests have verified that the foam has very low moisture absorption (0.01 percent at 90 percent RH in 24 hours) and good thermal conductivity (0.60 BTU/hr/ft^2/°F/in). Thermal conductivity for air under the same conditions is 0.17. The foam-in-place resin serves as a water tight cushion around the components and will captivate any extraneous loose particles which could appear during the life of the equipment.

During the next report period three additional prototype units will be manufactured. The completed units will be subjected to the tests outlined in Section 2.3.7. These test results will be used as a design validation criterion.

2.2.8 ELECTRICAL RECEPTACLE AND PLUG

During this report period a vendor for the electrical receptacle and plug was selected and an order placed.

The vendor selected was the Marsh and Marine division of Vector Cable Co. Some features of the Marsh and Marine receptacle and plug are:

- All exposed metal components will be made from Berylco 165 to preclude any galvanic corrosion problems between the pressure vessel and the receptacle.

- The receptacle-to-pressure vessel interface will incorporate a double O-ring seal. This seal will be redundant, as is the seal between the pressure vessel cover and body.

- The receptacle and mating cable connecting plug will be of existing proven design currently in production at Marsh and Marine.

- The receptacle will have 22 electrical pins mounted in a removable insert. This permits replacement of the insert in the event of damage during assembly or test.

- The cable connecting plug can be terminated in a standard sheathed cable or a double armored cable without changing its functional design. Thus a standard rubber sheathed cable can be used for test purposes when minimum size and maximum flexibility are required. No further development effort will be necessary to attach an armored cable to the units to be implanted.

- Both the receptacle, plug and connected cable will be fully hydrotested at the component level before use with a system.

A procurement specification, 3M-IPP-100, Rev. A, has been prepared to define the technical requirements of the receptacle and cable connecting plug. This specification is the controlling technical document for Marsh and Marine. A copy of this specification is included as Appendix A.

2.3 COMPONENT AND SUBASSEMBLY TESTING

2.3.1 FUEL CAPSULE

Four prototype fuel capsules were successfully assembled, welded, and hydrotested. Two of these capsules had dummy fuel pellets made from aluminum oxide (Alsimag 614) while the other two capsules were loaded with $Sr90TiO_3$ pellets of 186.5 and 186.8 watts respectively. The two fueled capsules are scheduled for ocean exposure studies by NRDL.

The inner liners were welded in argon by the TIG process using 20 amps and a travel speed of 10.6 inches/min. The outer capsules were electron beam welded at 30 kv with 140 ma and a speed of 65 inches/min. One of the dummy capsules was welded before and one after the two fueled capsules. Prior to welding the caps on the inner liners, the axial free volume was taken up by circular stainless steel shims.

Following final capsule welding, the capsules were subjected to a vacuum leak check. No leaks were detected. The capsules were then weighed and subjected to an external hydrotest of 10,000 psi. Following hydrotest, the capsules were again weighed to determine if there had been any in-leakage of fluid. There was no detectable increase in weight.

Some deformation of the capsules occurred during the hydrotest, however, the capsule dimensions were still within the tolerance limits allowed by the insulation system. A summary of the post-test dimensions compared with the pre-test dimensional range is shown in Table 3. Prior to testing, the fuel capsule components were inspected only for conformance to print, consequently, the actual dimensions were not recorded. As shown in Table 3, the actual fuel capsules experienced more permanent deformation than the dummy capsules. That is due to the fact that the dummy Alsimag pellet is much stronger in compression and therefore provides very good axial reinforcement. The actual pellet will allow some deformation, especially where the platinum jacket is folded over.

2.3.2 BIOLOGICAL SHIELD

a) Background

Six short term isothermal tests* were oven treated in vacuum at 1785°F for 100 hours. Five barrier materials were tested: tantalum (Ta), tungsten (W), molybdenum (Mo), copper (Cu) and aluminum oxide (Al_2O_3). The sixth test contained no barrier between the shield and liner material (U-8Mo and Hastelloy X). Figure 2-21 shows the make-up of the short-term test specimen.

b) Testing

Testing began with a 4-hour pump down of the sealed quartz tubes followed by two argon gas flushes and subsequent pump down to 15μ of Hg. The temperature was raised 50°F every half hour until 1785° was reached. At this point, cooling fans were directed at the greased glass to seal the glass and prevent sealant loss. After a 100-hour soak the furnace power was turned off to allow the test fixture to cool inside the furnace.

After about 4 hours of cool-down (1250°F), the specimen containing the molybdenum barrier cracked open, admitting air to all 6 fixtures for a period of 5 minutes. The fixtures were then blanked off and the remainder of the tests were subsequently pumped down to 10μ of Hg. However, the molybdenum test was open

*For full understanding of this report, the reader is referred to Isothermal Compatibility Test Plan, Ref. No. 3691-0695.

Table 3. Fuel Capsule Dimensions Before and After 10,000 psi External Hydrotest

	Post-Test Dimensions						
	A ' Dia	B ' Dia.	C ' Dia.	D 'Dim.	E Dim	F Dim	G Dim
Capsule No. 1 Dummy Fuel Pellet	3.172	3.190	3.193	3.338	3.416	0.027	0.02
Capsule No. 2 $Sr^{90}TiO_3$ Pellet 186.5 watts	(1)	(1)	(1)	3.33[illegible]	3.37	0.0[illegible]	0.067
Capsule No. 3 $Sr^{90}TiO_3$ Pellet 186.8 watts	(1)	(1)	(1)	3.334	3.37	0.061	0.06
Capsule No. 4 Dummy Fuel Pellet	3.175	3.190	3.194	3.337	3.41[illegible]	0.01[illegible]	0.014
Pre-Test Range							
Same Pre-Test Dimensional Range for all (4) Capsules	3.198 3.196	3.198 3.196	3.196 3.196	3.344 3.334	3.460 3.442	0.002 max (estimated)	0.00[illegible] max (estimated)

Notes (1) Dimensions not taken – hot cell limitations

A Dia – O.D. at center of capsule
B Dia – O.D. at top of capsule
C Dia – O.D. at bottom of capsule
D Dim. – Distance from top of capsule to bottom of capsule
E Dim – Distance from top of handle to bottom of capsule
F Dim. – Concavity of top of capsule measured at point OA
G Dim – Concavity of bottom of capsule measured at center of capsule

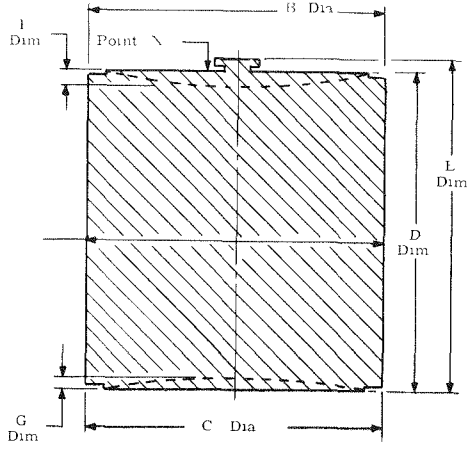

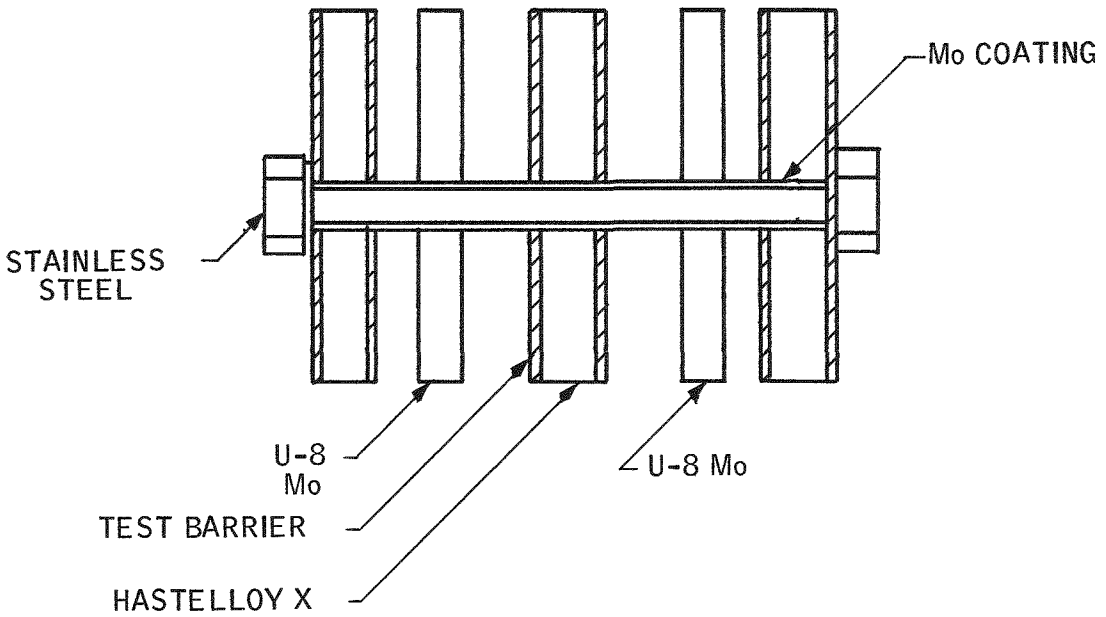

BARRIER MATERIALS TESTED:

TANTALUM
TUNGSTEN
MOLYBDENUM
COPPER
ALUMINUM OXIDE
NO BARRIER

Figure 2-21. Short-Term Test Specimens

to the air for the remainder of the cool-down (18 hours). Because of the broken tube in the molybdenum test, both the tungsten and molybdenum tests were re-run successfully.

c) Results

Examination of the post-test samples show the following:

Tantalum coating:	sound and adherent
Aluminum oxide coating:	sound and adherent
Copper coating:	sound but lifted off substrate
Tungsten coating:	allowed formation of eutectic reaction
*Tungsten #2 coating:	sound and adherent
Molybdenum coating:	heavily oxidized, no conclusions
*Molybdenum #2 coating:	sound and adherent
No barrier:	formation of expected eutectic melt

The test samples were metallographically mounted for further examination as shown in Figures 2-22 through 2-28. Polishing was difficult, permitting only rough semi-quantitative microprobe measurements. The Al_2O_3 and Mo tests were selected for this analysis.

Microprobe measurements indicated no significant diffusion of the Hastelloy-X components into either the Al_2O_3 or Mo barriers. In fact, beyond 40 microns into the barriers from the Hastelloy-X barrier interface, only X-ray radiation for the barrier constituents was observed.

Similarly, there was no significant diffusion of the barriers into the Hastelloy-X, of the barriers into the U-8Mo alloy, or of the U-8Mo alloy into the barriers.

The Al_2O_3 barrier Hastelloy-X and Al_2O_3 barrier U-8Mo alloy interfaces appear intact while there are separations at the Mo barrier Hastelloy-X and Mo barrier U-8Mo alloy interfaces.

*These tests were rerun.

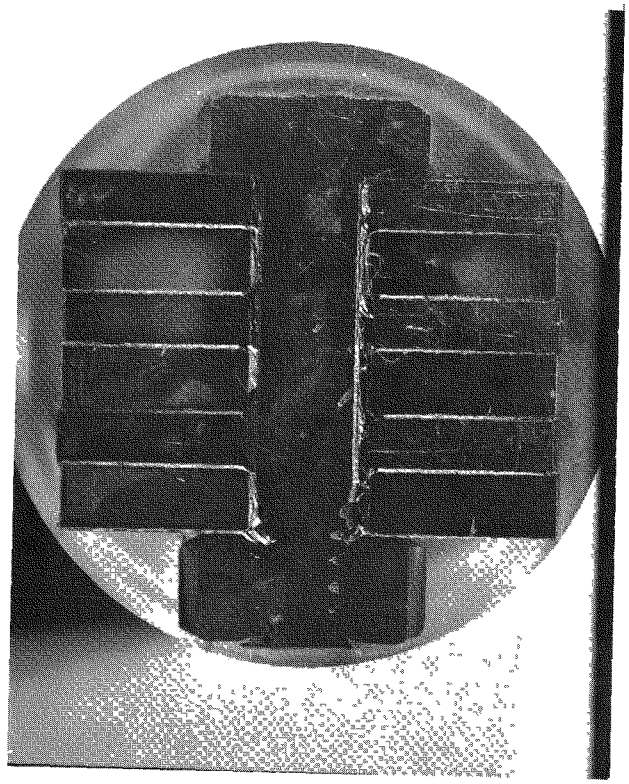

Figure 2-22. Aluminum Oxide ($A1_2O_3$)

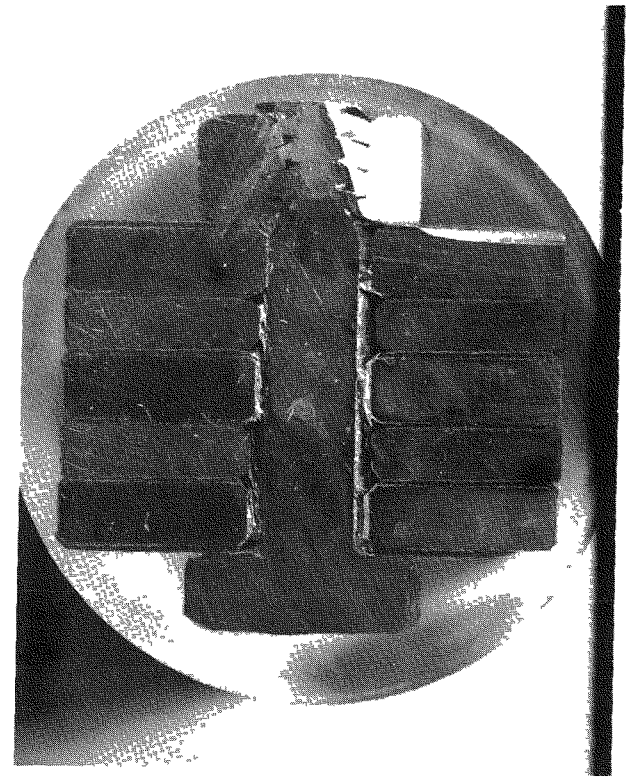

Figure 2-23. Tantalium (ta) Specimen

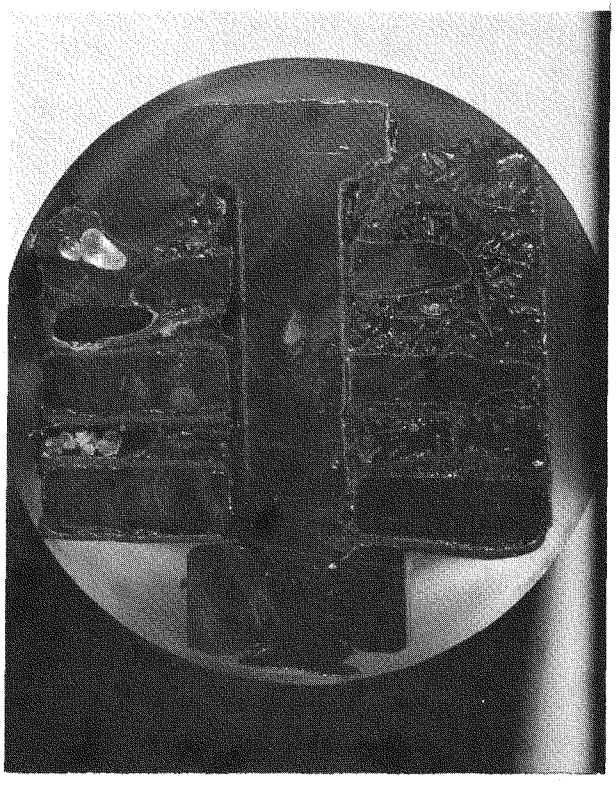

Figure 2-24. Tungsten (W) Specimen No. 1

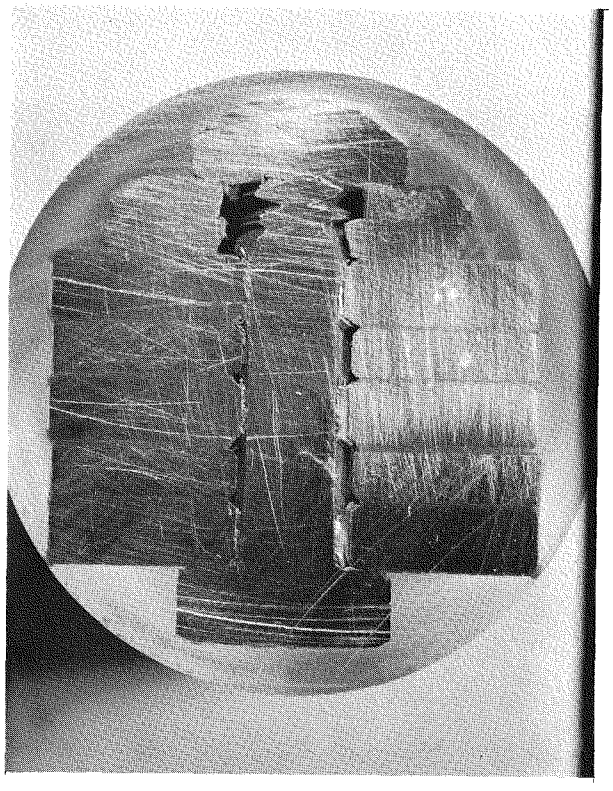

Figure 2-25. Tungsten (W) Specimen No. 2

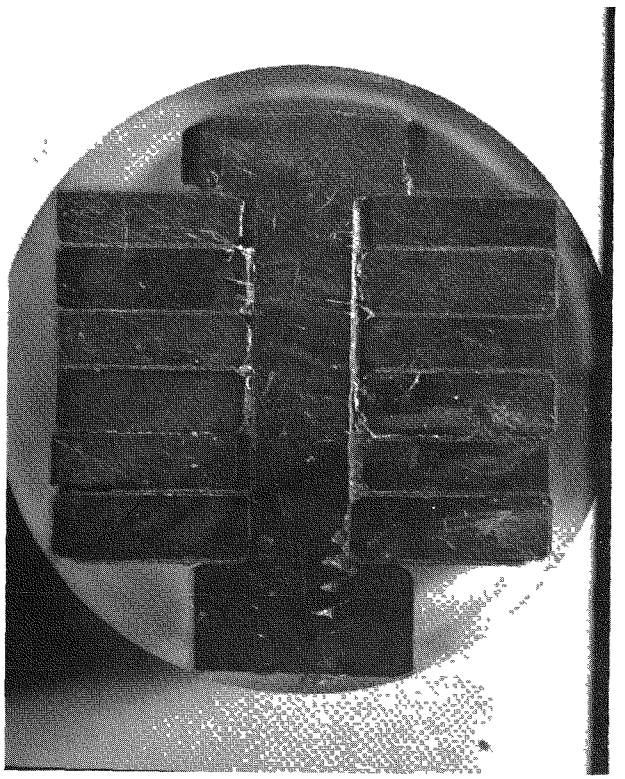

Figure 2-26. Molybdenum (Mo) Specimen No. 2

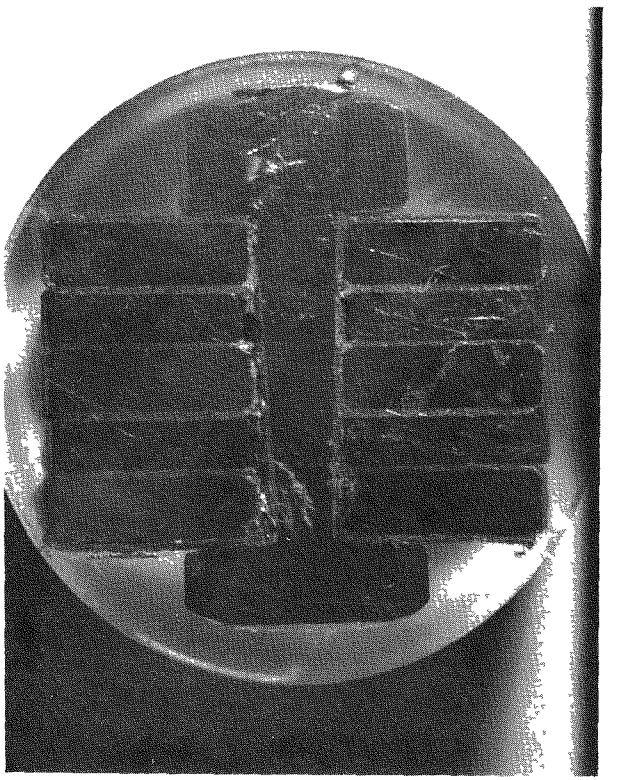

Figure 2-27. Copper (cu) Specimen

Future – This report completes the short-term testing and analysis. Long-term testing has been under way for about 2500 hours. Both the 500 and 2000 hour long-term tests have completed oven treatment. Visual examination showed very little reaction between the test components. Figure 2-29 shows the make-up of the long-term test specimens.

2.3.3 INSULATION SYSTEM

The getter evaluation test data was analyzed and the static proof test evaluation was performed during this report period. The tension rod prestressing investigation, the shipping container dynamic test and the dynamic test to specification of insulation unit 10D1 were also completed.

2.3.3.1 Getter Evaluation Test

The getter evaluation test completed during the last report period, was conducted in three parts by successively loading the same getter sample to determine the capacity of the getter. After each part of the test the residual gas was analyzed on the mass-spectrometer to determine the gas constituents and percentage composition. After each of the first two parts of the test where 52,170 micron-liters and 25,503 micron-liters were gettered (see Figure 2-30) the gas analysis taken showed the gas to be essentially all argon which is not gettered (see Table 4). After Part III of the test, where the getter capacity was completely used, the predominant residual gas was carbon monoxide. This shows that the getter had used up its capacity for this gas.

The settle-out pressure at the end of each part of the test compares well with the pressure expected from the non-getterable argon in the test gas. For example, at the end of Part I there was a settle-out pressure of 10.5 microns. The argon pressure expected is calculated by multiplying the total gas admitted (micron-liters) by the fraction of argon composition and dividing by the system volume (liters).

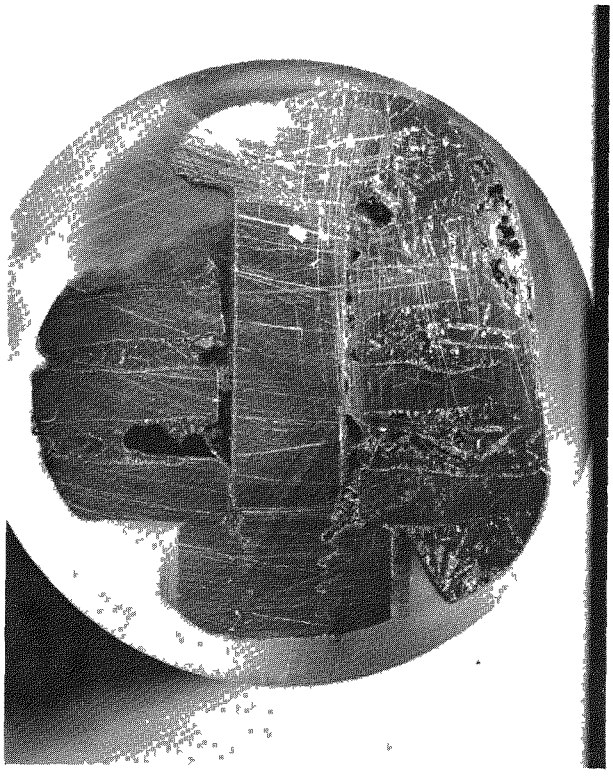

Figure 2-28. Specimen with No Barrier Material

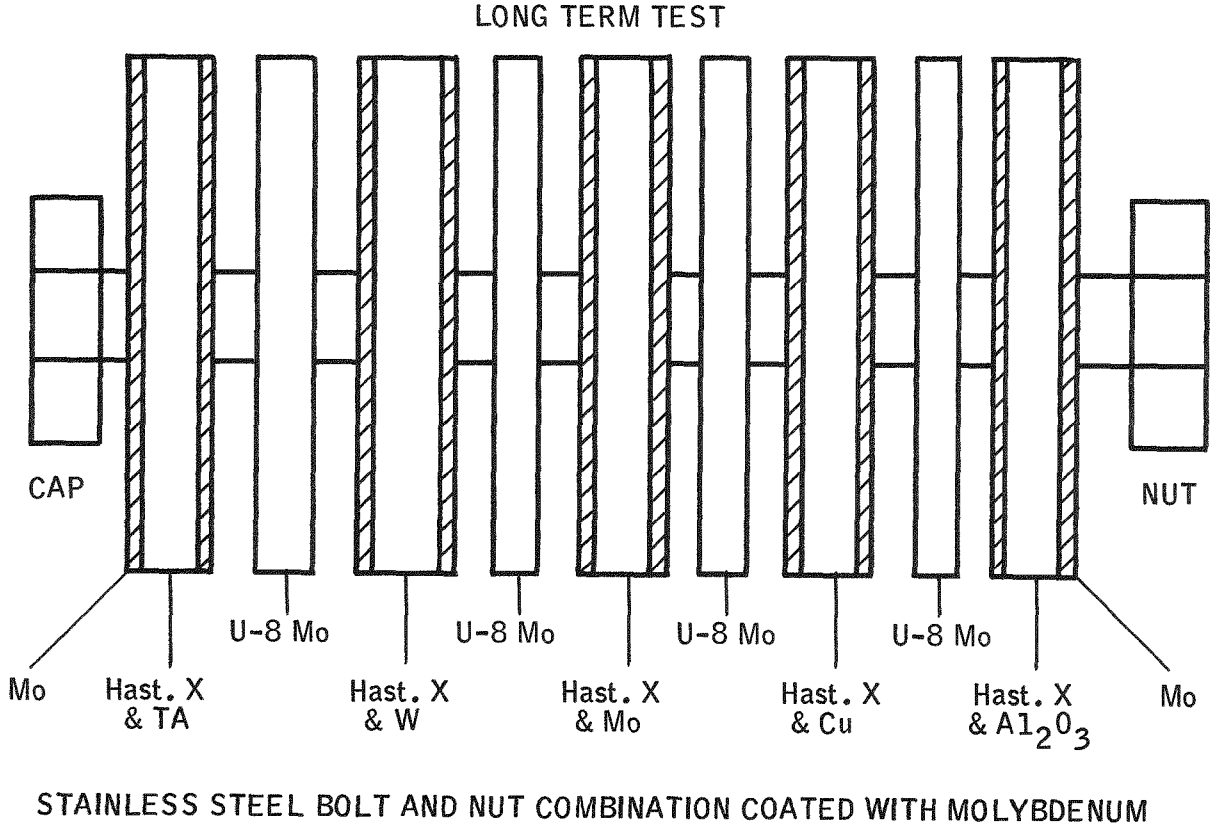

Figure 2-29. Long Term Test Specimen

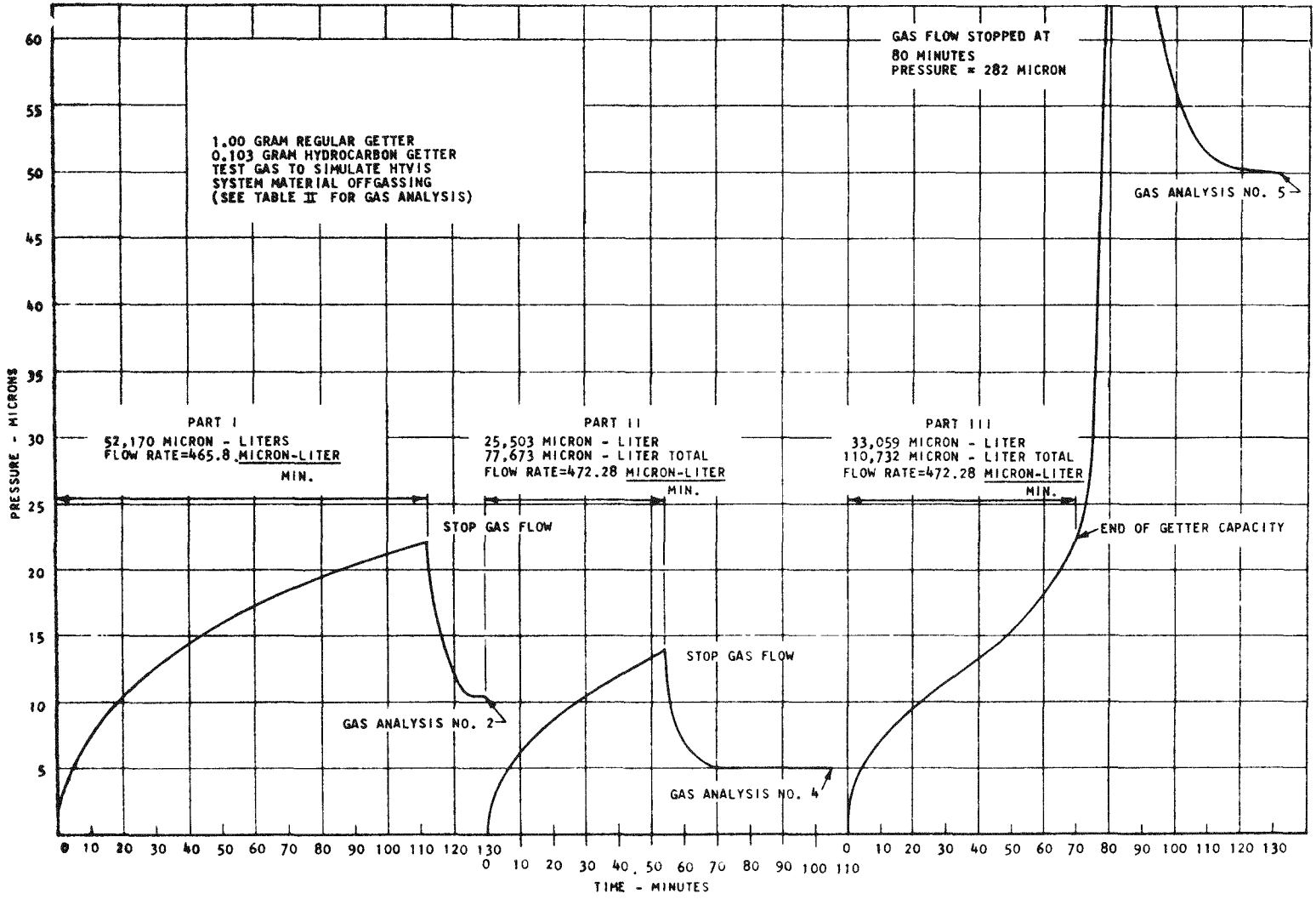

Figure 2-30. Getter Evaluation Test Results – System Pressure vs. Time

Table 4. Mass Spectrometer Analysis, Getter Evaluation Test

Analysis No.	Gas Composition Percent								Remarks	
	Description	H_2	A_r	Co	Co_2	O_2	CH_4 Group	H_2O		
1	Analysis of System Prior to Part I	3.20	------	4.20	------	-----	-----	92.6	9-25-67	1300 hr.
2	After Gettering 52,170 u-1 Test Gas	1.42	84.65	1.53	1.88	-----	6.2	4.32	9-25-67	1630 hr.
3	Analysis of System Prior to Part II	3.34	------	6.17	0.40	0.23	-----	89.86	9-26-67	0900 hr.
4	After Gettering 25,503 u-1 Additional Test Gas	1.84	88.34	0.94	1.54	-----	2.03	5.31	9-26-67	1145 hr.
5	After Gettering 33,059 u-1 Additional Test Gas	1.38	10.64	86.52	0.11	0.26	0.19	0.90	9-26-67	1500 hr.
6	Analysis of Test Gas (No. 4701)	97.07	0.0244	1.36	0.115	0.102	0.328	1.10	9-26-67	1130 hr.
7	Gas Lab Gas Analysis	98.4	0.026	1.20	0.0065	0.22	0.40	-----	----------	

Note: The H_2O percentage shown in this table results from residual H_2O in the line connecting the analyzer to the system as seen in Analysis No. 1 and No. 3.

$$\text{Expected argon pressure} = \frac{52,170 \text{ micron-liters} \times 0.00026}{1.415 \text{ liters}}$$

$$= 9.59 \text{ microns}$$

The actual argon pressure determined by multiplying the total settle-out pressure by the percentage of argon, as determined by the mass-spectrometer analysis (Table 4), is calculated as follows:

$$\text{Actual argon pressure} = 10.5 \text{ micron} \times 0.8465 \times \frac{100*}{95.68}$$

$$= 9.29 \text{ microns}$$

In the test apparatus the hydrocarbon getter was heated in order to maintain a reasonable CH_4 equilibrium pressure. At room temperature the getter pumping speed is sufficient to maintain a 1 micron CH_4 pressure for the CH_4 flow predicted in the actual container. In the getter test, however, the CH_4 flow must be considerably higher in order to complete the getter test in a reasonable length of time. As a consequence, the equilibrium CH_4 pressure will also be higher according to the equation:

$$P = (Q/S)^2$$

where:

P = Equilibrium CH_4 pressure

Q = CH_4 flow rate

S = Getter pumping speed

For example, the test flow was approximately 2,000 times higher than the actual flow. As shown by the preceding equation, the only way to keep the equilibrium pressure at a reasonable level is to obtain a corresponding increase in S. This is accomplished by heating the hydrocarbon getter to 300°C.

---

*This term is used to account for the percentage of H_2O in the test line.

The higher than 10 micron pressure shown on the pressure rise curves (see Figure 2-30) for the test is caused by the high flow rate used in order to conduct the test in a reasonable length of time. The flow rate used in this test for the regular getter (472.8 micron-liters per minute) is approximately 2,000 times greater than is expected in an actual HTVIS unit. The useful getter capacity of 110,732 micron-liters is in good agreement with the design getter capacity of 88,089 micron-liters. The design getter capacity was determined by dividing the total gas expected by the specified grams of getter.

2.3.3.2 Static Proof Test Evaluation

The static proof test was completed with the neck tube buckling at a load within 2 percent of the calculated buckling load. The deflections of the neck tube and the tension rod in the radial direction were 0.019 inch and 0.028 inch, respectively, at failure of the neck tube. The calculated deflections of the neck tube and tension rod were 0.0055 inch and 0.0045 inch, respectively.

The neck tube failed by forming 45° wrinkles, indicating that the mode of failure was shear buckling. The calculated stress in the tension rod at the load when the neck tube failed was 37,200 psi, which is above the proportional limit (30,000-32,000 psi at room temperature) of the tension rod material.

The strain measured in the tension rod indicated that the stress in the tension rod exceeded the proportional limit and that the proportional limit of the material was about 30,000 psi. The strain measured in the tension rod is shown on Figure 2-31.

The stress in the tension rod was expected to exceed the proportional limit of the material for the static proof test because the neck tube and tension rod were tested cold to failure. Since the neck tube is stronger in the cold condition then in the hot condition, the neck tube was designed to fail in the hot condition at the 9g design load of 3,121 pounds. When the neck tube is failed in the cold condition, the calculated load to fail the neck tube is 4,017 pounds.

The deflections of the neck tube and the tension rod in the radial direction were 0.019 inch and 0.028 inch, respectively, at failure of the neck tube. The calculated deflections of the neck tube and tension rod were 0.0055 inch and

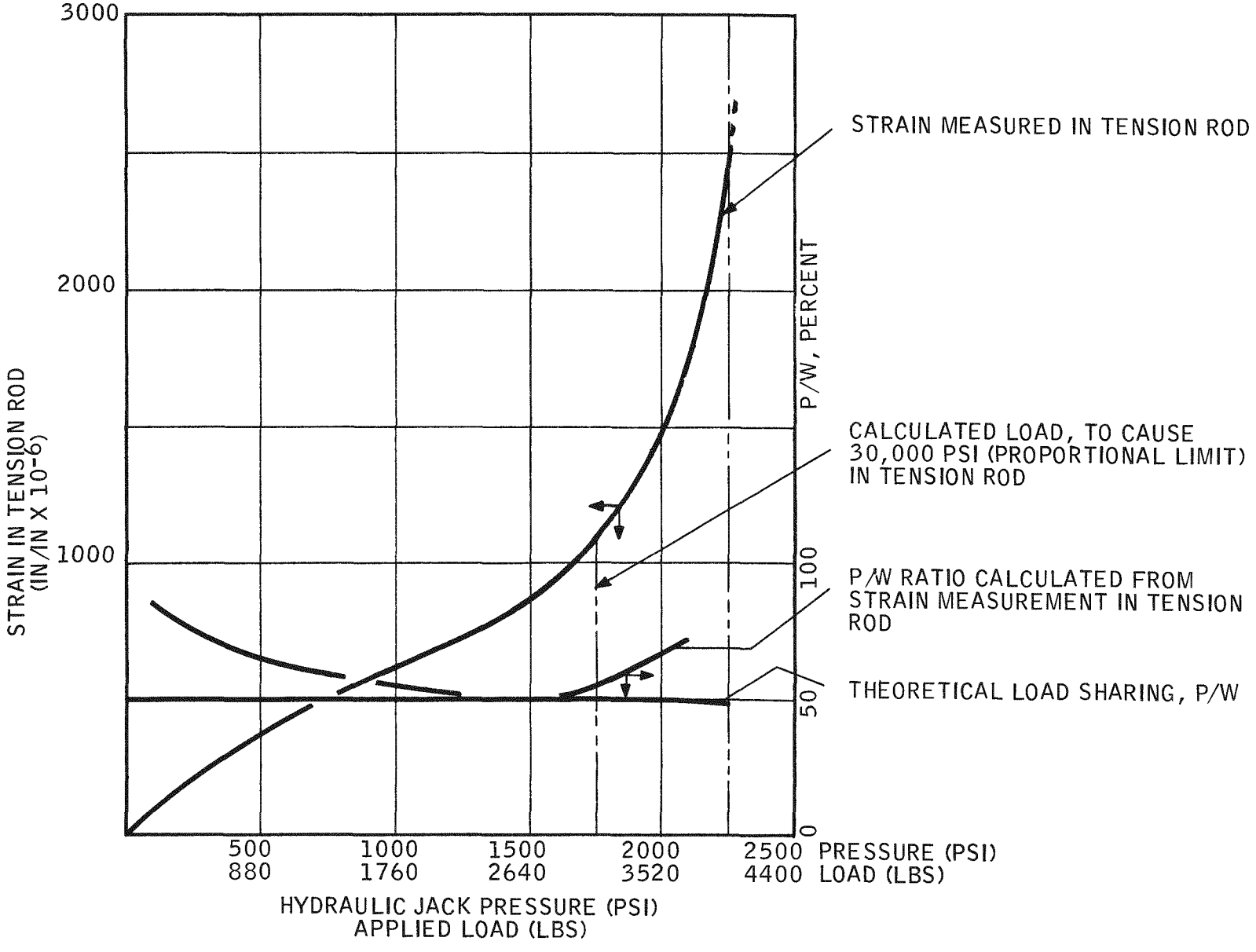

Figure 2-31. Strain vs. Applied Load in Tension Rod (Static Proof Test)

0.0045 inch, respectively. The measured and calculated deflections are shown in Figure 2-32 as a function of the applied load. Figure 2-32 shows that the measured deflections of the neck tube and tension rod varied linearly with the applied load from 0 to 3,700 pounds. In this load range the measured deflections of the neck tube and tension rod were 3.2 and 4.8 times larger than the calculated deflections.

Because the measured deflections of the neck tube and tension rod were larger than the calculated deflections a separate tensile test was made on the tension rod alone to determine the stress-strain relationship for the tension rod. One sample of Inconel 625 solution annealed male rod and one of Inconel 718 age hardened female rod was assembled into a tension rod and subjected to a tensile test. A picture of the tension rod tested is shown on Figure 2-33. The elongation of the tension rod was measured by an extensometer and load vs. strain was recorded on a stress-strain recorder. The load was first applied to 1,600 pounds or 27,350 psi stress, which is somewhat below the 30,000 psi proportional limit, and then the load was released to zero. In this load range the tension rod did not exhibit any permanent deflections. The test was repeated several times with the same results. The load then was increased to 2,895 pounds or 49,490 psi stress, which is above the proportional limit. From this test the actual proportional limit was determined to be at 31,600 psi.

The theoretical and measured load sharing between the tension rod and the neck tube are also shown on Figure 2-31 as a function of the applied load. The measured load sharing (ratio of load in tension rod to applied load) averaged 30.1 percent higher than the theoretical load sharing in the load range from 0 to 1,800 pounds. The measured and theoretical load sharing were in good agreement in the load range from 1,800 pounds to 3,100 pounds. The twelve strain gauges located on the four sides of the neck tube measured tensile and compressive strains. The maximum measured tensile strain on the top side was 120 micro-inch/inch and the maximum measured compressive strain on the bottom side was 400 micro-inch/inch. The calculated tensile and compressive strains on the top and bottom sides were 323 micro-inch/inch and 478 micro-inch/inch, respectively.

Length measurements taken on the male and female tension rods before and after the static proof test indicate that the male rod took a permanent set of 0.003 inch to 0.006 inch and the female rod took a permanent set of 0.004 inch to

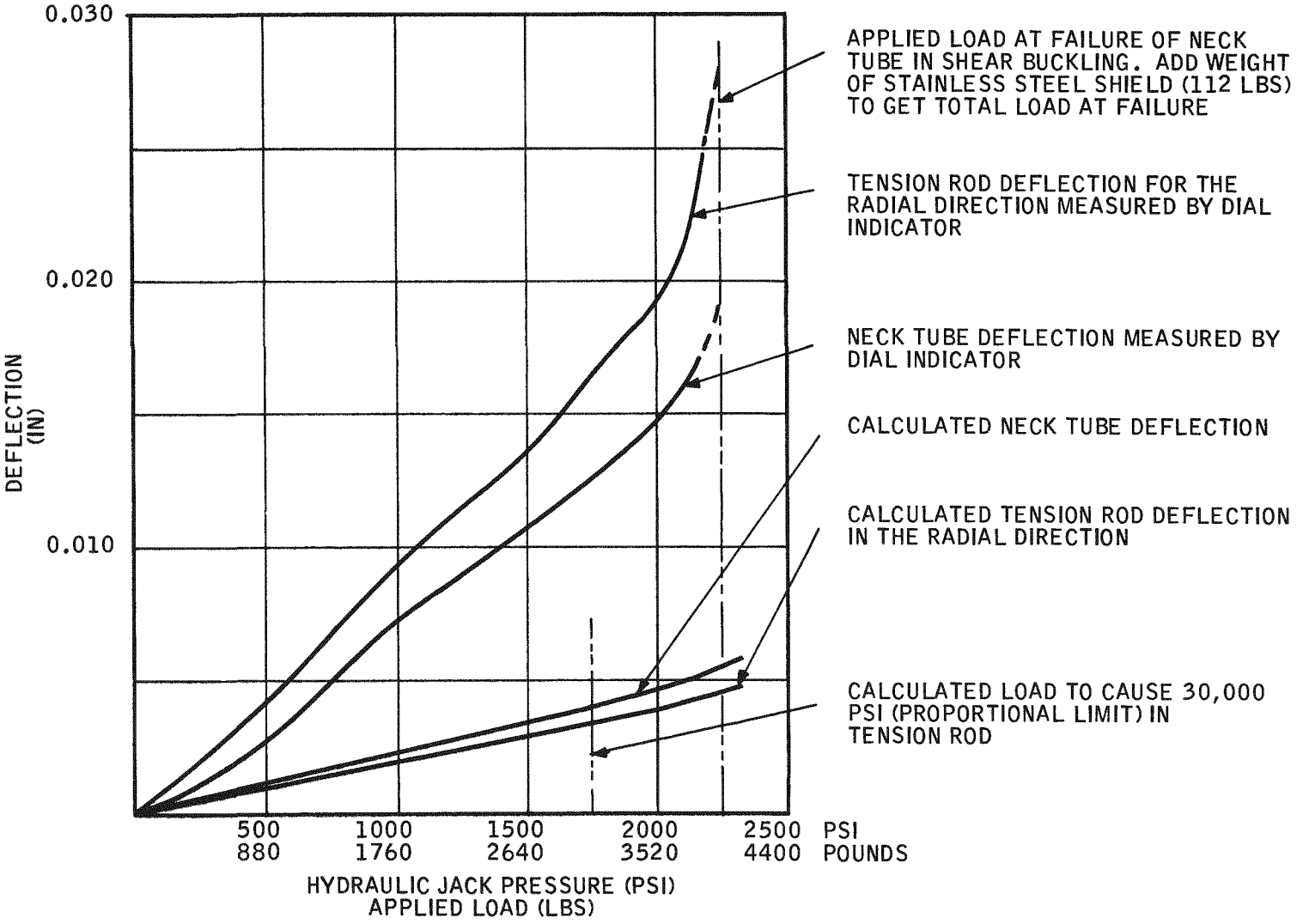

Figure 2-32. Deflection vs. Load for Neck Tube and Tension Rod (Static Proof Test)

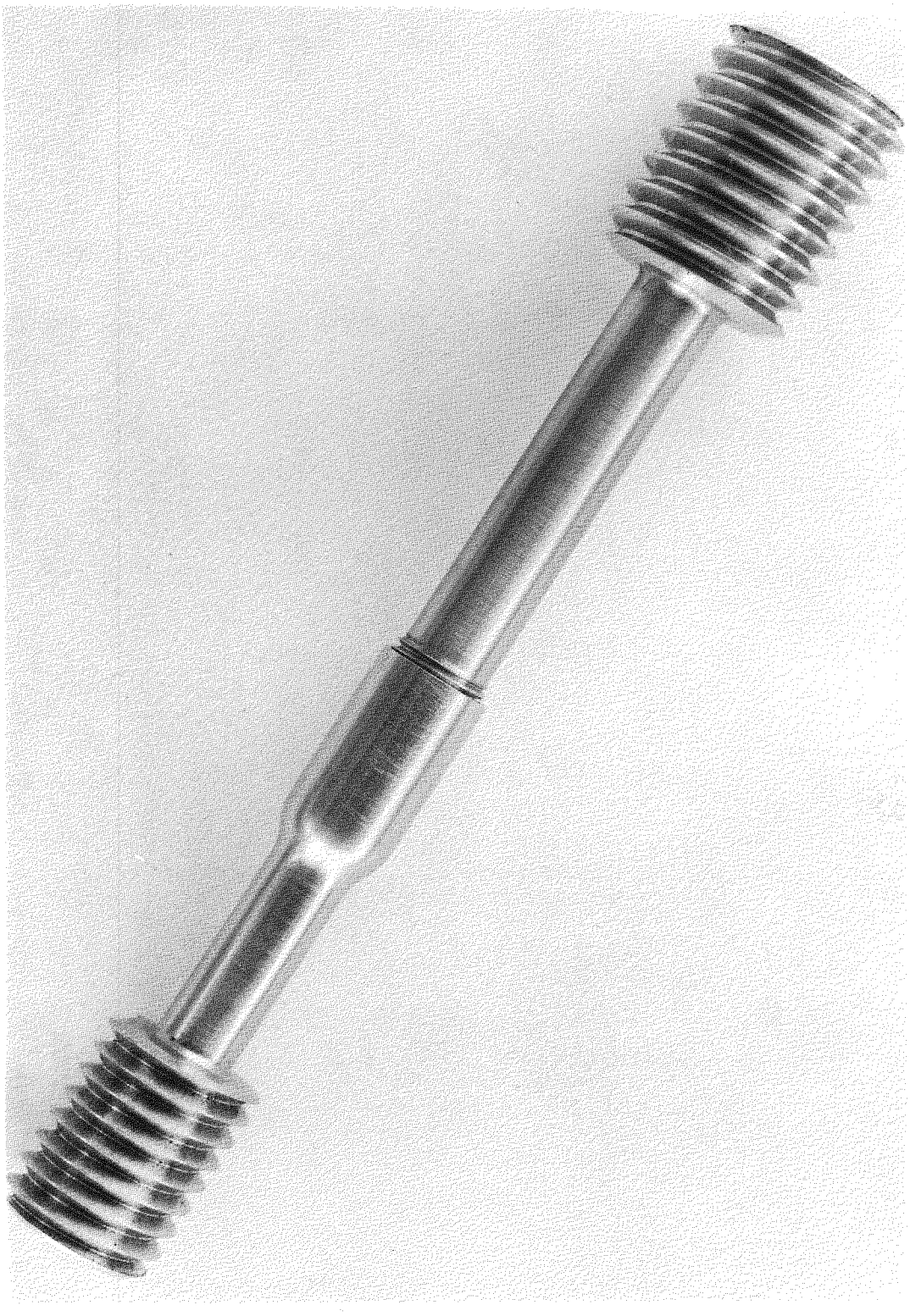

Figure 2-33. Tension Rod Assembly for Load Deflection Test

0.007 inch. The total permanent set for the two rod halves was 0.007 to 0.013 inch. The deflection in the test fixture was 0.001 inch under the maximum load applied, which is negligible.

Results of the static test showed that the mode of failure of the neck tube is shear buckling, as predicted by the analysis of the support system, and that the load to fail the neck tube in shear buckling was predicted accurately using the design information and experimental data available in the literature. The experimental and theoretical load sharing between the tension rod and the neck tube showed good agreement in the load range where the neck tube failed. The deflections of the neck tube and tension rod were 3.2 and 4.8 times larger than the calculated deflections for the neck tube and tension rod, respectively.

The load deflection test performed on the tension rod in the tensile test machine indicated that the rod halves deflected in the static proof test at the tension rod ends were not caused by the two tension rod halves. It is believed that the large deflection measured in the static proof test was caused by movement in the test fixture, specifically in the center plate of simulated spider which connected the tension rod to the shield. Calculations show that if this center plate was only one degree off from the vertical center line, which was entirely possible, the movement of this plate back to the vertical position under the applied load would have permitted the tension rod end to deflect 0.008 inch. The 0.007 to 0.013 inch permanent set measured in the tension rod is believed to be caused by loading the tension rod much above the proportional limit during buckling of the neck tube. The sum of the permanent deflections in the tension rod and the deflection caused by the possible movement of the center plate accounts for the difference between the calculated and measured deflections.

The calculations performed to predict the critical buckling load are presented in Appendix B.

2.3.3.3 Tension Rod Pre-Stressing Investigation

The tension rod pre-stressing investigation was completed. The test set-up containing the tension rod and the accessories are shown in Figure 2-34. The object of this test was to determine the amount of torque required to achieve the

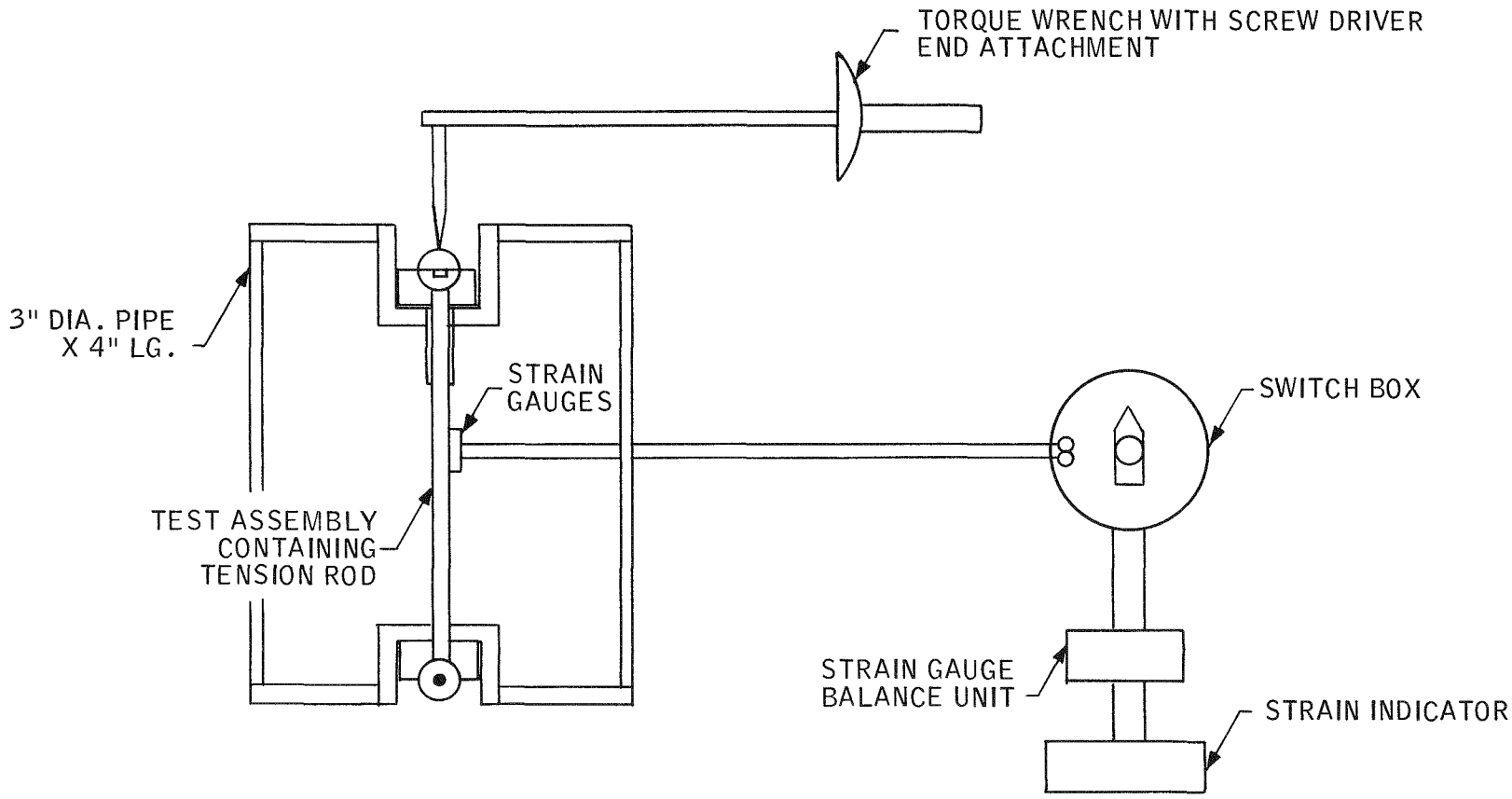

Figure 2-34. Schematic Test Assembly of Tension Rod Prestressing Investigation

desired pre-tension in the tension rod. The male and female tension rod and the spherical washers used in the static proof test were also used for the pre-stressing investigation. The strains measured in the tension rod were converted to load and results obtained at different torque values were plotted (Figure 2-35). The load vs. torque curve was found to be a straight line. Figure 2-35 shows that the torque required to achieve the desired pre-stress in the tension rod was 40 inch-pounds.

Strain gauges were attached to the tension rod receptacles of Unit 10D1 to confirm that the tension tie rods maintain their pre-stress after the unit has undergone heat-up.

2.3.3.4 Shipping Container Dynamic Test

Unit shipping container No. 1 was drop tested during this reporting period to determine if it would meet the contractural specifications, i.e., 4-inch flat drop on sides or ends shall not transmit greater than 6 g to the unit. The results of the drop tests show that the shipping container design is acceptable as the maximum g level recorded for a 4-inch drop was only 4.75 g.

For the shipping container drop tests, a dummy unit was used to simulate an actual unit in terms of weight and configuration. This unit was installed in the shipping container and secured by the container bolted flange. Two accelerometers were used to instrument the unit (Stratham ±20 g, A3-20-350; Statham ±6 g, C-6-350). A quick release drop device was used to insure uniform non-jerking drops. The data recorded during the test is presented on Table 5.

Following the successful demonstration of container No. 1, fabrication was started on the remaining three shipping containers.

2.3.3.5 Dynamic Test of Unit 10D1

After the thermal performance test of insulation system 10D1 was completed, the power was turned off and the unit was allowed to cool. The unit was then shipped to Ogden Technological Laboratory in Deer Park, Long Island, New York, for the dynamic test.

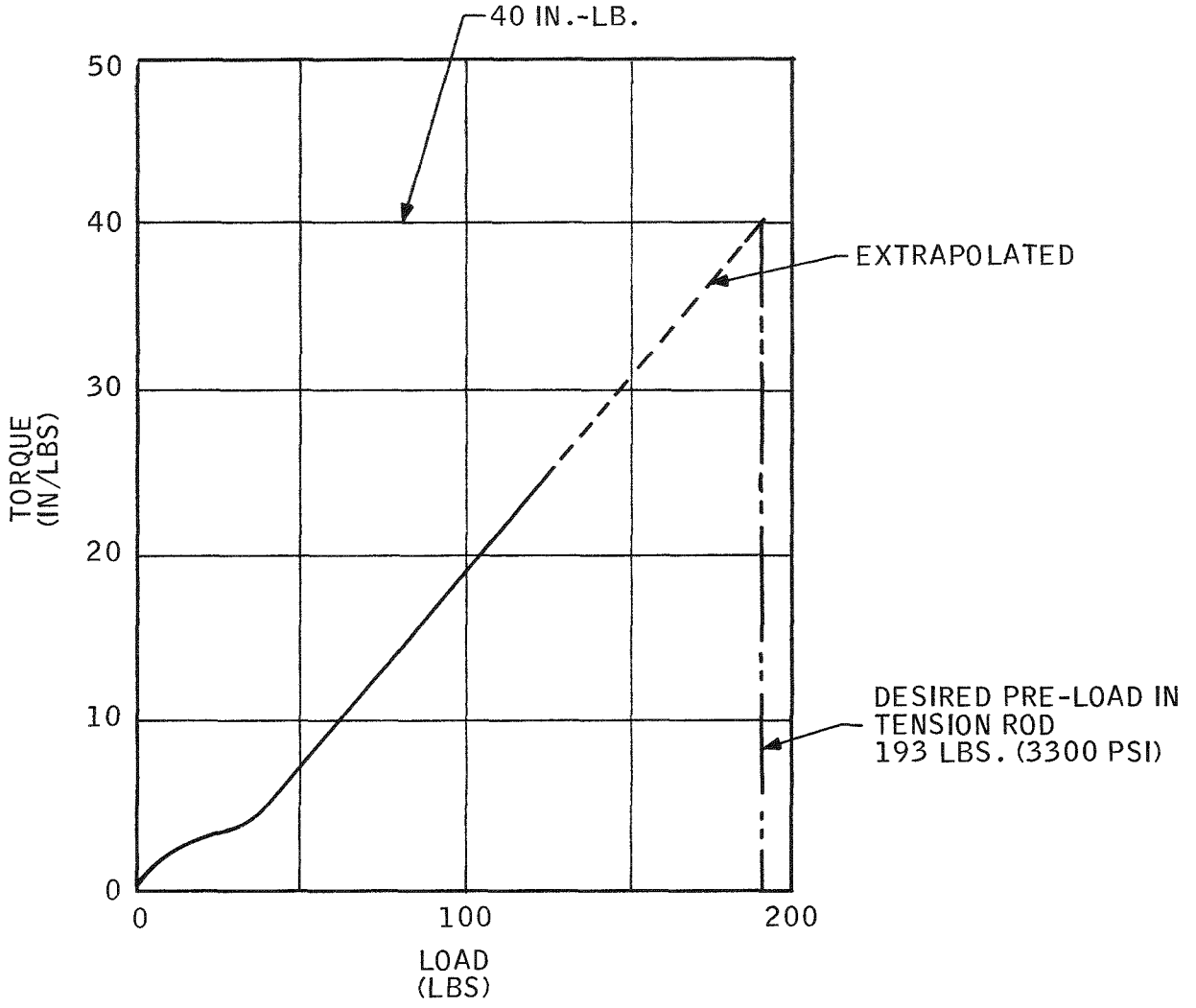

Figure 2-35. Tension Rod Torque vs. Load

Table 5. Shipping Container Drop Test Data

Container No. 1

Drop Direction	Drop Height Inch	Maximum "g" on Unit ±6 g Accelerometer	Maximum "g" on Unit ±20 g Accelerometer	Remarks
Vertical	1	2.0	2.5	Accelerometers
Vertical	2	3.0	3.25	mounted on top
Vertical	3	3.25	4.5	unit hold down
Vertical	3	4.0	4.0	flange. "g"
Vertical	4	4.25	4.5	measured in
Vertical	4	4.75	4.75	vertical direction.
Vertical	4	4.5	4.5	
Vertical	4	4.75	4.75	
Vertical	4	4.75	4.75	
Vertical	5	5.0	4.75	
Vertical	6	5.5	5.25	
Horizontal	4	3.0	4.0	Accelerometer
Horizontal	4	3.5	4.5	mounted on
Horizontal	4	3.25	4.5	cylindrical section
Horizontal	4	4.5	4.5	of shipping con-
Horizontal	4	3.75	4.5	tainer at unit
Horizontal	6	5.5	5.0	c.g.
Edge drop on side	2	2.0	3.25	
Edge drop on side	8	3.0	4.0	
Edge drop on base	8	2.75	2.0	

a) Vibration

The technical specification requires that the unpackaged system be designed to withstand the vibration level experienced during common carrier transportation as specified by MIL-STD-810A method 514-1, dated 23 June 1964, except that the maximum g level shall not exceed 3.

The insulation system was installed in the vibration test machine in accordance with section 3. 2. 2 of MIL-STD-810A specifications and attached by means of a rigid fixture capable of transmitting the vibration conditions specified herein. The test load will be distributed uniformly on the vibration exciter table to minimize effects of unbalanced loads.

The unit was vibration tested at the operating temperature of 1285°F at the bottom of the neck tube. The heat was supplied using four 250-watt heaters imbedded in a heater block. The vibration test schedule is as follows:

Cycling Sinusoidal

5-8 cps	0. 4-inch double amplitude
8-26 cps	1. 3 g peak
26-40. 5 cps	0. 036 inch double amplitude
40. 5-50 cps	3 g peak

5-50 cps cycled logarithmically from minimum to maximum in 7-1/2 minutes, 50-5 cps cycled logarithmically from maximum to minimum in 7-1/2 minutes, 15 minutes total per sweep. Total time each axis: 45 minutes (3 tests).

The internal pressure was monitored in the insulation system during the test and it was found that the pressure after the test was the same as the pressure before the test. The leak check which was performed after the test indicated no leak.

b) Shock

The technical specification for the shock test requires that the unpackaged system be designed to withstand the shock levels defined in MIL-STD-810A, Method 516-1, Procedure 1, except that the peak value shall be 6 g's and the nominal duration shall be 6 milliseconds. At the conclusion of the specified vibration tests, dynamic shock tests were performed. These tests were performed with the unit at operating temperature.

Three shocks in each direction were applied along the three mutually perpendicular areas of the unit. The shock pulse shape was saw-tooth in accordance with MIL-STD-810A. The internal pressure was monitored throughout the test and no increase in pressure was noted. A leak check after these tests showed no leaks.

Details of both the shock and vibration test will be reported after the data has been analyzed.

2.3.4 SEGMENTED RETAINING RING

A dynamic test of the redesigned segmented retaining ring was conducted during this report period. The objective of the test was to determine if the redesigned ring is capable of restraining the insulation system within the pressure vessel when the pressure vessel is subjected to the increased dynamic environment of 6 g's shock and 3 g vibration at frequencies up to 50 Hz.

The test was conducted by Environ Laboratories, Inc., on 6 October. A copy of the Environ Test Report is included in this report as Appendix C.

Post-test examination of the test components revealed no damage or anomalies.

Accelerometers on all three components (pressure vessel, insulation system envelope and biological shield) followed each other closely during both vibration and shock testing, indicating that there are no serious amplifications.

One exception to this was the accelerometer mounted on the bottom of the insulation system envelope. This accelerometer recorded some high frequency amplification when compared with the pressure vessel and shield accelerometers. It is felt this anomaly was due to a fault in the accelerometer calibration or the recording equipment. The analysis effort that led to this opinion is presented in the following paragraphs.

a) Component Description

The components used to test the redesigned segmented retaining ring consisted of the redesigned ring, a titanium pressure vessel (residual from Phase I), and a dummy insulation system consisting of outer envelope, simulated biological shield and shield support system. The shield support system consisted of a neck tube and three tension tie rods that closely simulated the actual system from a structural stiffness standpoint. This was done so that any dynamic amplification or attenuation that might be caused by the natural frequency of the actual insulation system would be simulated.

A schematic of the system tested is shown in Figure 2-36. This schematic shows accelerometer locations, axis identification and major component identification. Further explanation of accelerometer locations can be found in Appendix C. A summary of the accelerometer locations, axis orientation and accelerometers monitored during each test axis is shown in Table 6.

All accelerometers were bonded to the various components identified with their location. Those accelerometers mounted inside the insulation system were not moved during the testing; however, the accelerometer mounted on the exterior of the pressure vessel (LE61) was moved to record the axis being tested.

The test assembly shown in Figure 2-36 was mounted in a test fixture which consisted of top and bottom plates designed to mate with the contour of the pressure vessel and held together with tension tie rods. Consequently, the pressure vessel was in axial compression when installed in the test fixture. Several photographs of the test assembly in the test fixture during shock and vibration testing are shown in Figure 2-37.

b) Test Method

Three individual shocks were applied in each direction of the three mutually perpendicular axes (18 shocks). Input to the test assembly was monitored by an accelerometer mounted on the test fixture

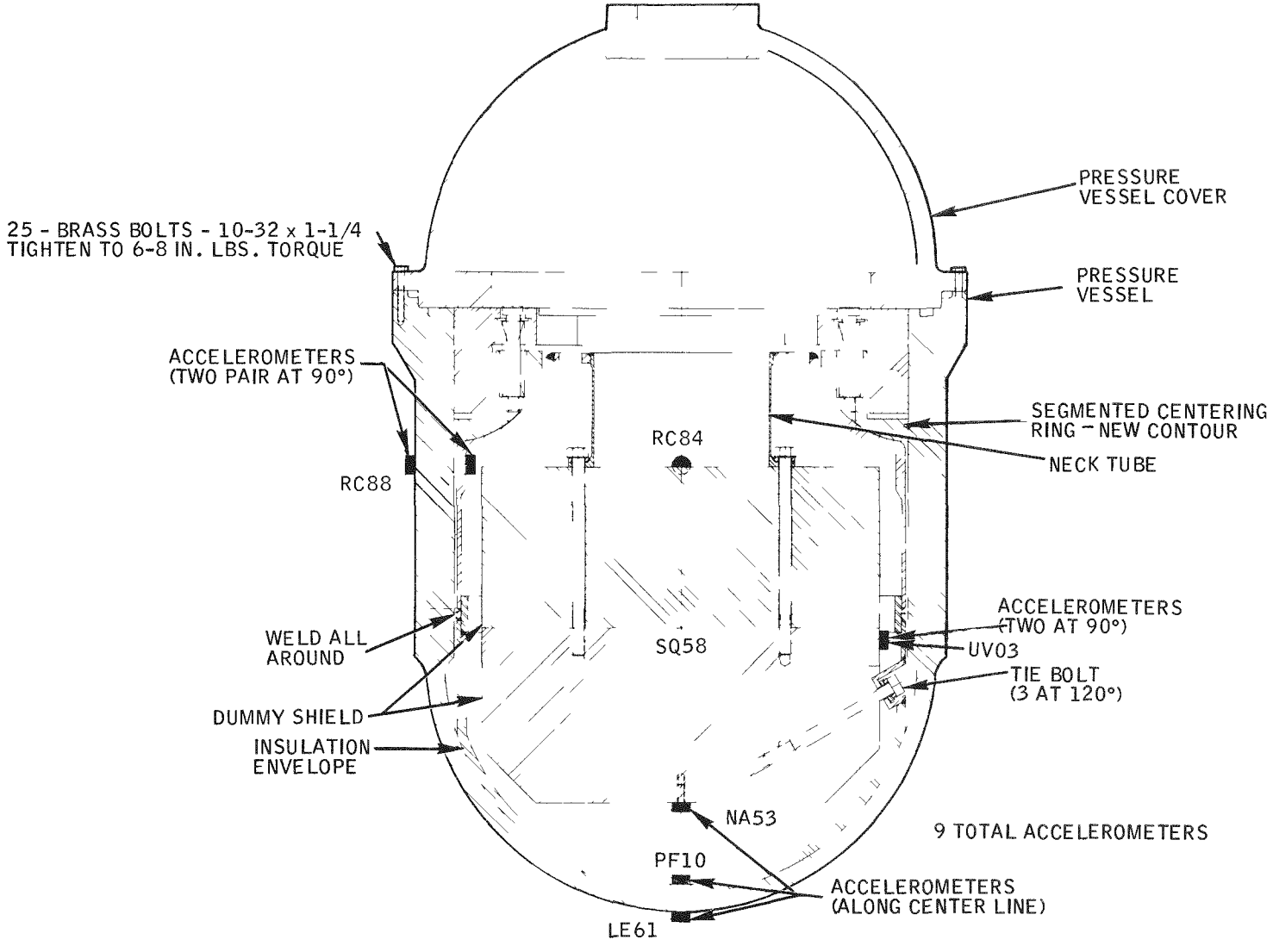

Figure 2-36. Schematic of Segmented Retaining Ring Dynamic Test Components

Table 6. Summary of Accelerometer Locations and Those Monitored During Shock Testing

Test Axis	Monitored Accelerom-eters	Accelerom-eter Axis Orientation	Accelerometer Location
Z and Z'	LE61	Z - Z'	Bottom external surface of pressure vessel.
	NA53	Z - Z'	Bottom of "dummy" biological shield.
	PF10	Z - Z'	Inside of insulation envelope on flat raised deck at bottom.
	UV03	X - X'	Outside surface of "dummy" shield at mid-height.
	SQ58	Y - Y'	Outside surface of "dummy" shield at mid-height.
Y and Y'	LE61	Y - Y'	Outer surface of pressure vessel at mid-height.
	RC84	Y - Y'	Outside surface of insulation envelope at mid-height.
	PF10	Z - Z'	Same as Z and Z' tests.
	UV03	X - X'	Same as Z and Z' tests.
	SQ58	Y - Y'	Same as Z and Z' tests.
X and X'	LE61	X - X'	Outside surface of pressure vessel at mid-height.
	RC88	X - X'	Inner surface of insulation envelope near top.
	PF10	Z - Z'	Same as Z and Z' tests.
	UV03	X - X'	Same as Z and Z' tests.
	SQ58	Y - Y'	Same as Z and Z' tests.

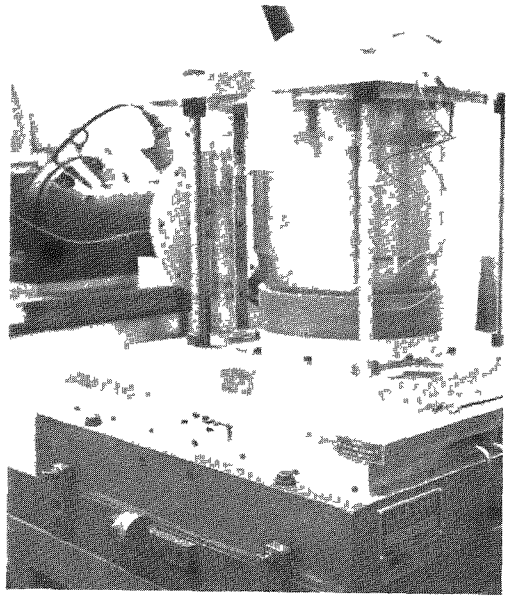

Vibration in "X" Axis

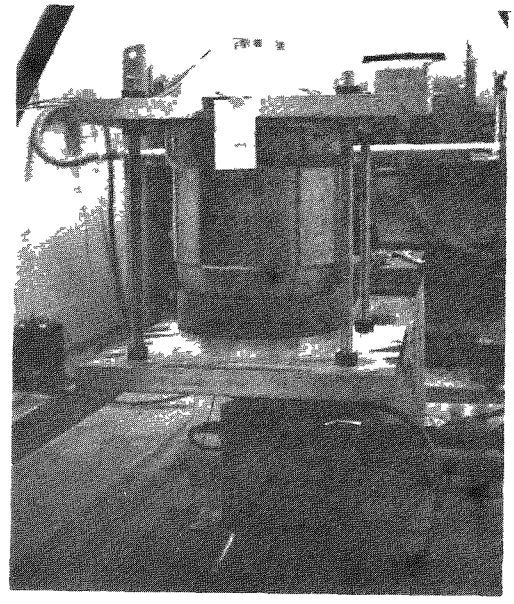

Vibration in "Z" Axis

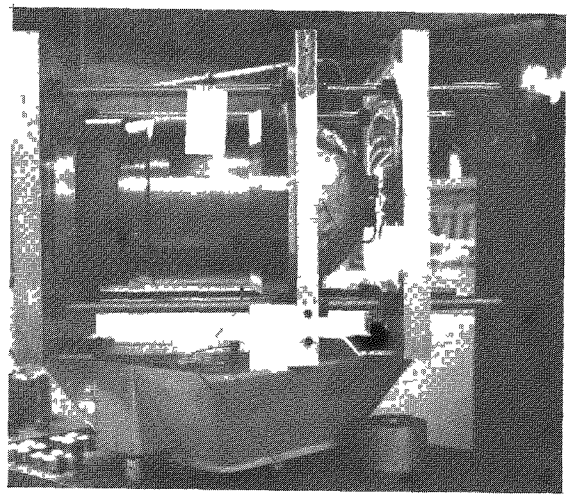

Shock in "Y" Axis

Figure 2-37. Photographs of Segmented Retaining Ring Dynamic Test Assembly in Test Fixture

(referred to as "Control"). Each shock impulse had an amplitude of 6 g's and a duration of 6 milliseconds. Refer to Appendix C for a complete description of the test.

c) Test Results

Table 6 describes the location and orientation of the various response monitoring accelerometers. Table 7 shows the values of input and response for each series of shock tests. Each value presented is the average of three separate shocks for a given direction. The shock values were measured from recorded traces in the case of the responses, and from oscilloscope trace photographs for the control accelerometer. Each initial shock impulse was of 0.006-second duration. During one of the Z-direction drops the maximum recorded response was 16 g, showing an amplification factor of nearly 3. This one instance was the highest recorded value and was the response generated by the accelerometer located at the bottom of the insulation envelope, PF10. There was close agreement between all of the accelerometers in a given test axis with the exception of accelerometer PF10.

Past test examination of the test components revealed no damage or abnormalities.

d) Discussion of Results

The only unusual occurrence noted during the test was the high frequency amplification indicated by accelerometer PF10 during the Z and Z' axis shocks. This accelerometer also indicated high frequency accelerations in excess of the input levels when the system was subjected to shocks in an axis transverse to its recording axis (see Table 7) and indicated accelerations in excess of 1 g during the free fall period in the shock test machine.

The unusual data from this accelerometer was investigated in an attempt to either explain the cause of the amplification or to determine if the data was erroneous. The findings of this investigation are presented in the following paragraphs.

Table 7. Summary of Maximum Accelerometer Response in G's During Shock Test

Accelerometer Identification	Test Axis					
	* Z	* Z'	* Y	* Y'	* X	* X'
Control	5.7	5.5				
LE61	4.9	6.4				
NA53	4.1	4.8				
PF10	12.5	12.6				
UV03	---	---				
SQ58	---	---				
Control			6.0	6.2		
LE61			5.1	4.8		
RC84			7.1	7.1		
PF10			7.2	7.4		
UV03			1.6	1.8		
SQ58			5.7	5.0		
Control					6.0	6.1
LE61					5.2	5.1
RC88					6.2	6.7
PF10					8.2	6.4
UV03					4.8	5.0
SQ58					---	---

*Direction of drop (see Figure 2-36).

1) The insulation system envelope used for this test had been used previously for getter seal-off tests and consequently it was necessary to modify the bottom end to provide a mounting surface for accelerometer PF10. The mounting arrangement for PF10 is shown in Figure 2-38.

Despite the small diameter and relatively large thickness of the disk, a certain amount of diaphragm action can take place, thereby permitting amplification. To check the stiffness of the accelerometer-disk assembly the natural frequency of the combination was calculated and found to be approximately 4800 Hz. This indicates that the diaphragm stiffness does not even remotely approach an infinite value, as would be the case for a "very stiff" component. It would therefore seem possible that the accelerometer mounting plate could be vibrating as a diaphragm due to the shock impulse in the Z or Z' axis.

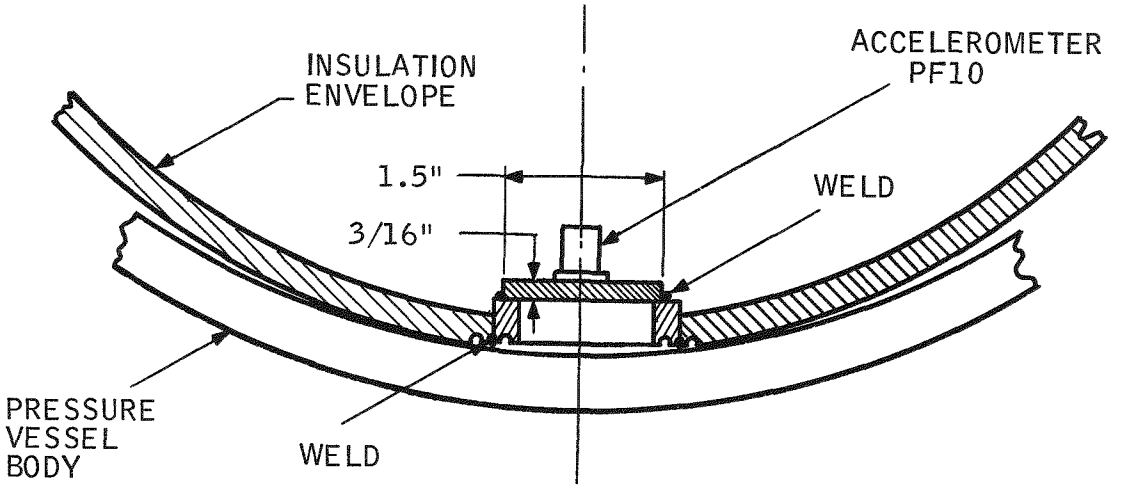

Figure 2-38. Accelerometer PF10 Mounting Schematic

It is, however, more difficult to explain the amplification exhibited by accelerometer PF10 (still located in the Z-Z' axis) when the shocks were applied to the Y, Y', X, and X' directions. Normally, accelerometers will pick up only a very small component of acceleration applied in their transverse directions. The particular unit involved (PF10) was checked on a vibration machine for transverse pick-up and was found to record approximately 20 percent of the applied signal. This would indicate that, for example, using data from the X-axis shock test, an acceleration of 5 x 8.2 = 41 g's existed in the Z-direction at the location of unit PF10. It is inconceivable that this condition could exist with an X-direction input of only 6.0 g's when it is realized that to experience acceleration in the Z-Z' axis (other than vibration of the mounting plate) there must be movement in that axis. Since the applied shock was in an axis transverse to the Z-Z' axis, the movement in the Z-Z' axis can only occur if the bottom of the insulation envelope slides along the spherical inner surface of the pressure vessel forcing the insulation system toward the retaining ring. The ring assembly springs resist this motion with a force of approximately 2200 pounds. In addition, there is the fact that with the 2200 pound force existing at the contact surface, a very considerable static-friction force must be overcome before the X-direction motion could occur. Both of these factors would tend to damp the motion rather than amplify it. In fact, had motion actually been present, the resulting recorded traces for both unit PF10 and unit UV03 would be expected to look very erratic. Actually, they are very similar to any of the traces recorded during the Z-Z' axis shocks, when this same type of motion could not occur.

2) Another possibility investigated was whether relative motion of the insulation system envelope with respect to the pressure vessel could occur during the Z-Z' axis shocks. This could occur only if the ring-assembly springs could be compressed, thus permitting axial movement of the insulation system envelope and an acceleration to be recorded. The insulation system assembly (as used in the test) weighed 329 pounds. With a 6 g input, the force exerted would be 6 x 329 = 1974 pounds. Since the opposing spring force is 2200

pounds, it does not appear that the motion could take place. For a shock in the opposite direction, with the insulation envelope pressed against the base of the pressure vessel by the spring force when impact occurred, the resulting inertia force would be in the same direction. This precludes the possibility of motion taking place during the initial input pulse. It is possible that compression in the material itself (of both the pressure vessel and the insulation envelope) could take place to cause a rebound which might be picked up by the accelerometer. It would then be expected that the recorded maximum trace for unit PF10 would occur at a displacement in time from the maximum recorded at the bottom of the pressure vessel. Careful examination of the recorded traces of these two accelerometers failed to reveal any lag.

3) Another possible explanation has to do with the fact that the insulation system envelope is bell-shaped and will "ring" when struck. This type of ringing involves many frequencies (harmonics of the fundamental) and, if one of those frequencies approximates the natural frequency of the accelerometer-mounting-disk assembly, an amplified acceleration could be recorded as a purely local condition. Furthermore, this phenomenon is not completely dependent upon the direction of impact.

4) None of the explanations offered in sections (1), (2), and (3) above account for the following observed anomally in the PF10 accelerometer data. For drops in both the Z and Z' directions, at the initiation of motion, a small acceleration (approximately 1 g) was recorded on all accelerometers in the Z and Z' axis. The approximate shape of the traces together with the pertinent time periods is shown in the sketch below.

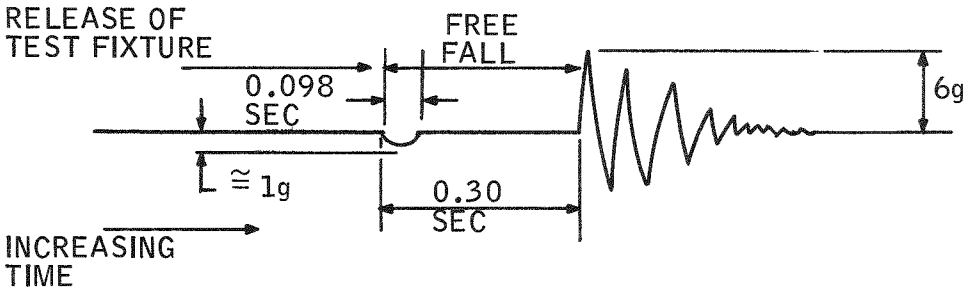

NOTE: The 1 g acceleration does not remain constant during the fall of the test fixture because it is part of a hydraulic system and is pumping fluid through the system during the fall. The system thus reaches a constant velocity and acceleration falls to zero.

Accelerometers LE61 and NA53 both recorded a level somewhat less than 1 g, while PF10 indicated a g-level greater than twice this amount. Under such a low g-level it is inconceivable that the insulation system would loose contact with the bottom of the pressure vessel, which is the only way this accelerometer could read different than the other two in the same axis. Remembering that the retaining ring springs exert a force of 2200 pounds at the contact surface, it can be seen that the required acceleration level would be roughly 6.7 g for the 329 pound insulation system. There is no discernable time lag between the initial motion-dip traces for each of the three accelerometers referred to above, such as would have to be present if the disk mounted unit were acting as a diaphragm and producing a local effect. Even if this were the case, the amplification would not be explained. The "ringing" theory also breaks down for this situation since no impact has yet occurred.

e) Conclusions

It must be concluded that some fault existed in either the calibration or the recording equipment used to minitor the accelerometer PF10.

Although there is not sufficient data available to quantatively explain the unusual data from accelerometer PF10, the close correlation between all the other accelerometers and the fact that there was no damage to any components provides a high degree of confidence that the redesign of the segmented retaining ring is adequate to withstand a 6 g shock load.

2.3.5 PRESSURE VESSEL

No effort was expended on the pressure vessel during the period covered by this report.

2.3.6 THERMOELECTRIC GENERATOR

2.3.6.1 Leg and Couple Testing

a) Background

Two 6-couple bell jar tests were conducted using SNAP-21 couples taken from the same lots and batches used in the Phase II Task I prototype generators. The couples tested were from Lot 24, Batches 4, 8 and 10.

The objectives of these tests were to:

1) Determine the feasibility of ingradient testing as a Q. C. check on manufactured leg materials;

2) Correlate the ingradient performance results with the total couple resistance (measured at room temperature by Q. C.), for the same legs;

3) Determine the performance characteristics of SNAP-21 Phase II Task I geometry legs.

b) Description of Bell Jar Tests

Both tests consisted of six couples electrically connected in series in a parallel plate configuration. All legs were instrumented with iron-constantan thermocouples at both hot and cold junctions. The cold frame was also instrumented.

The thermopile was packed with powdered Min-K 1301 and backfilled to 2 psig with argon to simulate SNAP-21 environmental conditions.

c) Test Procedures

Prior to testing, the test fixtures were processed using a modified version of the SNAP-21 Phase II generator processing procedure.

After processing, the bell jar fixtures were heated to the temperature conditions as described in Table 8.

Table 8. Temperature Conditions for Ingradient Tests

Test Number	T_h-°F (Hot Electrode)	T_{cf}-°F (Cold Frame)
1	1100°F	80°F
1	1000°F	80°F
1	900°F	80°F
2	1100°F	80°F

At each of the four temperature conditions listed, the output performance and cold electrode temperatures were determined for both individual legs and couples.

Excessive cold electrode temperatures (above 140°F) were noted for several of the operating legs in the two tests. It was noted during disassembly that powdered Min-K 1301 was trapped between the follower-cold cap interface for those particular legs. This is the suspected cause for the high cold electrode temperatures. Because of the large variations in cold electrode temperatures from leg to leg, it was necessary to normalize all of the data to a common temperature condition (cold electrode temperature – 120°F, hot electrode temperature 1100°F). The average power output per couple is summarized in Table 9.

Projecting the results in Table 9 to a 48-couple generator system, we have the results listed in Table 10.

Table 9. Average Power Output Per Couple (Normalized to 1100°F H. E., and 120°F C. E.)

Test Number	Seebeck's Voltage (Millivolts)	Resistance (Milliohms)	Power (Milliwatts)
1	225	36. 4	348
2	228	38. 3	338

Table 10. Expected Performance Output for a SNAP-21 Generator

Test Number	Resistance (Ohms)	Seebeck Voltage (Volts)	Power (Watts)
1	1. 75	10. 8	16. 7
2	1. 84	10. 9	16. 2

An attempt was made to correlate the ingradient couple performance results with the total couple resistance measured at room temperature. At this time no significant corrclation has as yet been established between the room temperature resistance measurements and the ingradient performance results.

d) Discussion of Results

It is interesting to note that the normalized (1100°, 120°F) generator data from A10D1, A10D2, and A10D4 agrees well with the ingradient data listed in Table 10. Normalized data for the generators after 200 hours of operation is as follows:

- A10D1 – 15. 7 watts
- A10D2 – 16. 6 watts
- A10D4 – 17. 3 watts

Ingradient testing of the type described in this report is an excellent tool for determining the performance characteristics of a particular couple geometry and for determining the output performance of a generator using the same couple geometry. However, these tests are too slow and cumbersome to be used as a Q. C. check on manufactured leg materials. Hot and cold electrode instrumentation for tests of this type are very extensive requiring patience and time to assemble properly. It is doubtful that the couple resistance measurements at room temperature can be used as a Q. C. check on the thermoelectric leg materials. However, this check can be used to verify the mechanical integrity (check for cracks, poor bonds, etc.) of manufactured couples.

2. 3. 6. 2 Generator Development Testing

a) Ball and Socket Generators

The initial four ball and socket generators have completed all short-term and dynamic testing with the exception of A10D3. This generator was dismantled because of a pressure transducer failure during dynamic testing.

Thermoelectric Generators A10D1, A10D2 and A10D4 are fabricated with Conax fittings for the instrumentation and power output readouts from the system. Early in the test sequence there was a gradual loss of gas pressure in the generators. Each generator was examined to determine the cause of this pressure loss. The examination showed that the Conax fittings were loosening affecting the hermetic seal. This loosening is probably due to the "plastic flow" of the inner Viton seal.

In view of the leaking Conax fittings on Generators A10D2 and A10D4, and possibly A10D1 which is destined for system integration, a positive and well documented system of eliminating the leaks by intermittently torquing the Conax fittings has been followed. Beginning on November 1, 1967, the following schedule has been followed on A10D2 and A10D4:

1) Torque each respective generator to the original level of tightness.

2) Record all temperatures on the two instrumented couples.

3) Record transducer exitation and millivolt output, translating millivolt output to pressure.

4) After 24 hours again monitor and record all instrumented couple temperatures and all mv readouts of pressure transducer.

5) Repeat Step 4.

6) Repeat Step 5.

7) If no change in pressure has occurred after the three day effort, the sequence is complete.

8) If a change in pressure has occurred, return to Step 1, increasing torque by 3 inch-pounds. Retighten Conax fittings.

9) Repeat Steps 2 through 6.

10) If necessary, repeat the process. Do not exceed 70 inch-pounds of maximum torque.

Generator A10D1 will require a special effort as the unit is not operating at design temperatures. Figures 2-39, 2-40 and 2-40 define leak rate and re-torquing effect on the Conax fittings with time.

Figures 2-39 through 2-41 indicate a partial or slowing trend in the leak rate; however, in a long-term test program the use of Conax fittings appears to have several problems.

Generator A10D4 was integrated with Insulation System S10D1A for early fueling and test operations at Oak Ridge National Laboratories, and is currently on test at that facility.

A test plan defining generator efficiency has been released (ref. to Report No. MMM 3691-9004). The actual test work will commence early in the next report period.

A topical report containing the evaluation of the initial four ball and socket generators is being prepared.

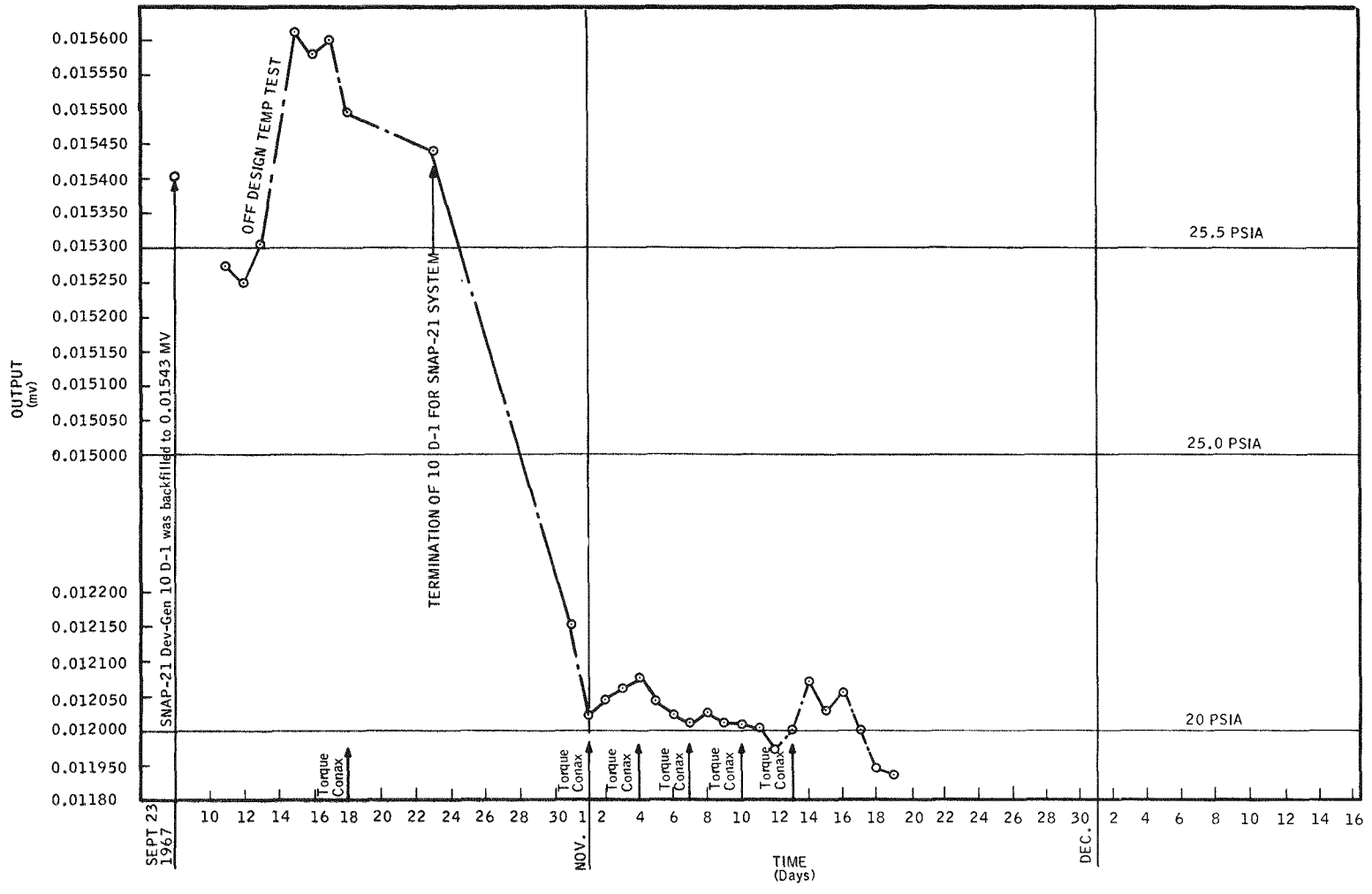

Figure 2-39. Generator A10D1: Effect of Tightening Conax Fittings

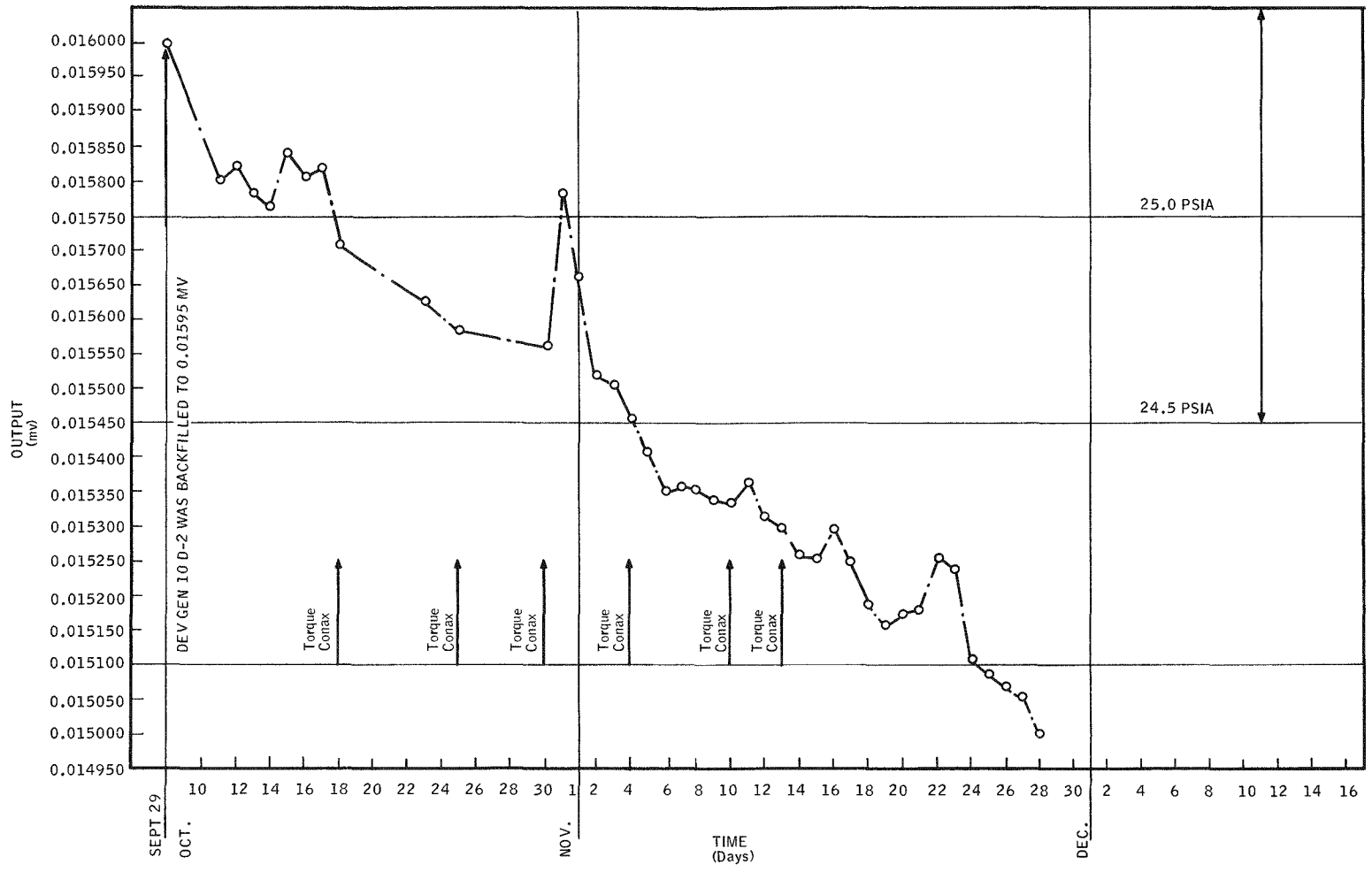

Figure 2-40. Generator A10D2: Effect of Tightening Conax Fittings

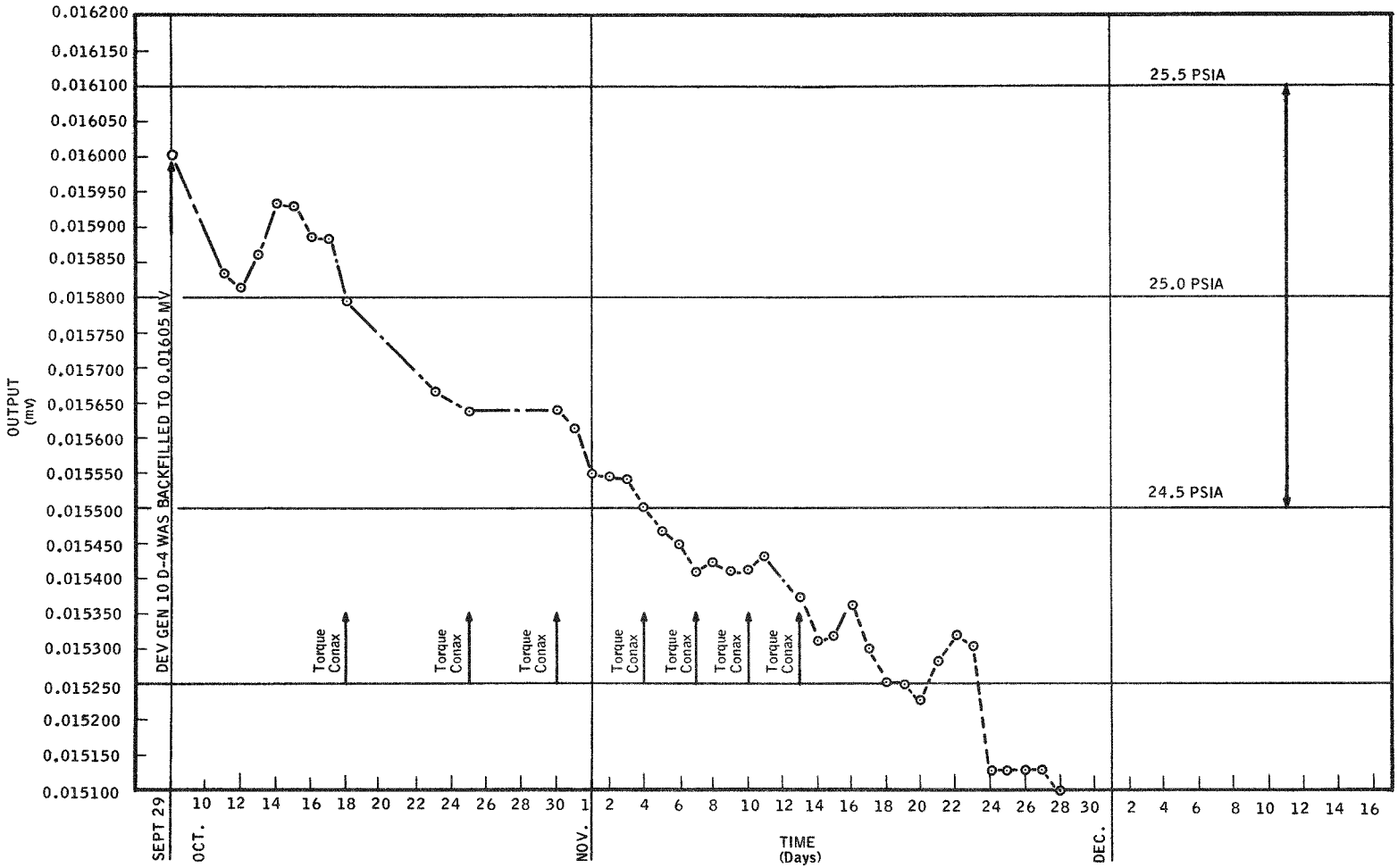

Figure 2-41. Generator A10D4: Effect of Tightening Conax Fittings

b) In-Line Generators

Two in-line generators, A10D5 and A10D6, have been on test. A10D5 has been stabilized and voltage-current performance mapping and specification level dynamic testing (see Appendix C) has been completed. The unit is currently on long-term test. Plots of the performance mapping are shown in Figures 2-41a through 2-41d.

Post vibration test data analysis of A10D5 showed a 5 percent increase in the thermopile resistance of from 1.84 to 1.94 ohms. After a stabilization period of 24 hours and before shock testing, the thermopile resistance was 1.89 ohms. After shock testing the resistance measured 1.87 ohms. A complete set of data was recorded on January 8, 1968. The thermopile resistance had increased to 1.93 ohms. A complete performance report will be forthcoming early in the next report period.

Generator A10D6 is scheduled for specification level dynamic testing early in the next report period. Both Generators A10D5 and A10D6 will be watched closely for the effects of dynamic testing on the thermopile resistance.

2.3.6.3 Generator Processing

Generator A10D5 began processing November 13, 1967. The processing was completed and the pinch-off made on November 15, 1967. The processing of this generator was a 26-hour procedure with an additional 24-hour hold and evaluation period. This process was shorter than that of the previous generators because Microquartz was used as the insulating material rather than Min-K 1301.

After Generator A10D5 was turned over to the test group, the anti-collapse restraining ring had to be removed. This ring is used only in the processing of the generator to protect and support the thin wall section of the generator long case (0.005-0.006 thick) while under hard vacuum. To remove the ring instrumentation wires had to be cut from the outer case because of insufficient slack in them. In the process of rewelding (T.I.G.) these wires back to the case, a pin hole was inadvertently burned through the generator case at the junction to the hot frame causing the generator to lose pressure and become exposed to atmosphere. The hole was repaired and the generator was returned to manufacturing on December 4, 1967, for reprocessing. This generator was completely reprocessed with the exception of the thermocouple seat-in operation. Reprocessing was completed on December 7, 1967, and the generator was returned to the test group.

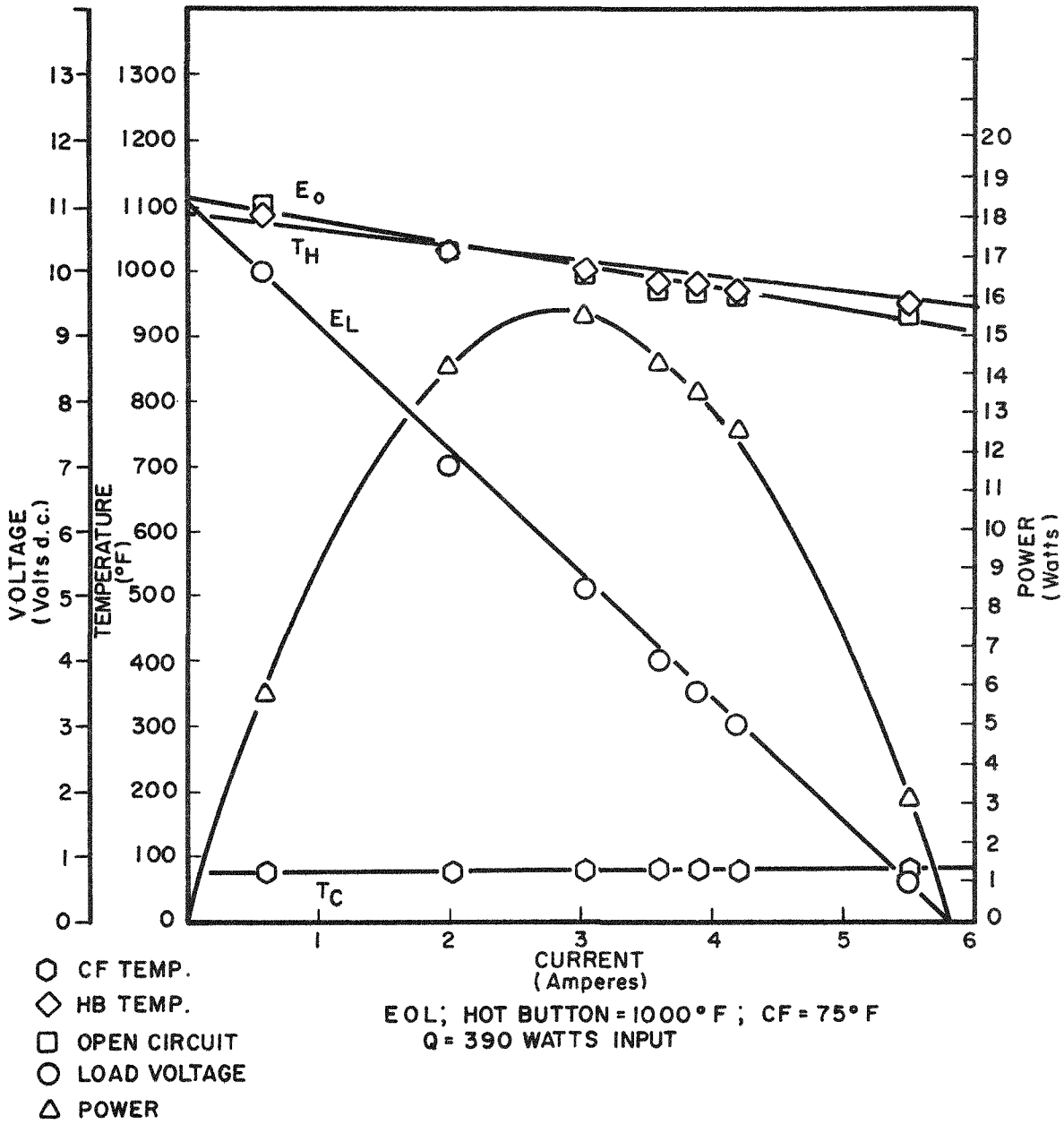

Figure 2-41a. SNAP-21 Development Generator 10D5: Performance Evaluation Map

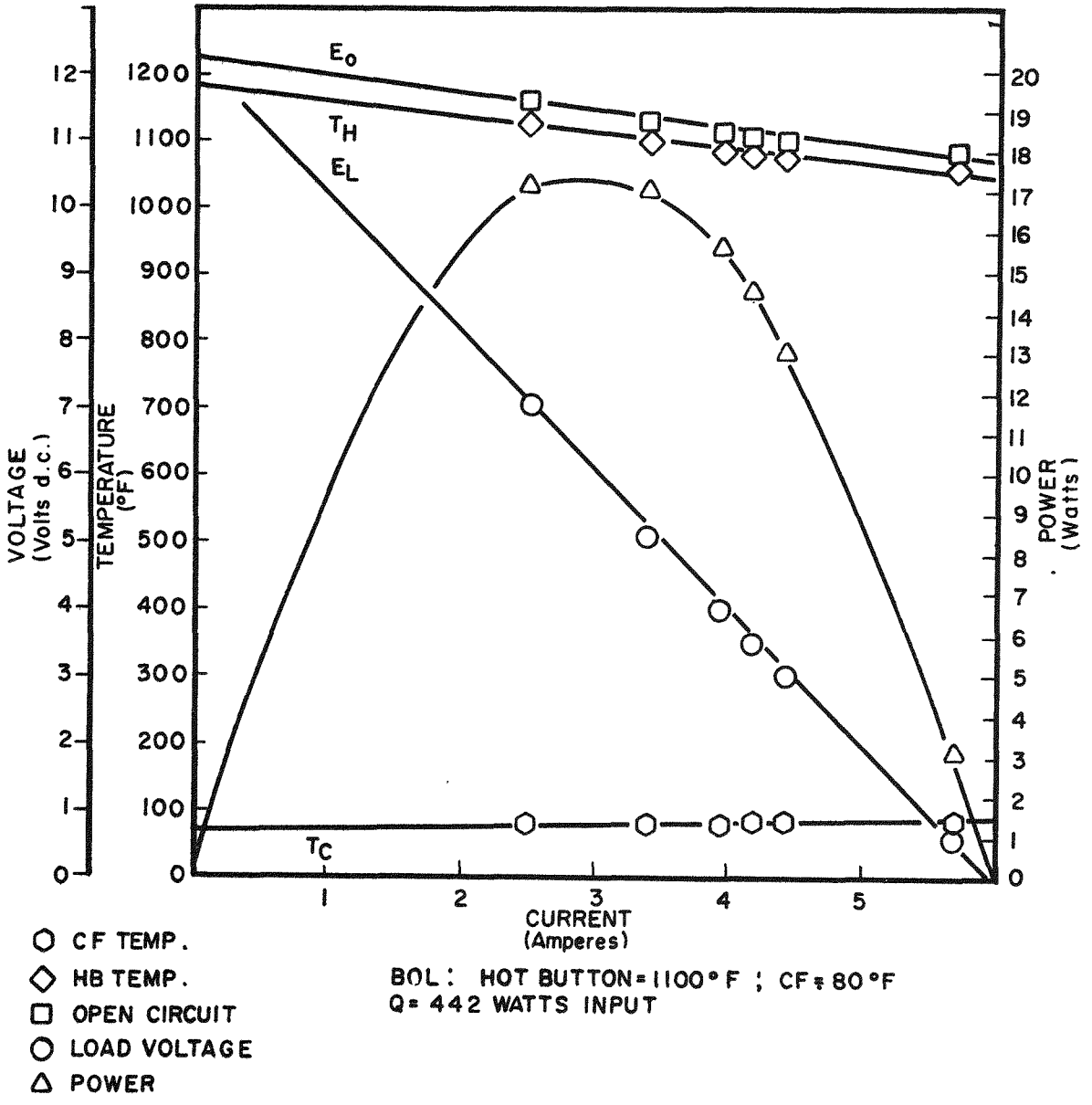

Figure 2-41b. SNAP-21 Development Generator 10D5: Performance Evaluation Map

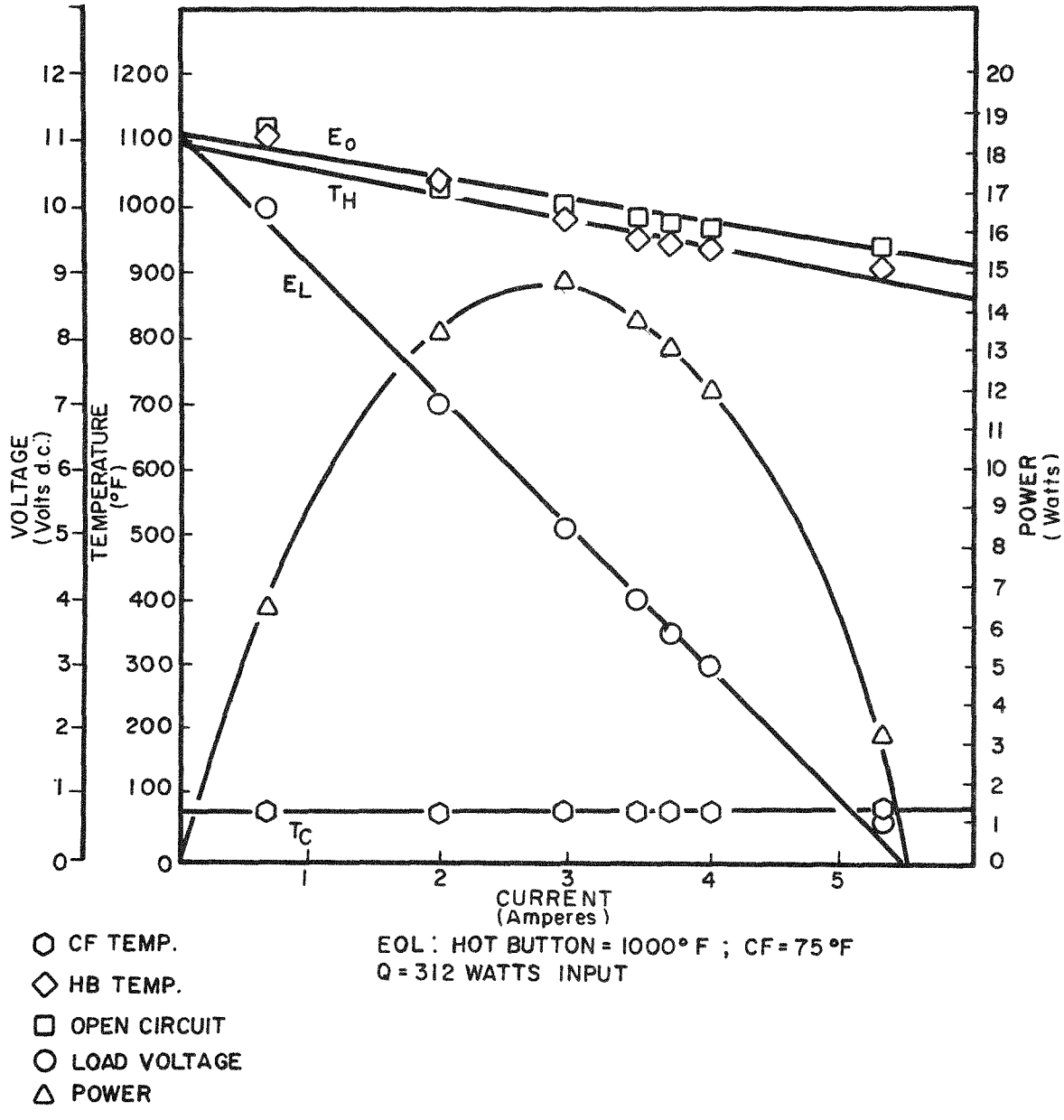

Figure 2-41c. SNAP-21 Development Generator 10D5: Performance Evaluation Map After Shock and Vibration Testing

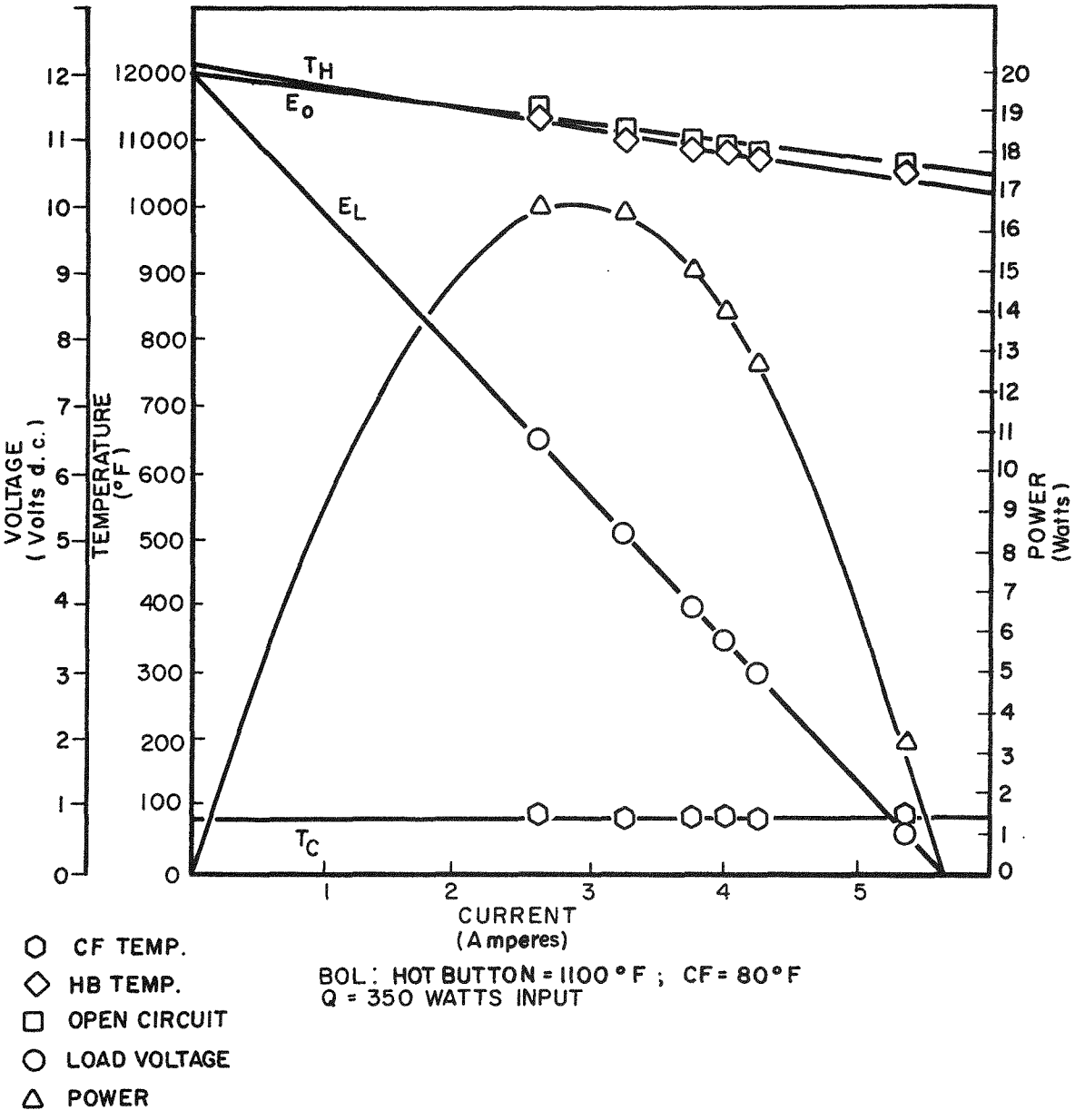

Figure 2-41d. SNAP-21 Development Generator 10D5: Performance Evaluation Map After Shock and Vibration Testing

Processing of Generator A10D6 was started and, after seating in the thermocouple legs, the generator was found to have developed a leak. The processing was stopped at this point and the generator was leak checked. A leak was detected in the solder joint of a 4-couple header to the cold frame. It was sealed with epoxy, cured, checked under 12 psig argon gas to assure that it was leak tight, and the processing was continued. The processing was on the last blank-off prior to the 24-hour hold and final seal-off when another leak was detected. The generator was immediately pressurized with argon and power shut off. The generator was removed from the processing station and leak checked.

A leak was confirmed in the area of the joint between the short case and cold frame. This is the same area that previously leaked and it had been soldered to eliminate this condition prior to assembly. This time the leak area was covered with Scotchweld. After an overnight cure pressure of 12 psig argon was applied and the generator was again leak checked. No leaks were detected and the generator was remounted into the processing and test station. Reprocessing was completed, with the exception of the seat-in operation, and the generator was pinched-off on December 17, 1967.

Effort for the next report period will be directed at completion of processing Generator A10D7. This generator has Min-K 1999 as insulating material. This material has a shortened process period similar to that of the Microquartz used in Generator A10D5. This will complete the effort for in-line generators.

2.3.6.4 Phase I Continuation Testing

During this report period the monitoring and analysis of thermoelectric test work initiated during Phase I of the SNAP-21 program continued. The units being tested and the accumulated hours on test are:

A1 – 30,147 hours

A3 – 28,785 hours

A4 – 27,945 hours

In October 1967, the input power to the modules was reduced to simulate the decay of a radioactive isotope.

Prototype generator units P5, P6 and P7 have amassed the following test hours:

P5 – 23,225 hours

P6 – 22,596 hours

P7 – 22,771 hours

All units are performing with no significant change in performance.

Performance data for these modules and generators are shown in Figures 2-42 through 2-45 and in Tables 11 and 12.

2.3.7 POWER CONDITIONER

The residual Phase I power conditioners and related electronic equipment has continued on test during the report period. The conditions and related equipment have accrued over 23,000 hours of actual test without significant change in system performance. Power conditioner test data is shown in Tables 13 through 16.

The four development power conditioners for Phase II of the SNAP-21 Program are scheduled for dynamic testing early in the next report period. A completed test plan defining the test program is currently being published.

2.3.8 ELECTRICAL RECEPTACLE

No test effort was expended in this area during the report period.

2.4 SYSTEM FABRICATION, ASSEMBLY AND TESTING

2.4.1 PHASE I CONTINUATION TESTING

Testing of Phase I system, Prototype Generator P4, was terminated on December 4, 1967, after being on test for 23,496 hours. The test was terminated for two

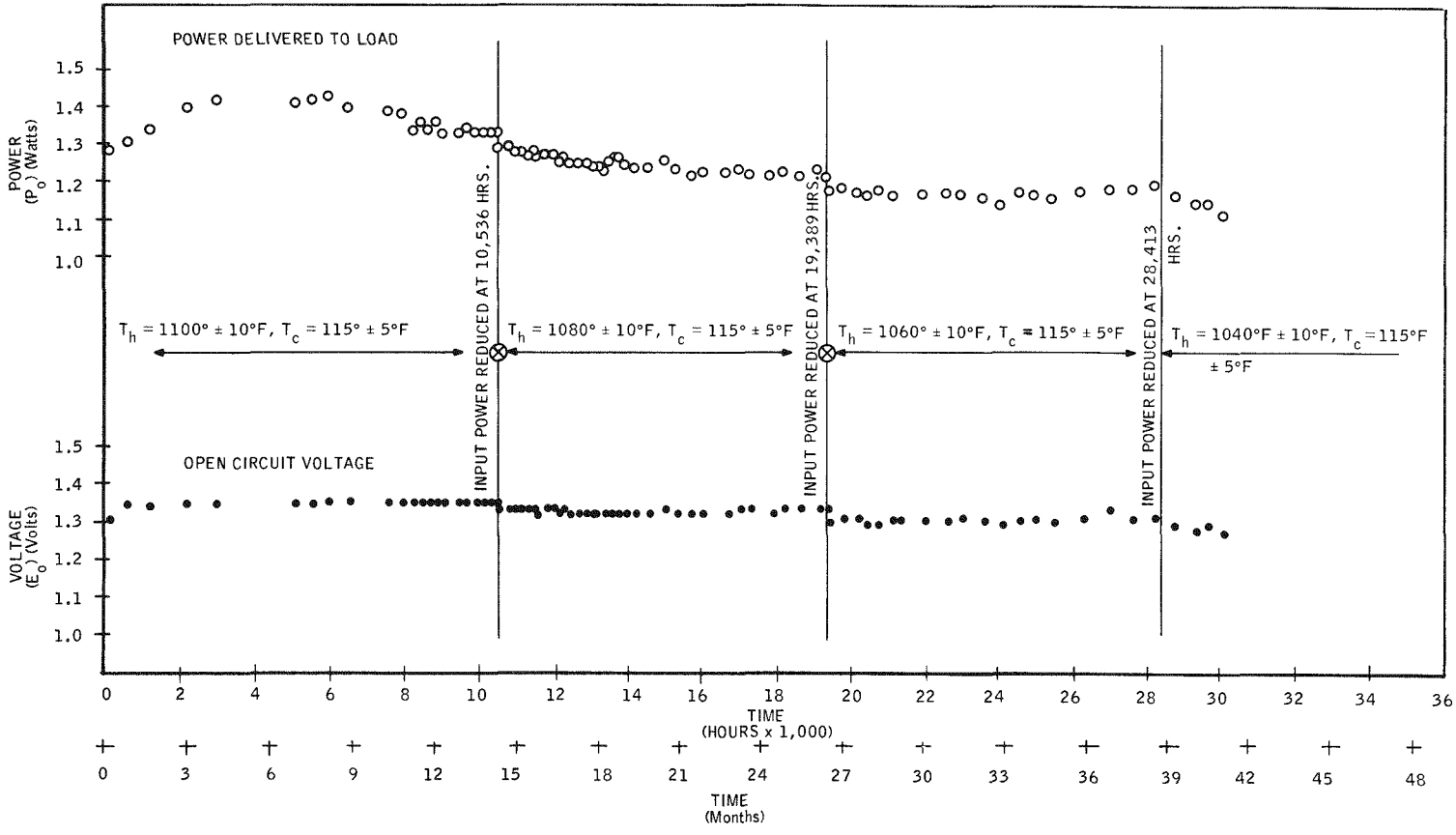

Figure 2-42. Performance of SNAP-21B 6-Couple Module A1

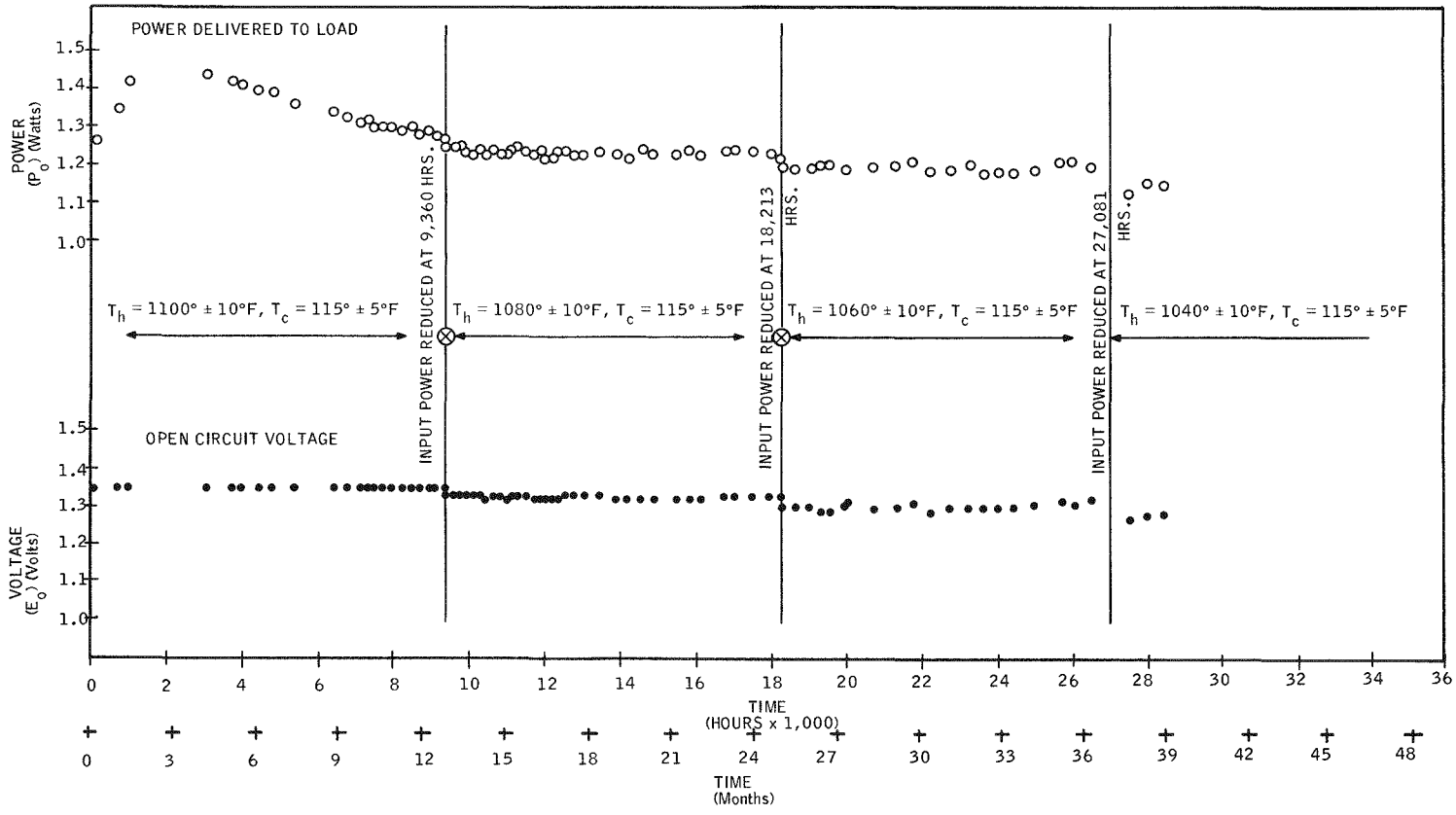

Figure 2-43. Performance of SNAP-21B 6-Couple Module A3

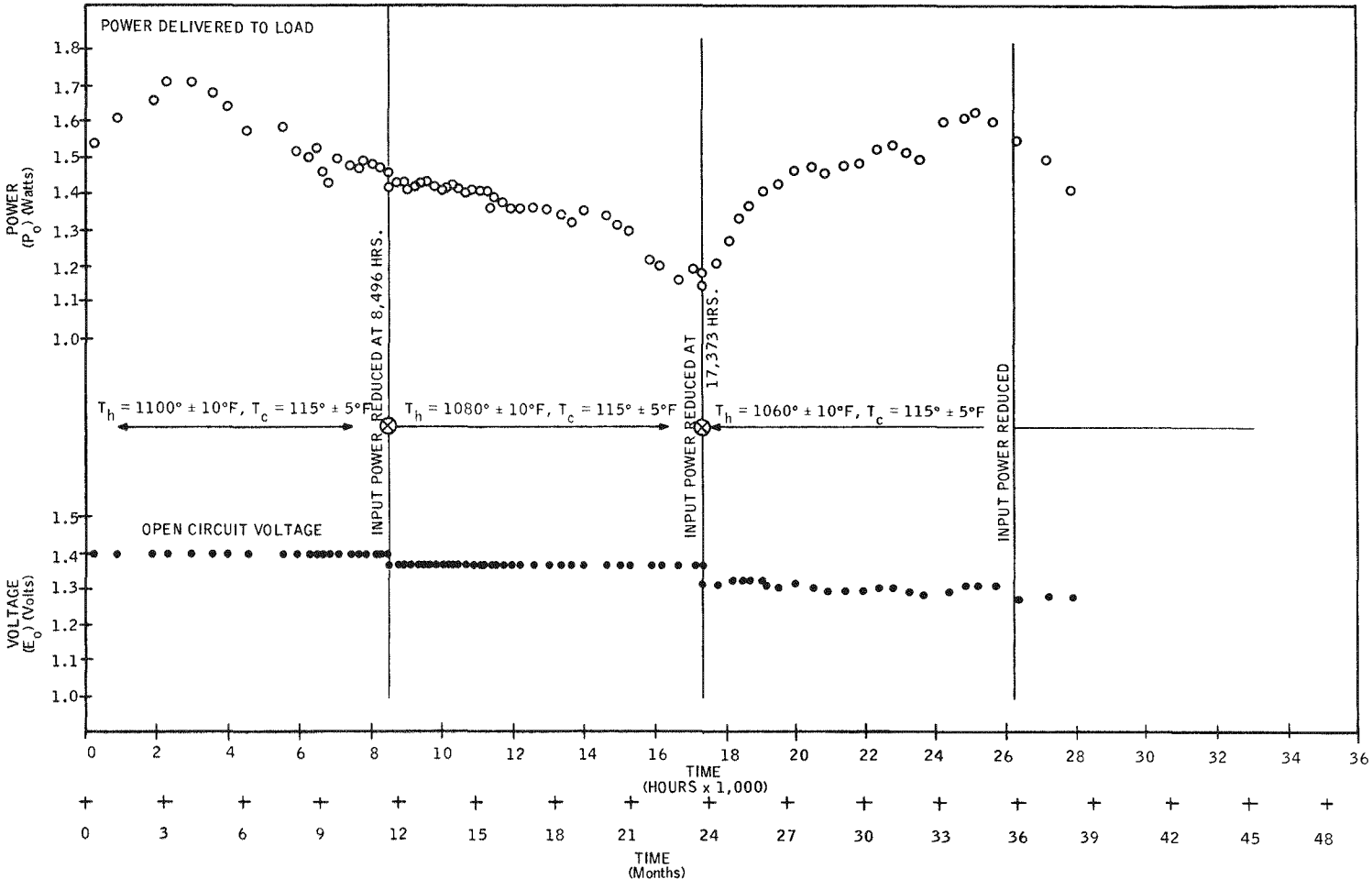

Figure 2-44. Performance of SNAP-21B 6-Couple Module A4

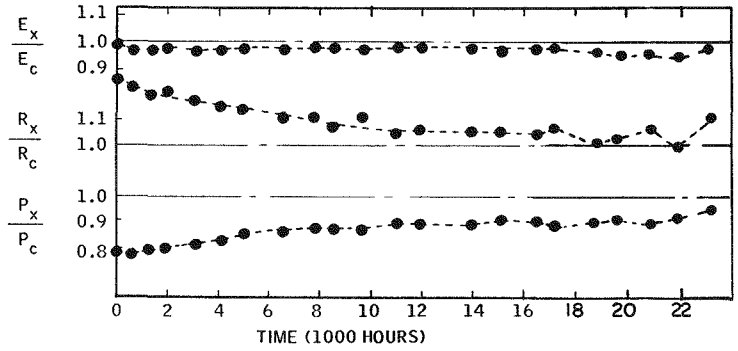

Prototype 3M-37-P5

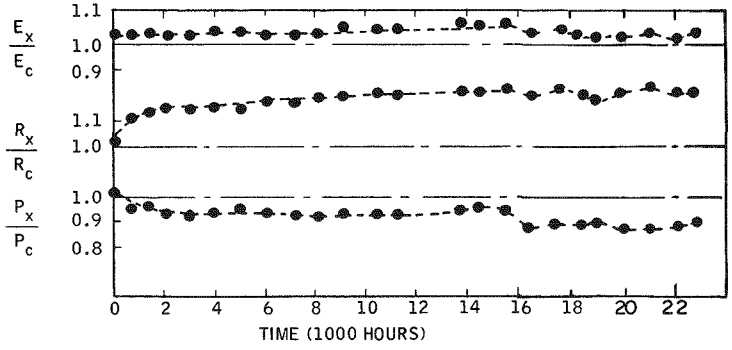

Prototype 3M-37-P6

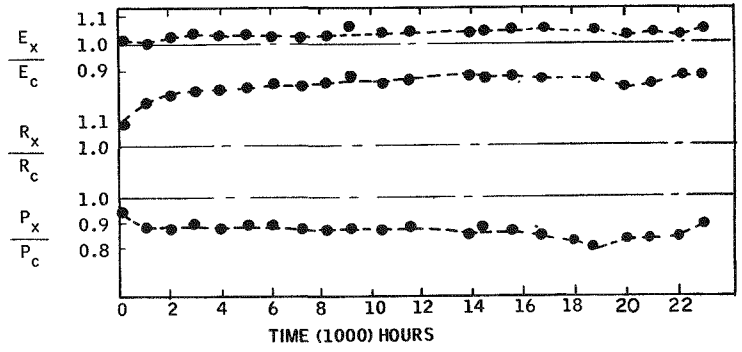

Prototype 3M-37-P7

Figure 2-45. Performance of Prototype 48-Couple Generator 3M-37-P5, P6, P7 (E = voltage, R = resistance, P = power, x = experimental, C = computer)

Table 11. SNAP-21 Six Couple Modules

Module	Date	T-Hot (est)	T-Cold	E_o (volts)	E_L (volts)	I_L (amps)	P_o (watts)	R (M-ohms)	P_I (watts)	Hours	
A1	9-30-67	1060	95	1.38	0.65	1.94	1.27	375	34	27,957	Moved Modules
	10-16-67	1060	115	1.30	0.64	1.86	1.18	356	34	28,341	
	10-19-67	Power Input Reduced								28,413	
	10-25-67	1041	115	1.27	0.63	1.82	1.15	351	32	28,557	
	11-6-67	1040	113	1.28	0.64	1.83	1.16	352	32	28,845	
	11-30-67	1040	114	1.27	0.63	1.80	1.13	356	32	29,421	
	12-15-67	1040	112	1.28	0.63	1.79	1.13	361	32	29.781	
	12-29-67	1040	113	1.26	0.63	1.75	1.10	360	32	30,147	
A3	9-30-67	1060	120	1.31	0.65	1.83	1.19	361	47	26,625	Moved to REG Power
	10-18-67	1060	119	1.31	0.65	1.82	1.18	364	47	27,057	
	10-19-67	Power Input Reduced								27,081	
	10-25-67	1040	120	1.27	0.63	1.77	1.12	360	45.5	27,225	
	11-6-67	1040	119	1.27	0.64	1.79	1.13	358	45.5	27,513	
	11-30-67	1041	118	1.28	0.64	1.80	1.15	357	46.0	28,089	
	12-15-67	1040	120	1.28	0.64	1.80	1.15	356	46.5	28,449	
	12-29-67	1040	120	1.27	0.64	1.79	1.14	353	46.5	28,785	
A4	9-30-67	1060	119	1.32	0.69	2.39	1.64	266	40	25,785	Moved to REG Power
	10-16-67	1060	118	1.30	0.68	2.38	1.63	259	40	26,169	
	10-19-67	Power Input Reduced								26,241	
	10-25-67	1040	116	1.27	0.64	2.44	1.55	259	39.5	26,385	
	11-6-67	1040	116	1.26	0.63	2.42	1.52	260	39.5	26,673	
	11-30-67	1040	116	1.27	0.62	2.39	1.49	271	39.0	27,249	
	12-15-67	1040	119	1.26	0.61	2.33	1.41	280	38.5	27,609	
	12-29-67	1040	118	1.27	0.61	2.33	1.41	285	38.5	27,945	

Table 12. SNAP-21 Prototypes P5, P6 and P7

Module	Date	T-Hot (est)	T-Cold	E_o (volts)	E_L (volts)	I_L (amps)	P_o (watts)	R (M-ohms)	P_I (watts)	Hours
P5	10-20-67	1057	159	9.90	4.95	2.17	10.74	2.28	175	21,545
	11-6-67	1067	158	10.08	5.04	2.19	11.04	2.30	174	21,953
	11-30-67	1070	150	10.10	5.05	2.20	11.62	2.30	175	22,529
	12-18-67	1070	145	10.22	5.11	2.22	11.34	2.30	175	22,961
	12-29-67	1066	150	10.20	5.10	2.22	11.32	2.30	175	23,225
P6	10-20-67	1055	176	9.92	4.96	2.01	9.97	2.47	188	20,916
	11-6-67	1055	172	10.08	5.04	2.02	10.18	2.50	185	21,324
	11-30-67	1055	166	10.00	5.0	2.04	10.20	2.45	190	21,900
	12-18-67	1055	165	10.00	5.0	2.04	10.20	2.45	190	22,332
	12-29-67	1055	172	9.99	4.99	2.03	10.13	2.46	190	22,596
P7	10-20-67	1055	171	10.14	5.07	1.91	9.68	2.65	176	21,091
	11-6-67	1055	165	10.24	5.12	1.90	9.73	2.69	180	21,499
	11-30-67	1055	167	10.26	5.13	1.91	9.80	2.69	180	20,507
	12-29-67	1055	173	10.19	5.10	1.92	9.79	2.65	178	20,771

Table 13. Automatic Selector Switch: Output Voltage vs. Time on Test

Time (Hours on Test)	Output Voltage		Remarks
	Conditioner MP-A	Conditioner MP-D	
13,583	24.54	24.59	
13,943	24.55	24.60	
14,471	24.56	24.60	
14,615	24.55	24.59	
15,095	24.62	24.58	NOTE: System turned
15,479	24.62	24.58	off from 4-24-67
15,887	24.50	24.59	to 6-6-67
16,343	24.46	24.58	
16,799	24.45	24.57	
17,327	24.47	24.55	
17,951	24.50	24.55	
18,479	24.47	24.59	
18,959	24.47	24.57	
19,319	24.48	24.59	
19,631	24.48	24.58	
20,111	24.47	24.58	
20,687	24.45	24.56	

Table 14. Regulator Test Fixture Performance Data

Operating Hours	A	C	D	F	HPR-A Operating Hours	HPR-A
18,369	21.75	21.86	22.49	21.93	17,552	26.78
18,729	21.72	21.79	22.47	21.90	17,912	26.77
19,257	21.72	21.78	22.46	21.89	18,440	26.80
19,401	21.72	21.78	22.46	21.88	18,584	26.81
19,881	21.54	21.63	22.41	21.88	19,064	26.46
20,265	21.53	21.55	22.42	21.90	19,448	26.51
20,673	21.53	21.46	22.42	21.88	19,856	26.51
21,117	21.49	21.39	22.40	21.84	20,360	26.51
22,161	21.52	21.37	22.39	21.85	21,344	26.51
22,617	21.60	20.79	22.40	21.88	21,800	26.48
23,145	21.46	21.45	22.35	21.82	22,328	26.45
23,769	21.46	21.13	22.31	21.82	22,952	26.36
24,297	21.35	21.52	22.41	21.82	23,480	26.31

Table 15. Converter Performance, Power Conditioner MP-B

E-In - Volts	I-In - Amps	P-In - Watts	E-Out - Volts	I-Out - Amps	P-Out - Watts	Efficiency Percent	Hours on Test
4.844	2.491	12.167	24.00	0.451	10.824	88.96	16,212
4.839	2.456	11.986	24.00	0.444	10.656	88.90	16,572
4.842	2.471	12.066	24.00	0.447	10.728	88.91	17,100
4.843	2.470	12.063	24.00	0.447	10.728	88.93	17,244
4.841	2.464	12.029	24.00	0.446	10.704	88.98	17,724
4.840	2.463	12.022	24.00	0.445	10.680	88.84	18,108
4.838	2.443	11.920	24.00	0.442	10.608	88.99	18,516
4.843	2.478	12.102	24.00	0.449	10.776	89.04	19,020
							19,620 Unit Shut Down for Experimental Testing (6-7-67)

Table 16. Converter Performance, Power Conditioner MP-C

E-In - Volts	I-In - Amps	P-In - Watts	E-Out - Volts	I-Out - Amps	P-Out - Watts	Efficiency Percent	Hours On Test
4.913	2.395	11.809	24.00	0.436	10.464	88.61	15,783
4.908	2.360	11.606	24.00	0.429	10.296	88.71	16,143
4.909	2.374	11.757	24.00	0.432	10.368	88.19	16,671
4.910	2.378	11.779	24.00	0.433	10.392	88.22	16,815
4.906	2.372	11.740	24.00	0.432	10.368	88.31	17,295
4.905	2.374	11.747	24.00	0.432	10.368	88.26	17,679
4.904	2.353	11.642	24.00	0.428	10.272	88.23	18,087
4.909	2.389	11.831	24.00	0.434	10.416	88.04	18,591
4.912	2.395	11.867	24.00	0.436	10.464	88.18	19,575
4.913	2.396	11.878	24.00	0.436	10.464	88.10	20,031
4.910	2.375	11.764	24.00	0.432	10.368	88.13	20,559
4.908	2.371	11.740	24.00	0.431	10.344	88.11	21,183
4.909	2.375	11.762	24.00	0.432	10.368	88.15	21,811
4.909	2.376	11.767	24.00	0.432	10.368	88.11	22,098
4.910	2.375	11.764	24.00	0.432	10.368	88.13	22,485
4.912	2.403	11.907	24.00	0.438	10.512	88.28	22,770
4.911	2.377	11.776	24.00	0.433	10.380	88.92	23,250

NOTE: Unit was discovered to have been accidentally shut down on 12/21/67. Power was restored on 12/22/67.

reasons: 1) some of the components were needed for Phase II tests, and 2) the system instrumentation had degraded to a point where it was difficult to control the test and no new information could be obtained. However, other SNAP-21B prototype generators are continuing on test.

A summary of the system performance data is shown in Tables 17 and 18. Data analysis shows system performance to be relatively constant throughout the past quarter.

Prior to the terminating of the test, the system power input was adjusted to its BOL value. Tables 19 and 20 show design, beginning of test and end of test data summary.

A preliminary analysis was made on the system. Comparison of the design and beginning of test data shows several disagreements. Of major concern is the difference in the cold electrode temperature. It is believed that this high temperature of 170°F was caused primarily by the cold cap-follower interface.

Comparison of the beginning of test and end of test results shows that the open circuit (Seebeck) voltage showed little change and the internal resistance increased. It is suspected that the increase in resistance is due to a sublimation of the thermoelectric material at the hot end of the legs. As a result, the power output of the thermoelectric generator decreased.

Table 17. SNAP-21B-1 System Test; Electrical Data, Generator Test Circuit

Date	1/20/67	2/14/67	3/18/67	4/22/67	5/24/67[1]	6/24/67
Open Circuit Voltage (volts)	10.23	10.25	10.28	10.20	10.28	10.00
Load Voltage (volts)	5.17	5.17	5.18	5.17	5.17	5.13
Load Current (amps)	2.27	2.29	2.27	2.25	2.26	2.20
Internal Resistance (ohms)	2.23	2.22	2.25	2.24	2.27	2.21
Power Output (watts)	11.74	11.84	11.75	11.64	11.66	11.29
Hours on test (start test 4/29/65)	15,711	15,771	16,539	17,379	18,147	18,891
Date	7/1/67	8/23/67	9/27/67	10/23/67	11/13/67	12/1/67
Open Circuit Voltage (volts)	9.90	9.95	9.42	9.90	9.98	9.85
Load Voltage (volts)	5.17	5.12	5.15	5.15	5.15	5.14
Load Current (amps)	2.20	2.20	2.15	2.12	2.17	2.18
Internal Resistance (ohms)	2.15	2.19	2.21	2.24	2.23	2.16
Power Output (watts)	11.37	11.26	11.12	10.92	11.18	11.21
Hours on test (start test	19,059	20,321	21,161	22,540	23,064	23,496

1. The thermal conditions which correspond to these electrical data are the same as those shown for the respective test date in the Summary of Data-System Test Circuit table.

Table 18. Summary of SNAP-21B System Performance

Date	7/29/66	8/9/66	9/15/66	10/1/66	11/12/66	12/12/66	1/20/67	2/14/67
Generator hot electrode temperature (°F)	1065	1061	1075	1062	1079	1076	1070	1070
Generator cold electrode temperature (°F)	179	178	181	181	179	180	180	180
Water temperature (°F)	40	40	39	37	38	38	38	37
Generator load voltage (volts)	5.18	5.18	5.19	5.15	5.19	5.17	5.17	5.17
Generator load current (amps)	2.30	2.27	2.30	2.30	2.29	2.29	2.25	2.27
Generator total power output (watts)	12.01	11.86	12.08	11.95	11.99	11.91	11.73	11.84
Conditioner load voltage input (volts)	4.87	4.87	4.87	4.84	4.88	4.88	4.85	4.85
Conditioner load current input (amps)	2.30	2.27	2.30	2.30	2.29	2.29	2.25	2.27
Conditioner total power input (watts)	11.29	11.14	11.29	11.22	11.27	11.24	11.00	11.10
System load voltage (volts)	24.00	24.00	24.00	24.00	24.00	24.00	24.00	24.00
System load current (amps)	0.42	0.42	0.42	0.42	0.42	0.42	0.41	0.42
System power output (measured) (watts)	10.08	9.96	10.08	10.08	10.08	10.01	9.84	9.96
System power output (corrected) (watts)	10.66	10.66	10.69	10.63	10.76	10.64	10.48	10.71
System power input (measured) (watts)	224	224	224	225	226	226	226	226
System power input (corrected) (watts)	220	220	220	221	222	222	222	222
Conditioner efficiency (percent)	89	90	90	90	89	89	89	90
System efficiency (percent)	4.8	4.8	4.9	4.8	4.8	4.8	4.7	4.8
Hours on test (start test 4/29/65)	10,923	11,187	12,075	12,531	13,515	14,235	15,171	15,771

Date	3/18/67	4/22/67	5/24/67[2]	6/24/67	7/1/67	8/23/67	9/27/67	10/23/67	11/13/67	12/1/67[3]
Generator hot electrode temperature (°F)	1070	1070	1070	1050	1050	1050	1050	1050	1050	1050
Generator cold electrode temperature (°F)	180	180	180	180	180	180	180	180	180	180
Water temperature (°F)	38	37	38	37	38	38	37	37	37	39
Generator load voltage (volts)	5.18	5.17	5.17	5.13	5.17	5.16	5.15	5.15	5.15	5.14
Generator load current (amps)	2.26	2.23	2.25	2.19	2.17	2.18	2.15	2.15	2.15	2.18
Generator total power output watts)	11.80	11.64	11.71	11.31	11.30	11.35	11.18	11.15	11.17	11.31
Conditioner load voltage input (volts)	4.86	4.86	4.86	4.84	4.86	4.83	4.85	4.83	4.86	4.83
Conditioner load current input (amps)	2.26	2.23	2.25	2.19	2.17	2.18	2.15	2.15	2.15	2.18
Conditioner total power input (watts)	11.07	10.93	11.00	10.67	10.61	10.62	10.51	10.45	10.54	10.61
System load voltage (volts)	24.00	24.00	24.00	24.00	24.00	24.00	24.00	24.00	24.00	24.00
System load current (amps)	0.41	0.41	0.41	0.40	0.40	0.40	0.39	0.39	0.39	0.40
System power output (measured) (watts)	9.86	9.74	9.84	9.60	9.48	9.48	9.36	9.41	9.48	9.48
System power output (corrected) (watts)	10.46	10.38	10.38	10.23	10.20	10.09	9.97	9.91	10.09	10.10
System power input (measured) (watts)	225	225	225	219	219	219	219	219	219	219
System power input (corrected) (watts)	221	221	221	215	215	215	215	215	215	215
Conditioner efficiency (percent)	89	89	89	90	89	89	89	90	90	89
System efficiency (percent)	4.7	4.7	4.7	4.8	4.7	4.7	4.6	4.6	4.7	4.7
Hours on test (start test 4/29/65)	16,539	17,379	18,147	18,891	19,057	20,310	21,150	21,774	23,064	23,496

[1]The system test was moved from T. C. A. to Space Center 6/28/66.

[2]The input power was reduced from 225 watts to 219 watts on May 24, 1967.

[3]Test terminated on December 4, 1967.

Table 19. SNAP-21B-1 System Test Comparison of Design, Beginning and End of Test Generator Data

	Design	Begin Test	End Test
Open Circuit Voltage (volts)	11.1	10.48	10.44
Load Voltage (volts)	6.51	5.23	5.18
Load Current (amps)	2.5	2.50	2.25
Internal Resistance (ohms)	-	2.10	2.33
Power Output (watts)	13.8	13.08	11.68
Test Hours	-	1,176	23,592

It may also be noted that the efficiency of the power conditioner showed very little change. It appears that the cause of the decrease in the system power output and system efficiency is due to the increase in the internal resistance of the thermoelectric generator.

The system (see Figure 2-46) was removed from the environmental water tank and disassembled. Figure 2-47 shows the lower half of the system with the cover removed. No detailed post-test analysis is planned for the system components.

Most of the system components will be used for other tests. Probable applications are:

Component	Test
Pressure Vessel and Power Conditioner	System S10D1A: early fuel system
Segmented Retaining Ring and Insulation System	Efficiency studies

Table 20. SNAP-21B-1 System Test Comparison of Design, Beginning and End of Test System Data

Item Instrumented	Design[5]	Begin Test	End Test
Generator hot electrode temperature (°F)	1100	1100	1100 Est
Generator cold electrode temperature (°F)	115	179	179 Est
Water temperature (°F)	41	39	38
Generator load voltage (volts)[1]	6.51	5.23	5.18
Generator load current (amps)[1]	2.5	2.48	2.23
Generator total power output (watts)	13.8	13.08	12.02
Conditioner load voltage input (volts)[1]	6.51	4.90	4.86
Conditioner load current input (amps)[1]	2.5	2.48	2.23
Conditioner total power input (watts)	13.8	12.24	10.92
System load voltage (volts)	24.0	24.00	24.00
System load current (amps)	0.421	0.45	0.41
System power output (measured) (watts)	-	10.90	9.84
System power output (corrected) (watts)[2]	11.7	11.65	10.54
System power input (measured) (watts)	-	230	230
System power input (corrected) (watts)[3]	203	226	226
Conditioner efficiency (percent)	N/A	89	90
System efficiency (percent)[4]	6.25	5.2	4.7
Test Hours	-	1,176	23,592

(1) Primary circuit only

(2) Corrected for measured instrumentation losses.

(3) Corrected for estimated instrumentation losses.

(4) Based on corrected power input and output

(5) SNAP-21B Program, Phase I, Deep Sea Radioisotope-fueled Thermoelectric Generator Power Supply System, Final Summary Report, No. MMM 3321-19, C-92a, M3679 (44th Ed.)

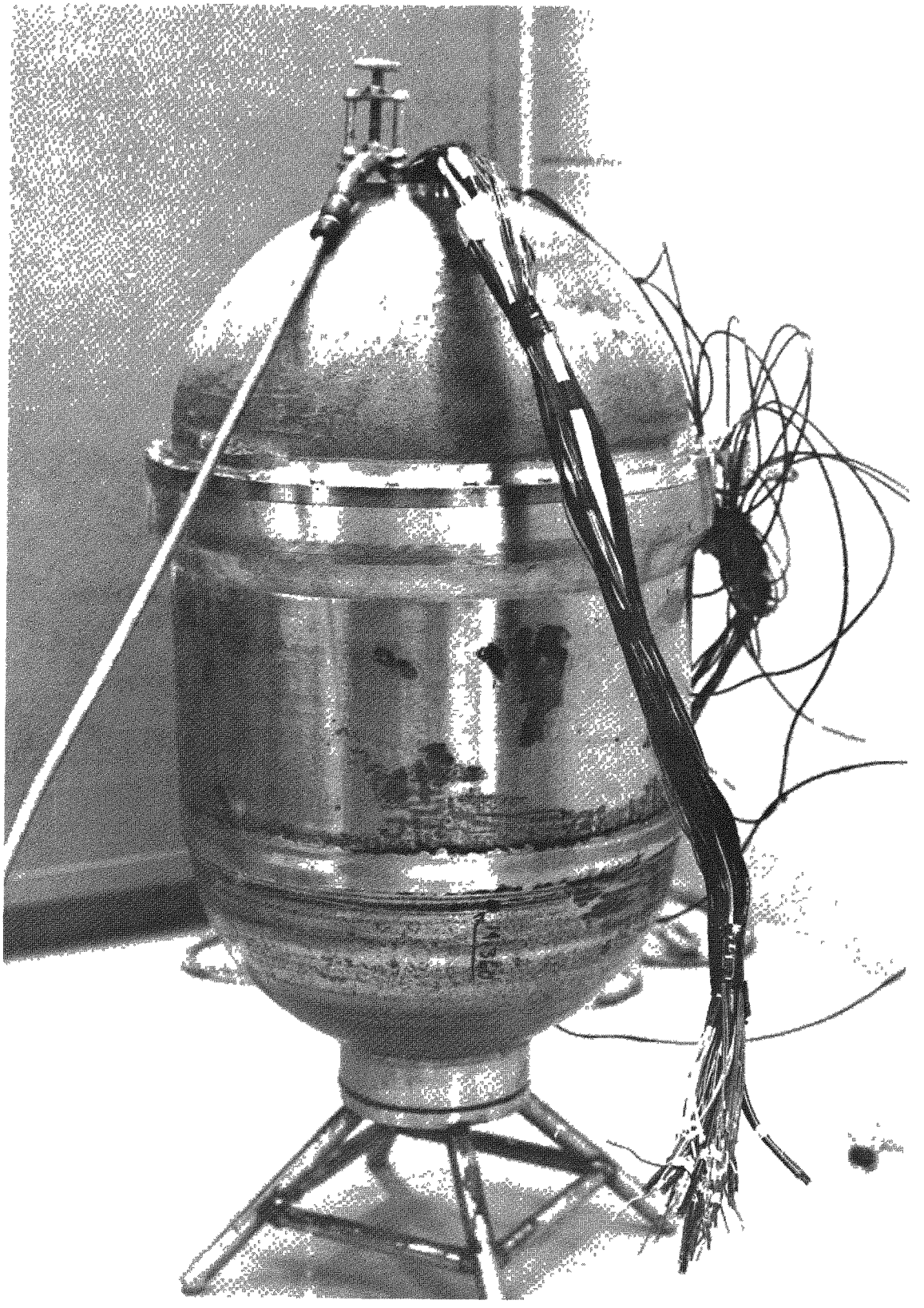

Figure 2-46. Prototype Generator P_4 After Removal from Water Tank

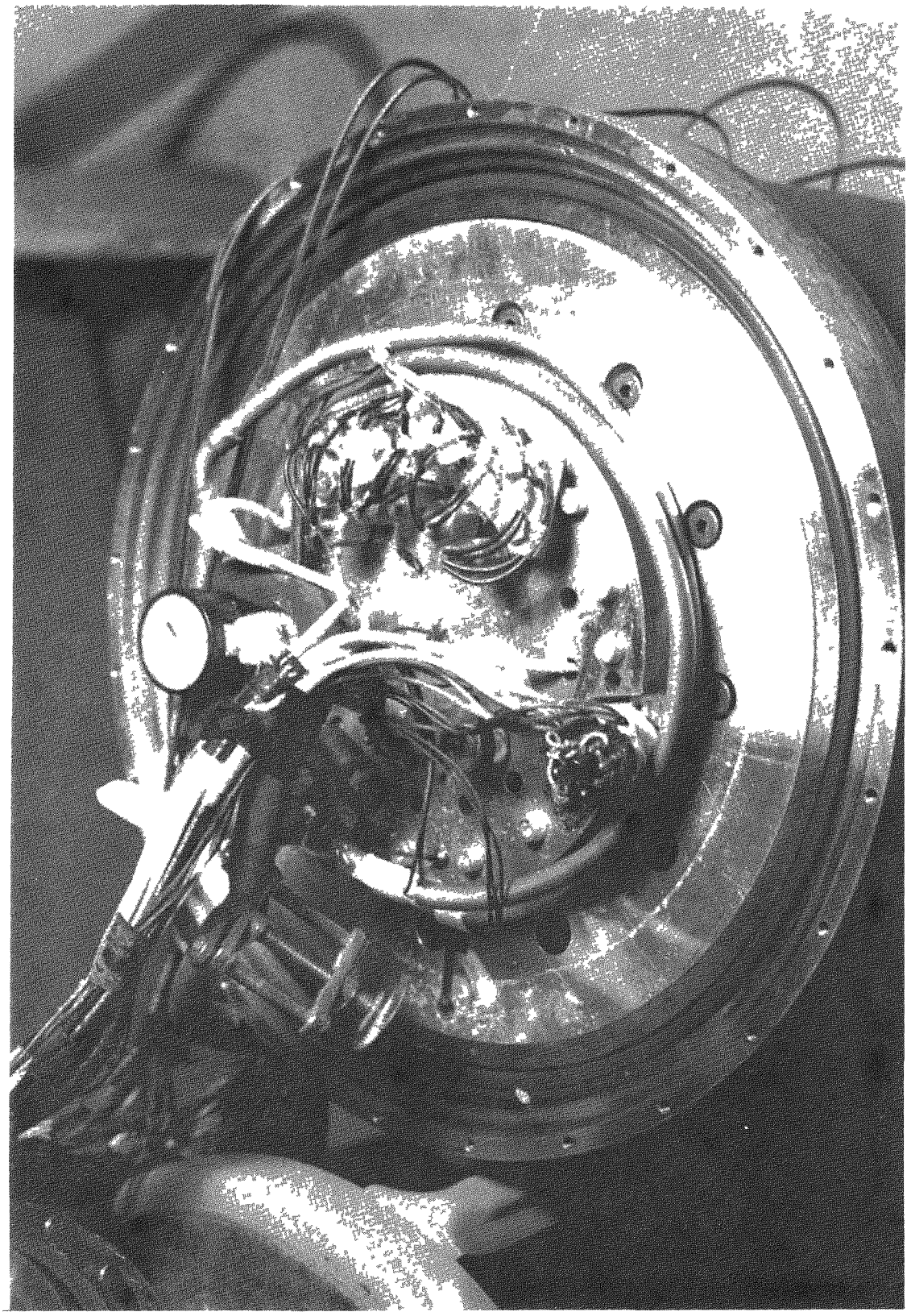

Figure 2-47 Prototype Generator P_4, Lower Half with Cover Removed

2.4.2 PHASE II SYSTEM

2.4.2.1 System S10D1

System S10D1 was assembled using the following components:

Pressure vessel (titanium 621) – Phase I

High vacuum thermal insulation system – Phase II

Segmented retaining ring (low spring constant) – Phase I

Heater block with four 200-watt heaters

Thermoelectric Generator A10D1 – Phase II

Power Conditioner MP-F – Phase I

To provide a thermal profile, thermocouples were installed in various key locations throughout the system. The thermocouples can be seen in the photograph, Figure 2-48. Those in hot areas were either TIG welded or capacitance discharged in position. The thermocouples were initially routed through isotherms for a minimum of two inches on their way to the exterior of the system. Thermocouples located in system cold areas were fastened with epoxy.

As the first step in the assembly process, the pressure vessel was inserted into a stand constructed of epoxy molded to the shape of the vessel. The high vacuum thermal insulation system with the segmented retaining ring was lowered into the pressure vessel. After thermocouples were attached to the heater block and the insulation neck tube, the heater block was inserted into the biological shield cavity and bolted into place. The thermal emitter plate was bolted to the heater block and a thermocouple fastened to its center.

The getter pod of the thermal insulation system was located in such a position as to make the separation of the segmented retaining ring from the thermal insulation system impossible. Without the capability of removal, the ring could not be disassembled for internal (spring area) thermocouple location. Only those thermocouples intended for external surface locations could be positioned.

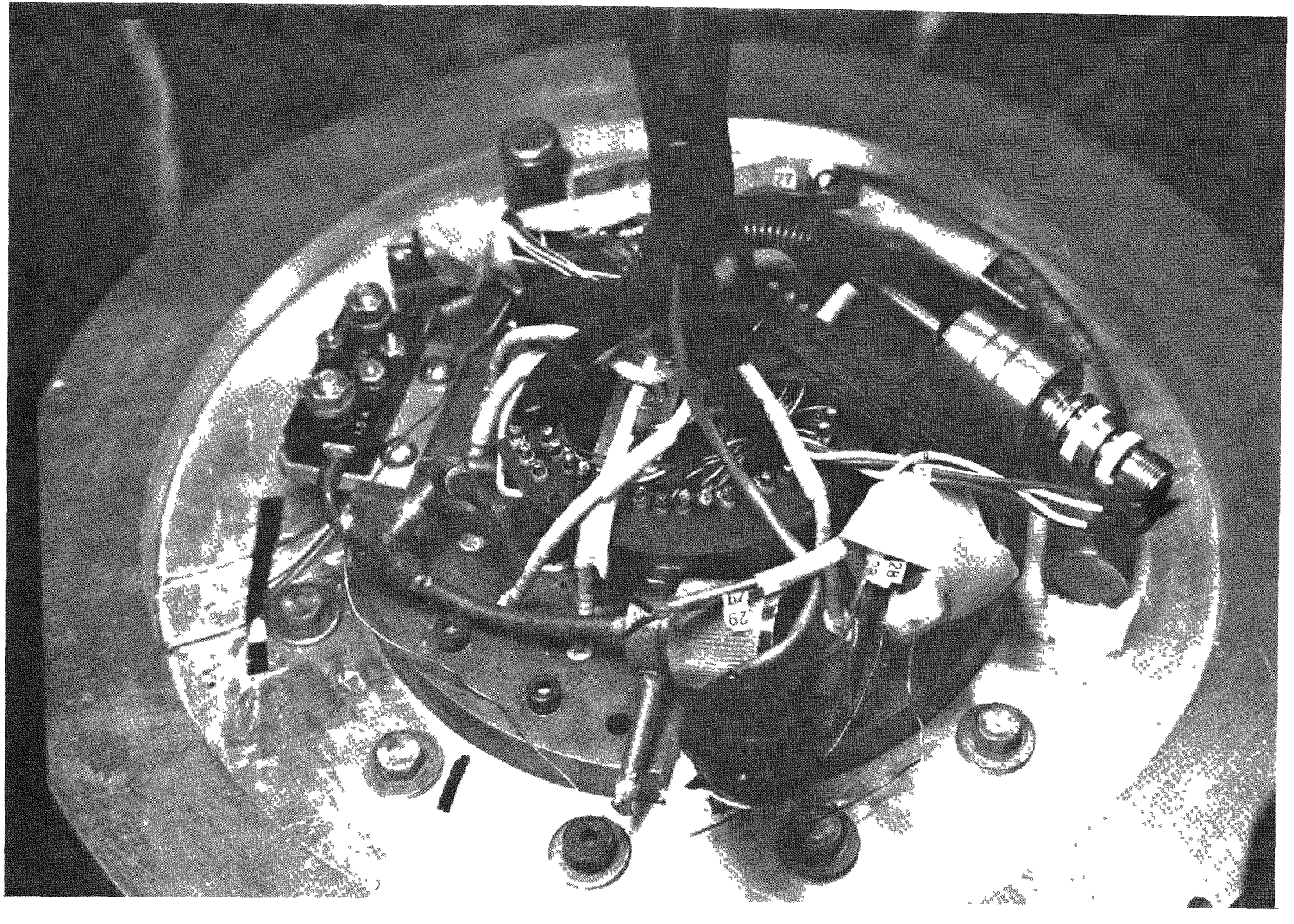

Figure 2-48. System S10D1, Thermoelectric Generator

A Microquartz pad was located about the periphery of the emitter plate and the instrumented thermoelectric generator was positioned above the plate by bolting to the segmented retaining ring. Min-K 1301 was charged through ports in the generator cold frame into the annulus between thermoelectric generator case and high vacuum thermal insulation system neck tube.

The instrumentation wiring of the thermoelectric generator was extended sufficiently (approximately fourteen feet) so that it would reach the test panel located outside the system and its environmental housing. The power leads and thermocouples for the heat source were also extended by the same amount. The completed and pre-tested power conditioner was fastened to the inside dome of the pressure vessel cover. With the cover suspended above the remainder of the system, the electrical wiring was completed.

Following the wiring, the cover was lowered into place and fastened to the body of the pressure vessel with 24 stainless steel bolts tightened diametrically to 10 inch-pounds of torque. One bolt was left out to provide for locating a thermocouple.

To avoid the situation of the biological shield mass being suspended by volts whose creep would be excessive at operating temperature, it was determined that the system should be tested in the normally inverse position, i.e., pressure vessel cover down. Therefore, it was necessary to assemble the system in its normal position, pressure vessel body down, and then rotate it prior to test initiation. After accomplishing the rotation in a special fixture the system was picked up in its inverse position and lowered into the test stand. The wires emerging from the pressure vessel cover were fed through a U-tube, which in turn, fastened to the cover. Thermocouples were fastened at various positions on the pressure vessel exterior, and the wires routed up the outside wall of the U-tube.

The system, including its test stand, was picked up and lowered into the test tank. The tank was filled with water and the power lead and instrumentation were wired to the test panel. The test tank contained a refrigeration coil. An immersion heater was lowered into the tank along with the system and its stand.

Table 21 is a summary of test data for System S10D1. Because the test started late in the quarter a complete system analysis could not be made for this report. However, indications are that system performance is quite stable.

2.4.2.2 Early Fueled System

During this report period, it was decided that a complete system would be assembled at Oak Ridge National Laboratory (ORNL) using fuel capsule #2 which was loaded with 186.45 watts (T_h) of 90 Sr as titanate for the heat source. The system was designated S10D1-A.

System S10D1-A will use the following components:

Pressure vessel (stainless steel-347) Phase I

High vacuum thermal insulation system 10D2, Phase II

Segmented retaining ring 10D1, Phase II

Thermoelectric Generator A10D4, Phase II

Power conditioner, undesignated, Phase I

The pressure vessel from Phase I is made of a type 347 stainless steel casting. It has seen nearly 23,000 hours of service as Phase I system pressure vessel. It was machined on the inside only to accept the insulation system and the power conditioner. After system teardown, the outside diameter of the pressure vessel and cover were finished machined to dimensions and tolerances of the Berylco 165 pressure vessels to more closely approximate conditions in future systems. Environmental conditions are controlled by a refrigerated water tank (28° - 40°F).

The insulation system to be used in the early fueled system will be high vacuum thermal insulation system 10D2. This is the back-up system and uses a heavy neck tube in the inner liner and tension support rods for the biological shield. It will be delivered to ORNL by special carrier. Two men will drive from the Linde Corporation to ORNL to assure safe delivery of the system. Their entire trip will be monitored by a recording accelerometer.

Table 21. SNAP-21 System S10D1 Test Data Summary

	BOL
System Power Input (measured) (w)	230
Generator Hot Electrode Temperature (°F)	1050
Generator Cold Electrode Temperature (°F)	130
Generator Cold Frame Temperature (°F)	115
Water Temperature (°F)	41
Generator Primary Load Voltage (v)	5.16
Generator Bias Load Voltage (v)	0.725
Generator Primary Load Current (a)	2.85
Generator Bias Load Current (a)	0.134
Generator Primary Power Output (w)	14.8
Generator Bias Power Output (w)	0.097
Generator Total Power Output (w)	14.897
Conditioner Primary Voltage Input (v)	5.14
Conditioner Bias Voltage Input (v)	0.701
Conditioner Primary Current Input (a)	2.85
Conditioner Bias Current Input (a)	0.134
Conditioner Primary Power Input (w)	14.7
Conditioner Bias Power Input (w)	0.094
Conditioner Total Power Input (w)	14.794
System Load Voltage (v)	24
System Load Current (a)	0.528
System Power Output (measured) (w)	12.67
Conditioner Efficiency (percent)	85.8
System Efficiency (percent)	5.5
Test Hours*	629.0

*As of 12/23/67.

Segmented retaining ring G10D1, Phase II design, was used in the dynamic test conducted in October of this year. Results of this test provided a high degree of confidence that the redesign of the segmented retaining ring is adequate to withstand a 6g shock load. (Ref. 2.3.4 of this report.)

The Phase II biological shield plug 10D1 will be used in this and future systems. Incorporation of the plug into the system required that it be encapsulated in three parts: an emitter plate, tube and end plate. Prior to encapsulation, the plug had to be sprayed with a barrier material, aluminum oxide (Al_2O_3). The sprayed plug was then ground to fit the encapsulated parts within a tolerance of 0.002 inch. The plug was assembled with the three parts of the encapsulated assembly and TIG welded to achieve a hermetic seal.

Thermoelectric Generator A10D4 will be used in the early fueled system. This generator is one of the first four of Phase II Design No. 1 and consists of the ball and socket configuration at the cold end junction to the follower. This generator, as well as all of the first four generators, used Conax fittings to convey instrumentation wires from inside. These headers initially leaked but periodic tightening to a prescribed torque value eventually achieved a leak-tight condition.

The power conditioner has not yet been designated but it will be one of Phase I design.

As much work as possible has been done at 3M to minimize the assembly effort at Oak Ridge. All instrumentation from the generator through the pressure vessel cover has been prewired terminated at a receptacle. The test console was completely wired through to plugs. Relatively few thermocouples remain to connect before closing the system.

All components will be transported by leased truck under the supervision of a cognizant member of Manufacturing Engineering. It is estimated that the trip to Oak Ridge will take 2-1/2 to 3 days.

Planned effort for the next report period will be the safe transportation of all components to ORNL and the fueling and setting up of the complete system. The system will be monitored by 3M Space and Defense Products Department personnel until equilibrium has been reached. ORNL personnel will become familiar with taking data during this period. Data will be forwarded to Space and Defense Products Department on a weekly basis.

The system will remain in operation for a period of about one month. The system will then be dismantled before returning it to 3M's Space and Defense Products Department.

2.5 SAFETY ANALYSIS AND TESTING

2.5.1 ELECTRICALLY HEATED FUEL CAPSULES

During this report period parts for ten electrically heated fuel capsules were fabricated. Instrumentation and heater block assemblies were supplied to 3M by NRDL. After trial assembly of the components (Figures 2-49 through 2-52) at 3M they were delivered to ORNL for final cleaning, assembly and welding. Electron beam welding was completed and after welding and leak checking the capsules were forwarded to PNL for ultrasonic testing. The ultrasonic inspection was completed and the capsules are ready for implantment.

Implantment was originally planned for mid-December; however, NRDL has indicated that this will not be possible and that they were now estimating mid-January. The test plan for ocean exposure of fueled capsules has been revised and will be released next month.

2.5.2 LABORATORY CORROSION STUDIES

Laboratory corrosion studies were conducted on samples of Berylco-165 rolled sheet stock. These samples indicated some pitting, which was not anticipated because of the demonstrated corrosion resistance of Berylco-165 in sea water. It was suspected that the pitting was due to surface inclusions created by the rolling process. A second set of samples were tested that had machined surfaces. These samples did not exhibit any pitting.

2.5.3 FUELED CAPSULE OCEAN EXPOSURE TESTS

The two fueled capsules that will be used for the ocean exposure tests were fabricated during this report period. Details of their fabrication and testing are presented in Section 2.3.1 of this report.

Based on the projected delivery of the capsule exposure tasks, ocean implantment at the NRDL test site at San Clemente Island will take place about 1 March 1968.

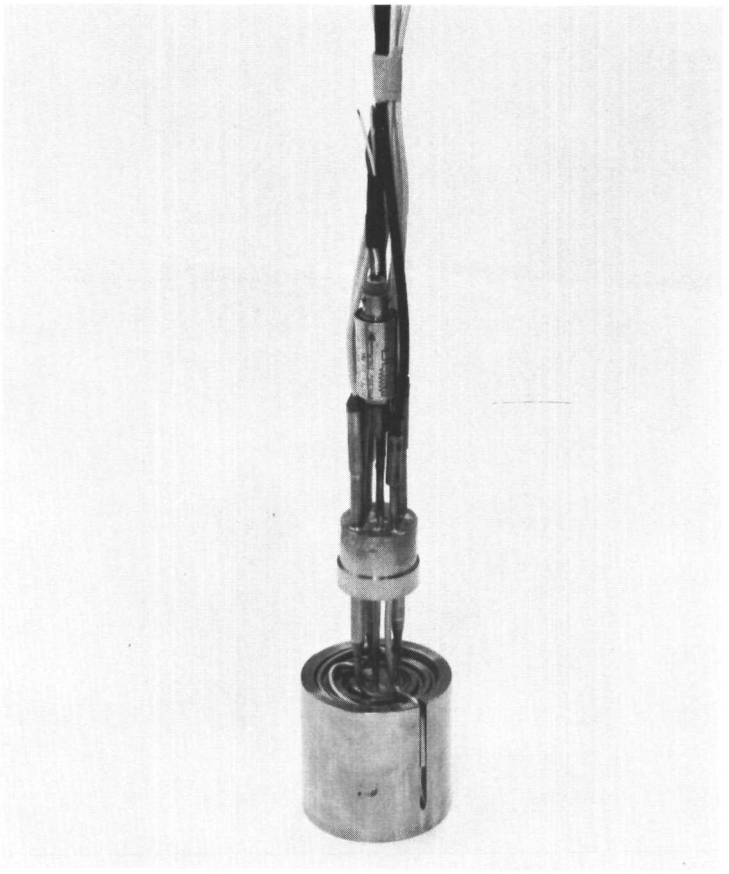

Figure 2-49 Electrically Heated Fuel Capsule Instrumentation and Heater Block Assembly

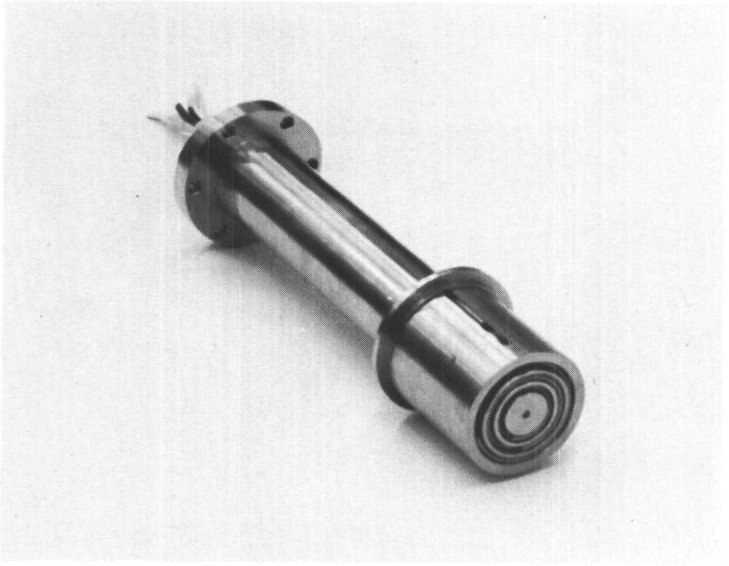

Figure 2-50 Partially Assembled Electrically Heated Fuel Capsule (showing Heater Block Assembly)

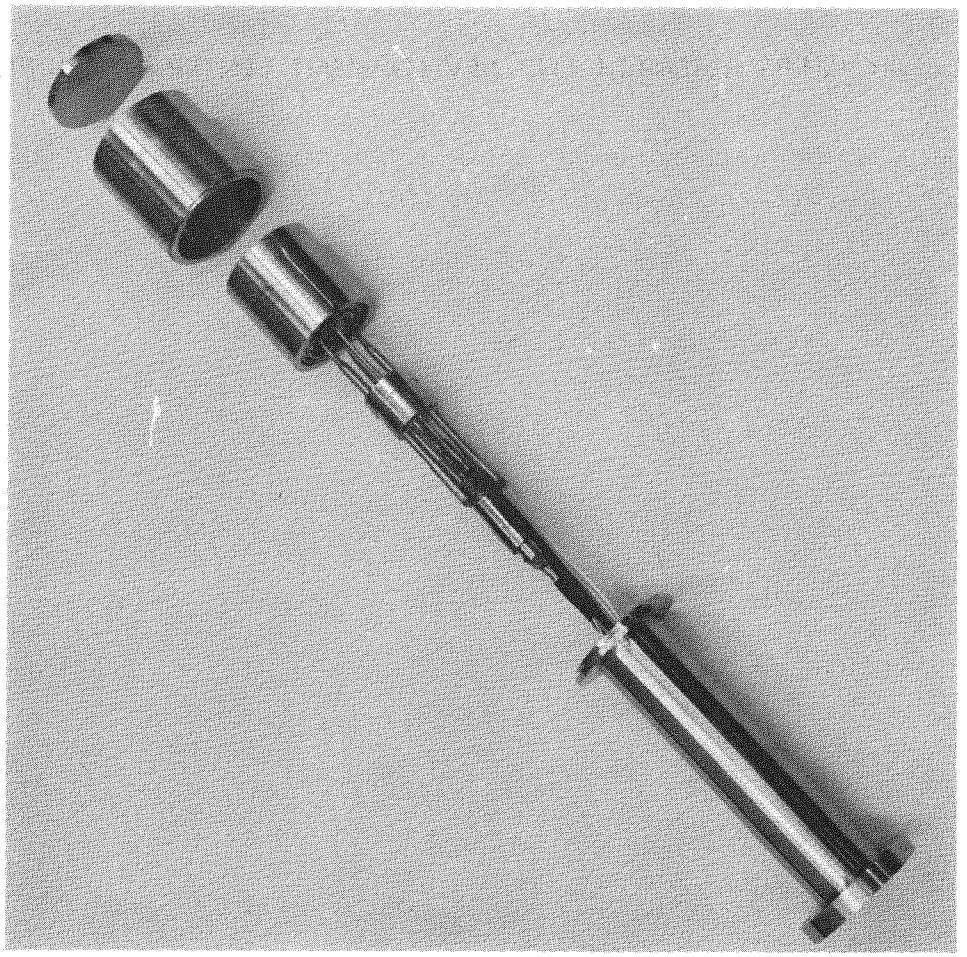

Figure 2-51
Exploded View of
Electrically
Heated
Fuel Capsule

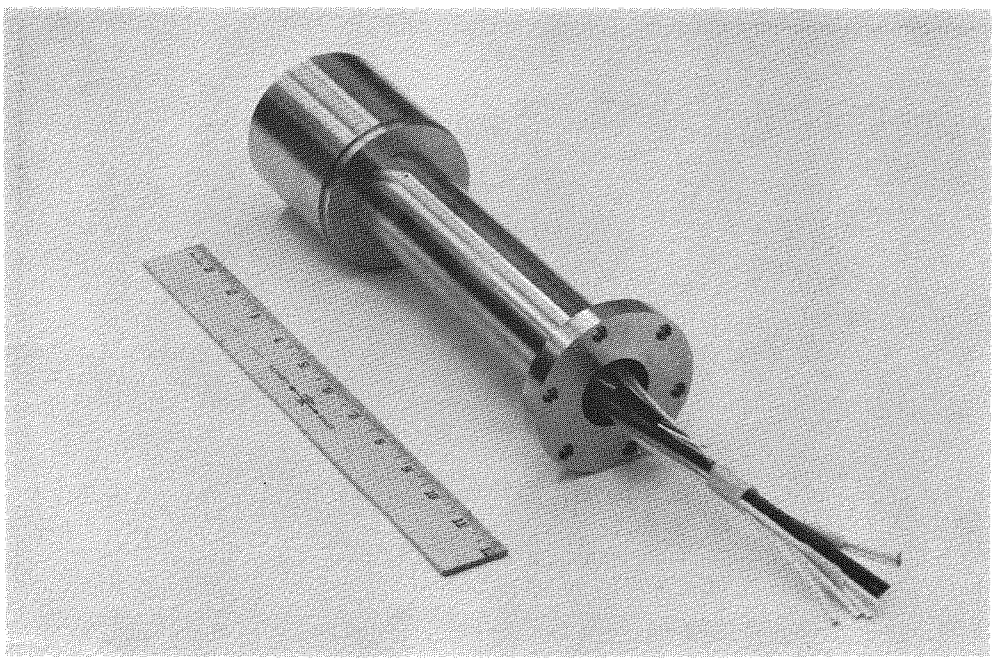

Figure 2-52 Assembled Electrically Heated Fuel Capsule

2.6 NAVSHIPS RESEARCH AND DEVELOPMENT CENTER 10-COUPLE MODULES

Design effort was completed on this task during this reporting period. All drawings have been released and submitted to MEL.

2.6.1 INTERFACE MEETINGS

An interface meeting with NAVSHIPS R&D Center personnel was held at 3M Company on October 4, 1967. The purpose of the meeting was to review the SNAP-21 10-couple module program. The meeting consisted of a review of preliminary drawings released from MEL to start raw-material procurement for tooling and components and a review of processing equipment at 3M for MEL personnel.

An interface meeting with NAVSHIPS R&D Center personnel was held at NAVSHIPS R&D on December 14, 1967. The purpose of the meeting was to discuss the present status, problem areas and schedule and to survey the MEL facilities so that work done by MEL and 3M could be more smoothly integrated.

2.6.2 PROCUREMENT

The critical procurement item, and at this time the pacing item for starting the assembly of the first module, is the ceramic header used for the feedthroughs for power and instrumentation. A purchase order was placed on December 14, 1967, but no delivery date had been established.

Delays have been encountered in obtaining the 304L stainless steel in that two shipments have been lost during transit from the west coast. Material has now been received at MEL.

An alternate pressure gauge, Ashcroft No. 1084P, was specified because of long lead times involved in obtaining the regular gauge.

2.6.3 DESIGN

The drawing review was completed and all drawings and bills of material have been released and submitted to MEL. As a result of the drawing review, the spines in the cold end heat exchanger were changed from stainless steel to copper for better heat transfer, an air bleed pipe was added, ceramic headers were incorporated in place of the Conax fittings and a steel wool and micro-quartz filter added to the evacuation tube fitting. A protective shield for the pinch-off tube will also be incorporated.

2.6.4 MANUFACTURING

Manufacturing activity was directed toward the processing and manufacturing of 3M furnished hardware.

All tooling prints, test cabinet prints, processing equipment requirements, handling, cleaning and passivating specifications were furnished to MEL.

Approximately 40 percent of the manufacturing process procedures for the fabrication of the modules have been written.

The development of procedures for soldering the ceramic headers into the cold base has been started. Samples have been prepared and will be evaluated.

All hardware to be furnished by 3M Company has been received or due in January. No schedule delays are anticipated.

A revised schedule will be made when the delivery date for the ceramic headers has been established.

The following work is anticipated for the next quarter:

- Complete the soldering development.
- Complete manufacturing process procedures.
- Assemble four test cabinets.

- Process Min-K 1301.
- Fabricate all other components.
- Assemble and process three modules.

3.0 TASK II–20-WATT SYSTEM

No effort was expended on this subtask during this report period.

BLANK

4.0 EFFORT PLANNED NEXT QUARTER

The following items are planned for the next quarter:

- Initiate test of System S10D1A at ORNL.
- Terminate test of System S10D1.
- Terminate test of System S10D1A at ORNL.
- Start integration of System S10D2.
- Implant electrically heated fuel capsules.
- Establish fuel capsule weld acceptance criteria.
- Deliver biological shields Nos. 5, 6, 7 and 8.
- Complete Insulation Systems 10D3 and 10D4.
- Conduct Linde Final Design Review.
- Start assembly of Insulation Systems 10Q1 and 10Q2 (electrically heated systems).
- Complete fabrication of first segmented retaining ring.
- Forge and machine body and cover for first pressure vessel.
- Hydrotest pressure vessel D10D1.
- Conduct final design review on pressure vessel.
- Determine efficiency of Generators A10D2, A10D5, A10D6 and A10D7.

- Complete assembly and short term test of Generators A10D5, A10D6 and A10D7.
- Determine final design of generator.
- Complete dynamic test of power conditioners H10D1 and H10D2.
- Assemble and test power conditioner H10D3 and H10D4.
- Conduct final design review of power conditioner.
- Complete assembly of first electrical receptacle and strain relief plug.

APPENDIX A

SPECIFICATION
SNAP-21
ELECTRICAL RECEPTACLE
(Beryllium Copper Housing)

SPECIFICATION
SNAP-21
ELECTRICAL RECEPTACLE
(Beryllium Copper Housing)

1.0 SCOPE

This specification delineates the requirements for an electrical receptacle and mating cable connector plug that will be used in a deep sea application.

2.0 APPLICABLE DOCUMENTS

AMS 2800A	(10-1-51) Identification, finished parts.
QA-STD-32	(Special Quality Control/Inspection Purchase Order Clauses)
QA-STD-44	(Vendor Inspection System Requirements)
MIL-C-5015D	Connectors, Electric, "AN" Type
MIL-STD-453	Inspection, Radiographic

3.0 REQUIREMENTS

3.1 Design Objectives

The function of this electrical receptacle is to provide a means of transferring electrical power and instrumentation signals through the wall of a pressure vessel that operates in an ocean environment at pressures up to 10,000 psi. It must be designed to mate with a pressure vessel boss on one side and with a cable connector plug on the other side. The interface requirements of the cable connector plug have not been specified. This interface

has been intentionally omitted because it is anticipated that the receptacle supplier will design the receptacle to mate with an existing, proven plug of his own design.

3.2 Physical Requirements

3.2.1 Pressure Vessel Interface

The pressure vessel interface of the receptacle shall be as shown in Fig. 1.

3.2.2 Cable Connector Plug Interface

The connector plug interface is not defined, however the receptacle shall be designed to mate with an existing, proven plug design. The mating plug design shall be capable of incorporating strain relief features that will allow a tensile load of 1000 lbs. to be applied to the electrical cable during the in-air condition without affecting the electrical pins or the seal integrity of the plug.

The receptacle and mating plug shall incorporate indexing features that will allow the plug to be mated with it in only one angular orientation.

In addition, the plug specified for use with this receptacle shall incorporate the design features specified in paragraphs 3.3.1

and 3.3.1.2 of MIL-C-5015D except that the test pin diameter specified in paragraph 3.3.1.2 shall be .007 in. larger than the maximum allowable diameter of a mating pin.

3.2.3 Electrical Interface

3.2.3.1 Number of Pins

From a system standpoint it is advantageous to have as many electrical pins in the receptacle as possible. However, it is recognized that development and manufacturing problems are increased by the number of pins. Therefore the procurement document accompanying this specification will request prospective vendors to quote on a range of pin quantities ranging from a minimum of 12 to a maximum of 36. The actual number of pins will be selected on the basis of vendor proposals considering such factors as schedule, cost and development risk.

In any case, the receptacle and plug must be compatible with respect to the number of pins.

3.2.3.2 Size and Type of Pins

The pins shall not be smaller than size 16

and shall conform to Paragraphs 3.2.5, 3.3.1, 3.3.1.1, 3.3.1.3 and 3.3.1.4 of MIL-C-5015D. The pins shall be fused to the receptacle insert by a glass or ceramic sealing system.

3.2.3.3 Pin Arrangement

Pin arrangement is optional.

3.4.2 Weight

Weight of the receptacle should be kept to a minimum consistent with good design practice. In any case the weight shall not exceed 6.5 lbs.

3.2.5 Material

The receptacle housing must be made from the same material as the pressure vessel to preclude galvanic corrosion. This material is beryllium-copper alloy Berylco-165. Design properties of this material are shown below:

Ultimate Tensile Strength, ksi	150	(1)
0.2% Tensile Yield Strength, ksi	130	(1)
Elongation, %	3	(1) Min.
Modulus of Elasticity, psi	19×10^6	
Proportional Limit (Tension) ksi	75	
0.2 Compressive yield strength, ksi	130	(1)

Coefficient of Thermal Expansion, in/in/°F x 10^6 + 68°F to + 572°F	9.9
+ 68° F to + 112°F	9.3
Density, lbs/in^3	.298

(1) Data based on Beryllium Corp. of America Technical Bulletin No. 1010-A.

Further information on the properties of this alloy can be obtained from the supplier, Beryllium Corp. of America, Reading, Pennsylvania.

To prevent galvanic corrosion, the plug specified for use with this receptacle must be fabricated from the same material or from a material that is compatible in the sea water environment.

3.3 Electrical Requirements

3.3.1 Receptacle

The minimum resistance from pin-to-pin or from pin-to-housing shall be 2,000 megohms at 300 VDC.

3.3.2 Cable Connector Plug

The minimum resistance from pin-to-pin or from pin-to-housing shall be 2,000 megohms at 300 VDC.

3.4 Design Requirements

3.4.1 Service Conditions

Service conditions for the electrical receptacle, either separately or joined with its mating plug, are as follows:

PARAMETER	CONDITIONS	
	Handling and Storage	Operation
Environment	Air	Sea Water
Pressure, psig	0-10 internal	0-10,000 external
Temperature, °F	-65 to +150	+30 to +80
Vibration (MIL-STD-810A)	Method 514.1 class 6 except that frequency shall be limited to 50 cps and acceleration to 4.5 g's max.	Same
Shock (MIL-STD-810A)	Method 516.1 Procedure 1, except that peak shock shall be limited to 9 g's and shock duration to 6 m's.	Same
Nuclear Radiation (continuous) (total Integrated dose over 5 year life - 10,000 rads)	200 mr/hr	200 mr/hr

3.4.2 Structural Design

The electrical receptacle shall be designed so that stresses calculated for a design pressure of 16,500 psi do not exceed the yield strength of the housing material.

3.4.3 Seal Integrity

3.4.3.1 External Seals

The receptacle design shall incorporate seals at the pressure vessel and electrical plug interfaces to prevent leakage of air or water when exposed to the service conditions defined in paragraph 3.4.1 and a hydrostatic proof test of 11,000 psi. In addition, the seal integrity must be maintained when the 1,000 lbs. tensile load specified in paragraph 3.2.2 is applied to the electrical plug simultaneously with the service conditions.

3.4.3.1 Internal Seals

The glass or ceramic sealing system used to seal the electrical pins to the receptacle insert and the seal between the insert and the receptacle body must be capable of withstanding an external hydrostatic pressure of 11,000 psi.

4.0 QUALITY ASSURANCE REQUIREMENTS

4.1 General

The receptacle supplier shall have a Quality Assurance

organization and procedures that conform to 3M/IPP QA-STD-44. All components and assemblies shall be inspected and tested in accordance with sampling plans and test procedures that have been developed during the receptacle development effort. This will include qualification and acceptance testing of delivery units. All inspection and test plans must be approved by 3M.

4.2 Proof Test

4.2.1 Receptacle

Each receptacle shall be subjected to an open face (electrical pins exposed) proof test at 11,000 ± 200 psi. The proof test cycle shall consist of the following sequence:

(1) 25 cycles from 0 to 11,000 ± 200 psi.

(2) Hold at 11,000 ± 200 psi for 8 ± 1 hour.

(3) One final cycle from 0 to 11,000 ± 200 psi.

Leakage shall not occur at the receptacle-to-pressure vessel interface or at the pin-to-insert or insert-to-receptacle housing interfaces.

Electrical resistance checks shall be conducted following the first, fifth, twenty-fifth and final hydrotest cycle. Electrical resistance shall not be less than that specified in paragraph 3.3.1.

In addition, the pin-to-receptacle insert seals

shall be leak tested using a mass spectrometer leak detector. Leakage shall not exceed 1×10^{-6} std. cc/sec. He.

4.2.2 Cable Connector Plug

Each cable connector plug shall be subjected to a hydrostatic proof test at 10,000 $\pm$ 200 psi. This test shall be conducted with the plug mated with an electrical receptacle or a test plug that simulates the receptacle. The proof test cycle shall consist of the following sequence:

(1) 25 cycles from 0 to 10,000 $\pm$ 200 psi.

(2) Hold at 10,000 $\pm$ 200 psi for 8 $\pm$ 1 hour.

(3) One final cycle from 0 to 10,000 $\pm$ 200 psi.

Leakage shall not occur at the cable connector plug-to-receptacle housing interface.

Electrical resistance checks shall be conducted following the first, fifth, twenty-fifth and final hydrotest cycle. Electrical resistance shall not be less than that specified in paragraph 3.3.1.

4.3 The following special Quality Control Inspection Purchase Order clauses are applicable in the performance of this contract: QA-STD-32 (6-19-67) Paragraphs: 1.0, 1.1, 1.2, 1.3, 1.3.2.2, 1.34, 1.37, 1.4.1, 1.8, 1.9.1, 1.10, 1.13, 1.13.1, 1.14.

4.4 Prior to hydrotest the receptacle shall be x-ray inspected in accordance with MIL-STD-453 and change notice #1 thereto dated 4 September 1963. Interpretation of x-rays will be on an individual basis until sufficient data is obtained to establish accept-reject criteria.

5.0 PREPARATION FOR DELIVERY

The receptacles shall be packaged for shipment to 3M in accordance with ICC shipping regulations and in accordance with good commercial packaging practice.

6.0 NOTES

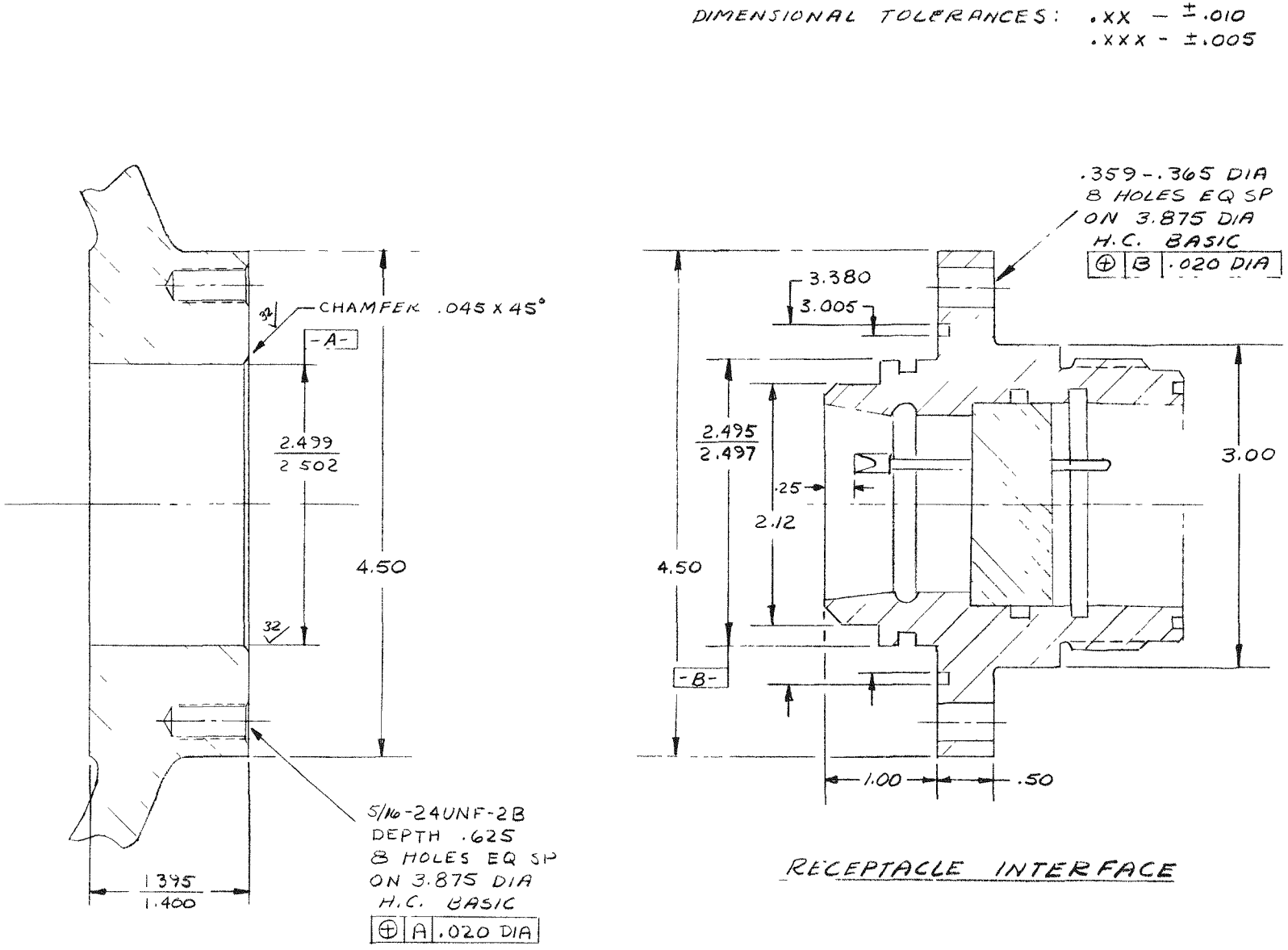

Figure A-1. Interface Requirements

APPENDIX B

STATIC PROOF TEST CALCULATIONS

APPENDIX B

STATIC PROOF TEST CALCULATIONS

The structural components used for the static proof test were made from the following materials: Neck Tube - Inconel X-750, Male Rod - Inconel 625 solution annealed, Female Rod - Inconel 625 solution annealed.

1. Derivation of Load Sharing Equation for Static Proof Test

The load sharing equation derived in report No. 9, Appendix C, May 29, 1967, for the HTVIS support system is modified slightly for the static proof test to incorporate the stiffness of the top flange which is connecting the neck tube to the test fixture and the center plate (spider) which is connecting the tension rod to the shield.

The deflection of the flange,

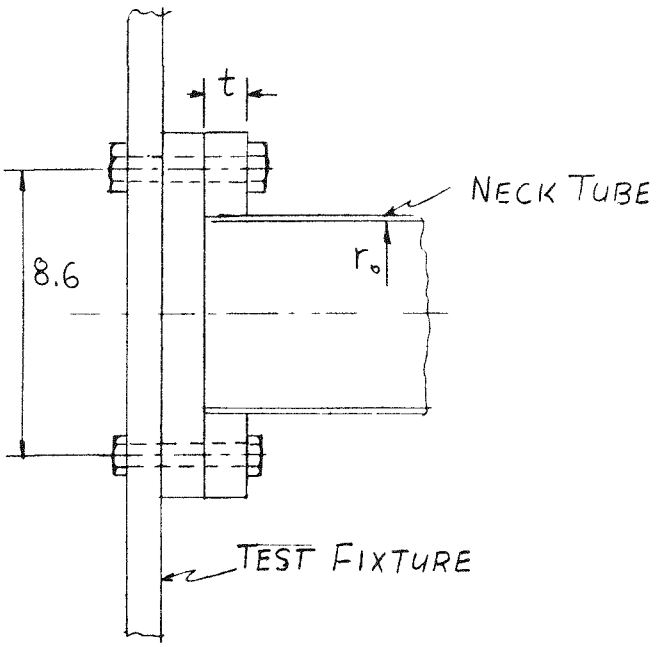

$t = .375$
$2a = 8.6$ in.
$a = 4.3$ in.
$r_o = 2.45$ in.
$E = 29.8\ 10^6$ psi

$$Q_{3F} = \frac{M}{\alpha Et^3} = \frac{W(\ell_{1N} + \ell_2) - P(\ell_{1N} + \ell_2 + \ell_3)}{\alpha Et^3}$$

$$\frac{r_o}{a} = \frac{2.45}{4.3} = .56$$

α = 20.5 from Ref. 2 Topical Report dated January 31, 1967.

$$\alpha Et^3 = 20.5 \times 29.8\ 10^6\ (.375)^3 = 32.2\ 10^6$$

$$y_{3_1F} = \frac{W(\ell_{1N} + \ell_2) + P(\ell_{1N} + \ell_2 + \ell_3 + e \tan\alpha)}{32.2\ 10^6} (\ell_{1N} + \ell_2 + \ell_3)$$

The reciprocal of the spring constants of the tension rod components were as follows:

a) Tension Rod,

$$\frac{1}{k} = \frac{\ell}{EA} = \frac{2.619}{29.8\ 10^{-6}\ (.0585)} = 1.502\ 10^{-6} \text{ in/lbs.}$$

E = 29.8 10^6 psi (Inconel 625, at room temperature)

A = .0585 in.^{2}

ℓ = 2.936 - 2(.16) = 2.619 in.

b) Spherical Washer,

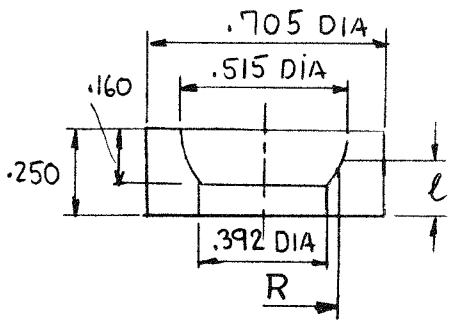

$$\ell = (.250 - .16) + .16/2 = .170$$

$$\frac{1}{k} = \frac{\ell}{EA} = \frac{.170}{29.8\ 10^{6}\ (.0875)} = .0651\ 10^{-6}\ \text{in/lb.}$$

$E = 29.8\ 10^{6}$ psi (stainless steel at room temperature)

$A = (.515^{2} - .392^{2})\ \pi/4 = .0875\ \text{in.}^{2}$

Calculation of tension rod displacement in the direction of the load due to the radial deflection of the spherical washer. The radius where the concentrated load is applied,

$$R = \frac{.515 - .392}{2}\ \frac{1}{3} + \frac{.392}{2} = .216\ \text{in.}$$

The radial component of the load P_r, at radius R,

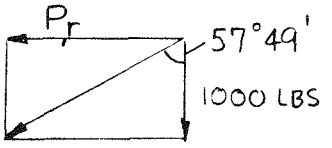

$$P_r = 1000 \tan 57°49' = 1550\ \text{lbs.}$$

The average pressure in the radial direction,

$$p_i = \frac{P_r}{\pi DL} = \frac{1550}{\pi(.216)2(.250)} = 4570\ \text{psi}$$

The maximum tangential stress due to the internal pressure p_i,

$$\sigma_t = \frac{a^2 p_i}{b^2 - a^2}\left[1 + \frac{b^2}{r^2}\right] = \frac{(.216)^2\ 4570}{(.352)^2 - (.216)^2}\left[1 + \left(\frac{.352}{.216}\right)^2\right] = 10{,}091\ \text{psi}$$

where,

$a = R = .216$ in.

$b = .352$ in. (outside radius of washer)

The deflection of the spherical washer in the radial direction at $r = a = R$

$$u_r \Big|_{r=a} = \frac{ap_i}{E} \left[\frac{a^2 + b^2}{b^2 + a^2} + \mu \right] =$$

$$= \frac{.216\ (4570)}{29.8\ 10^6} \left[\frac{.216^2 + .352^2}{.352^2 - .216^2} + .3 \right] = 82\ 10^{-6} \text{ in.}$$

The displacement of the rod in the direction of the load,

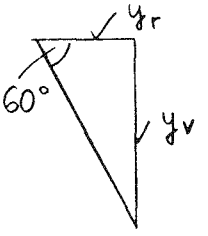

$$y_v = y_r \tan 60 = 82\ (1.73) = 141\ 10^{-6} \text{ in.}$$

$$\frac{1}{k} = \frac{141 \times 10^{-6}}{1000} = .141\ 10^{-6} \text{ in./lbs.}$$

The sum of the reciprocal of spring constants for the spherical washer is,

$$\frac{1}{k \text{ (compression)}} + \frac{1}{k \text{ (radial deflection)}} = .0651\ (10^{-6}) + .141\ 10^{-6} =$$

$$= .206\ 10^{-6} \text{ in./lbs.}$$

c) Center Plate (Spider),

$$\frac{1}{k} = \frac{\ell}{EA} = \frac{3.125}{29.8\ 10^6 (.75)} = .0139\ 10^{-6} \text{ in./lbs.}$$

$A = 1.5 \times .5 = .75 \text{ in.}^2$

$\ell = 3.125 \text{ in.}$

$$\sum \frac{1}{k} = (1.502 + .206 + .0139)\ 10^{-6} = 1.721\ 10^{-6} \text{ in./lb.}$$

The Load Sharing Equation,

$$P\alpha = \frac{W}{\cos \alpha} \left\{ \frac{\ell_1^2(2\ell_1 + 3\ell_2 + 3\ell_3) + 3\ell_1 \ell_2(\ell_1 + 2\ell_2 + 2\ell_3)}{6EI} + \frac{2\ell_1\ (2.58)}{EA} + \right.$$

$$+ \frac{(\ell_{1N} + \ell_2)\ (\ell_{1N} + \ell_2 + \ell_3)}{32.2\ (10^6)} \Bigg| \frac{\ell_R}{E_R\ A_R} \quad \frac{1}{\cos^2 \alpha} +$$

$$+ \frac{\ell_1^2(2\ell_1 + 3\ell_2 + 3\ell_3) + 3\ell_1(\ell_1 + 2\ell_2 + 2\ell_3)\ (\ell_2 + \ell_3 + e \tan \alpha)}{6EI} +$$

$$\left. + \frac{(\ell_{1N} + \ell_2 + \ell_3 + e \tan\alpha)\ (\ell_{1N} + \ell_2 + \ell_3)}{32.2\ (10^6)} + \frac{2\ell_1\ (2.58)}{EA} \right\}$$

2.) Calculation of Predicted Load to Fail the Neck Tube in Shear Buckling

The neck tube is made from Inconel 750 X material. The modulus of elasticity of the neck tube is, $E = 31.0\ 10^6$ psi at room temperature, 80°F.

$I = (4.922^4 - 4.9^4)\ \pi/64 = .5113 \text{ in.}^4$

$A = (4.922^2 - 4.9^2)\ \pi/4 = .1696 \text{ in.}^2$

Calculating each term in the load sharing equation.

ℓ_1 = 2.497 in.
ℓ_{1N} = 2.78 in.
ℓ_2 = 4.43 in.
ℓ_3 = 4.385 in.
e = 3.125 in.
α = 27°49'

$\sin\alpha$ = .4666
$\cos\alpha$ = .8844
$\tan\alpha$ = .5276

$$X_1 = \frac{\ell_1^2 (2\ell_1 + 3\ell_2 + 3\ell_3) + 3\ell_1 \ell_2 (\ell_1 + 2\ell_2 + 2\ell_3)}{6EI} =$$

$$= \frac{(2.497)^2 [2(2.497) + 3(4.43) + 3(4.385)] + 3(2.497)4.43(2.497 + 2(4.43) + (2)\,4.385)}{6(31.0)\ 10^6\ (.5113)}$$

$$= 9.07\ 10^{-6}$$

$$X_2 = \frac{2\ell_1\ (2.58)}{EA} = \frac{2(2.497)(2.58)}{(31.0)\ 10^6\ .1696} = 2.44\ 10^{-6}$$

$$G = \frac{E}{2(1+\mu)} = \frac{31.0\ 10^6}{2(1 + .29)} = 12.01$$

$$\frac{E}{G} = \frac{31.0}{12.0} = 2.58$$

$$X_3 = \frac{2(\ell_{1N} + \ell_2)\ (\ell_{1N} + \ell_2 + \ell_3)}{32.2} = \frac{(2.78 + 4.43)\ (2.78 + 4.43 + 4.385)}{32.2} =$$

$$= 2.59\ 10^{-6}$$

$$X_4 = \frac{\ell_1^2(2\ell_1 + 3\ell_2 + 3\ell_3) + 3\ell_1\ (\ell_1 + 2\ell_2 + 2\ell_3)\ (\ell_2 + \ell_3 + e\tan\alpha)}{6EI} =$$

$$= 2.497^2 \left[2(2.497) + 3(4.43) + 3(4.385)\right] + 3(2.497) \left[(2.497 + 2(4.43) + 2(4.385)\right]$$
$$\left[4.43 + 4.385 + 3.125\ (.5276)\right] \Big/ 6\ (31.0)\ 10^6\ (.5113) = 18.64\ 10^{-6}$$

$$X_5 = X_2 = 2.44\ 10^{-6}$$

$$X_6 = \frac{(\ell_{1N} + \ell_2 + \ell_3 + e\ \tan\alpha)\ (\ell_{1N} + \ell_2 + \ell_3)}{32.2\ 10^6} =$$

$$= \frac{\left[2.78 + 4.43 + 4.385 + 3.125\ (.5276)\right]\left[2.78 + 4.43 + 4.385\right]}{32.2\ 10^6} = 4.76\ 10^{-6}$$

$$P_\alpha = \frac{W}{.8844}\ \frac{(9.07 + 2.44 + 2.59)\ 10^{-6}}{\frac{1.721\ 10^{-6}}{(.8844)^2} + (18.64 + 2.44 + 4.76)\ 10^{-6}}$$

$$P_\alpha = \frac{W}{.8844}\ \frac{14.10\ 10^{-6}}{2.20\ 10^{-6} + 25.84} = .567\ W$$

$$P = (.502)\ W$$

Calculate the critical shear load for the neck tube at failure in shear buckling.

$$\frac{R}{t} = \frac{2.450}{.011} = 222$$

$\frac{\tau_{cr}}{E_r}\ 10^3 = .66$ from Figure A12 Report No. 9, dated May 29, 1967.

$$\tau_{cr}\ (\text{shear}) = 1.2\ (.66)\ E_r\ 10^{-3} = 1.2\ (.66)\ (31.0)\ 10^6 = 24{,}552\ \text{psi}$$

The shear load,

$$V = \pi R\, t\, \tau_{cr} = \pi\ (2.450)\ (.011)\ 24{,}552 = 2077\ \text{lbs.}$$

$V = W - P = (W - .502\ W) = .498\ W = 2077$ lbs

$$W = \frac{2077}{.498} = 4172 \text{ lbs.}$$

The load applied at the center of gravity of the support system to fail the neck tube in shear buckling is 4172 lbs. This load was calculated on the basis that the modulus of elasticity of the tension rod is constant.

Calculation of bending moments at neck tube ends and the ratio of critical shear stress to critical torsion stress

$$M_{(\text{Bottom End})} = W\ell_2 - P(\ell_2 + \ell_3 + e \tan\alpha) =$$

$$= 4172(4.43) - (.502)(4172)\left[4.43 + 4.385 + 3.125\ (.5276)\right]$$

$$= -3432 \text{ in-lbs.}$$

$$M_{(\text{Top End})} = W(\ell_1 + \ell_2) - P(\ell_1 + \ell_2 + \ell_3 + e \tan\alpha) =$$

$$= 4172\ (2.497 + 4.43) - (.502)(4172)\ \ 2.497 + 4.43 + 4.385 + 3.125(.5276) =$$

$$= +1755 \text{ in-lbs}$$

$$\left(\frac{M}{RV}\right)_{(\text{Bottom End})} = \frac{-3432}{2.450(2094)} = .66$$

$$\left(\frac{M}{RV}\right)_{(\text{Top End})} = \frac{1755}{2.450\ 2094} = .34$$

$\frac{fv}{s_S} = 1.2$ (bottom end of neck tube)

$\frac{fv}{s_S} = 1.2$ (top end of neck tube)

The $f_v/v_S = 1.2$ ratio used in the calculation for determining the critical shear stress for the neck tube was correct.

Since the maximum stress in the tension rod exceeded the proportional limit (see Figure A-1) it is necessary to make correction in the load sharing equation to include the effect of changing modulus of elasticity. A stress-strain curve for the tension rod material is presented in Figure A-1.

In the load sharing equation, the variable modulus of elasticity of the tension rod only affects the first term in the denominator.

$$\frac{P}{W} = \frac{14.10\ (10^{-6})}{\left[\frac{2.619}{E_R\ (.0585)} + .219\ 10^{-6}\right] \frac{1}{(.88445)^2} + 25.84\ (10^{-6})}$$

For small increments of strain, it is assumed that the modulus of elasticity is a constant, and therefore the load sharing equation and the deflection equations are applicable. The increments of strains used in the calculations are shown in Figure A-1.

Increments	psi Stress in Rod	E_R	Calculated P/W from Load Sharing Equation
1	0-30,000	$29.8\ 10^6$	.502
2	30,000-35,000	$23\ 10^6$	.492
3	35,000-37,500	$16\ 10^6$	.474

The maximum radial force P and the corresponding load W is calculated for each increment of strain.

Increments	σ Max (rod)	$P = \sigma A \cos\alpha$, lbs	$W = P \frac{1}{(P/W)} \frac{1}{1.76}$
1	30,000	1552	1756 psi
2	35,000	1810	2090
3	37,500	1940	2325

Calculations of radial deflection of the tension rods.

$$y_1 - y_o = (P_1 - P_o) \frac{\ell}{EA} \frac{1}{\cos^2 \alpha} = (1552-0) \left[\frac{2.619}{29.8\ 10^6\ (.0585)} + .219\ 10^{-6} \right] x$$

$$x \frac{1}{(.88445)^2} = .00341 \text{ in.}$$

$$y_2 - y_1 = (P_2 - P_1) \frac{\ell}{EA} \frac{1}{\cos^2 \alpha} = (1810-1552) \left[\frac{2.619}{23.0\ 10^6\ (.0585)} + .219\ 10^{-6} \right] x$$

$$x \frac{1}{(.88445)^2} = .000714 \text{ in.}$$

$$y_3 - y_2 = (P_3 - P_2) \frac{\ell}{EA} \frac{1}{\cos^2 \alpha} = (1940-1810) \left[\frac{2.619}{16\ 10^6\ (.0585)} + .219\ 10^{-6} \right] x$$

$$x \frac{1}{(.88445)^2} = .000501 \text{ in.}$$

The calculated radial deflections of the tension rod at different applied loads W are shown on Figure 5.

Calculation of neck tube deflection.

$$y_1 = \frac{(W-P)\ \ell_1^3}{3EI} =$$

$$y_2 = \frac{\left[W\ell_2 - P\ (\ell_2 + \ell_3 + e \tan\alpha)\right] \ell_1^2}{2EI}$$

$$y_3 = \frac{2(W-P)\ \ell_1\ 2.58}{EA}$$

$$y_F = \frac{\left[W(\ell_{1N} + \ell_2) - P(\ell_{1N} + \ell_2 + \ell_3 + e \tan\alpha)\right] \ell_{1N}}{C}$$

$$y_{tot} = y_1 + y_2 + y_3 + y_F$$

Increments	E psi	P, lbs	$\triangle$P, lbs	W, lbs	$\triangle$W, lbs
1	29.8	1552	1552	3090	3090
2	23.0	1810	258	3678	588
3	16.0	1940	130	4092	414

Increments	$y_1 \times 10^{-6}$ in.	$y_2 \times 10^{-6}$ in.	$y_3 \times 10^{-6}$ in.	$y_F \times 10^{-6}$	y Total, in.
1	503	-323	3769	149	.00392
2	108	- 12	813	72	.00097
3	92	+ 60	695	109	.00095
					.00584 Inch

Calculated neck tube deflections for different applied loads W, were plotted on Figure 6. The calculated P/W ratios are shown on Figure 5. The P/W ratio at the load where the neck tube failed (W = 2250 psi) is calculated by a trial-error procedure.

Assume W/P = .483

$$W = 2250 = P \frac{1}{P/W} \frac{1}{1.76} = \frac{P}{(.486)(1.76)}$$

P = 1924 lbs.

The maximum stress in the rod,

$$\sigma = \frac{1924}{.0585\ (.88445)} = 37{,}196 \text{ psi} \sim 37{,}200 \text{ psi}$$

The modulus of elasticity for the increment between 35,000 psi and 37,200 psi from Figure A-1 is E = 18 10^6 psi. Recalculating the W/P ratio from the load sharing equation using E = 18 10^6 modulus of elasticity gives W/P = .481. Using W/P = .483 ratio, the predicted load to fail the neck tube in shear buckling is,

$$V = 2077 = W - .483W = .517\ W$$

$$W = \frac{2077}{.517} = 4017 \text{ lbs.}$$

The actual load applied on the support system at the failure of the neck tube was 4072 lbs. (The load applied by the hydraulic jack was 3960 lbs. and the weight of the stainless steel shield was 112 lbs.)

FIGURE A-1

STRESS STRAIN CURVE FOR INCONEL 625 SOLUTION ANNEALED
TENSION ROD AT ROOM TEMPERATURE
(STATIC PROOF TEST)

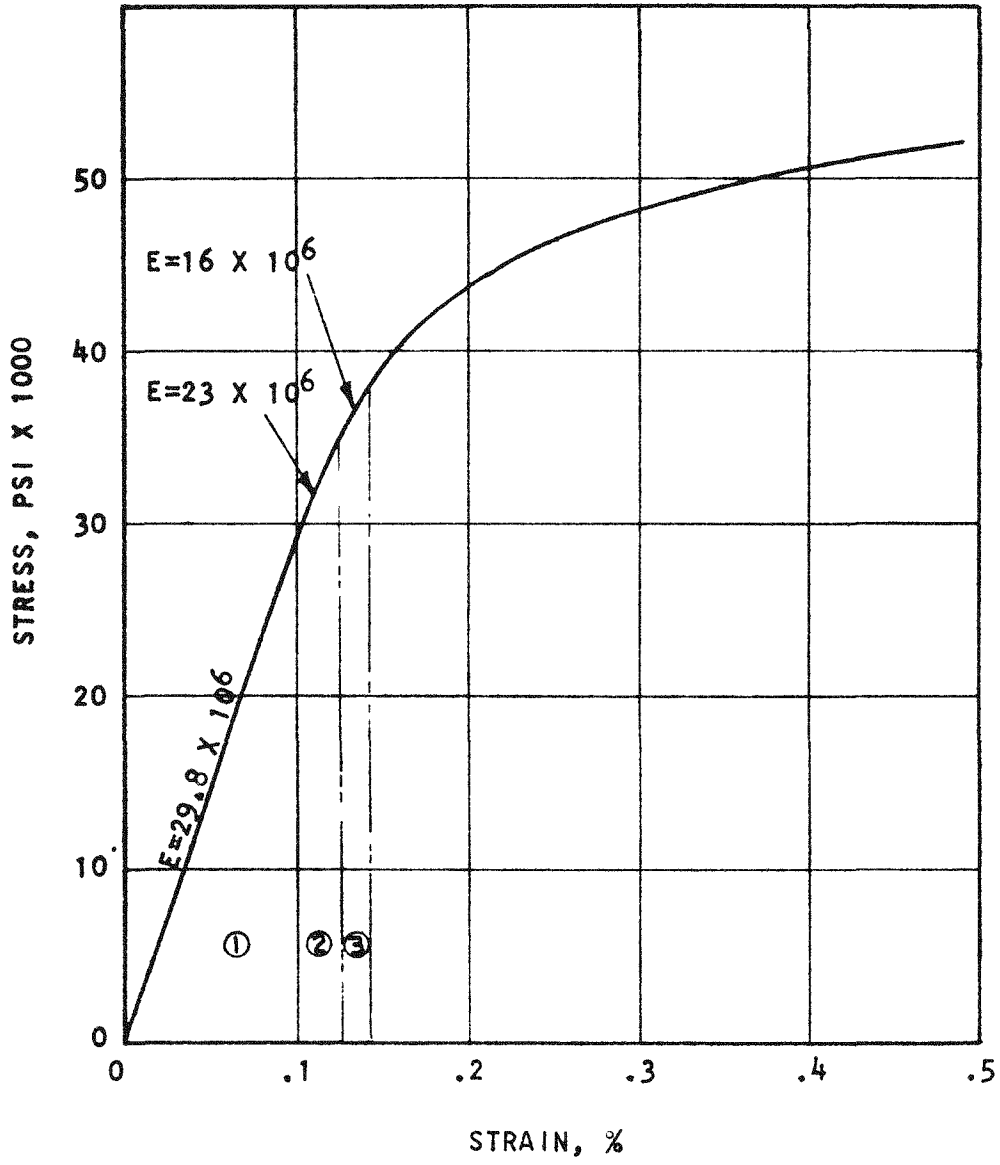

APPENDIX C

ENGINEERING REPORT NO. 3938-1

Prepared for:

3 M COMPANY
2501 Walnut Street
Space Center - Building 551
St. Paul, Minnesota 55113

Subject: VIBRATION TESTING

1. ABSTRACT

Subject one Thermoelectric Generator to the Vibration Test requirements of the SNAP 21 project.

The generator appeared to have functioned satisfactorily both during and at the completion of this test.

2. UNIT TESTED

One Thermoelectric Generator identified as Unit No. 10-D-5 was submitted for testing by the 3 M Company.

3. TEST REQUESTED

Subject the test sample to the following vibration test requirements in its three mutually perpendicular axes:

Input Levels:

5 cps to 26 cps at 1.3 gs peak acceleration

26 cps to 40 cps at 0.036 inch displacement

40 cps to 50 cps at 3.0 gs peak acceleration

Duration:

Sweep thrice from 5 cps to 50 cps to 5 cps in a period of 45 minutes.

4. INSTRUMENTATION

M-B Model C-50 Vibration Exciter

M-B Model T-665 Vibration Amplifier

M-B Model T-88 Vibration Control Console consisting of:

- M-B Model N-572 Oscillator
- M-B Model N-163 X-Y Plotter
- Environ No. 300-005 Oscilloscope

Endevco Model 2226 Accelerometer

Endevco Model 2614B Accelerometer Amplifier

Environ No. 201-001 Oscillograph Recorder (Sanborn)

Environ No. 201-501 Amplifier (Sanborn)

Environ No. 201-502 Amplifier (Sanborn)

5. PROCEDURE AND RESULTS

5.1 Axis Orientation of the Test Sample

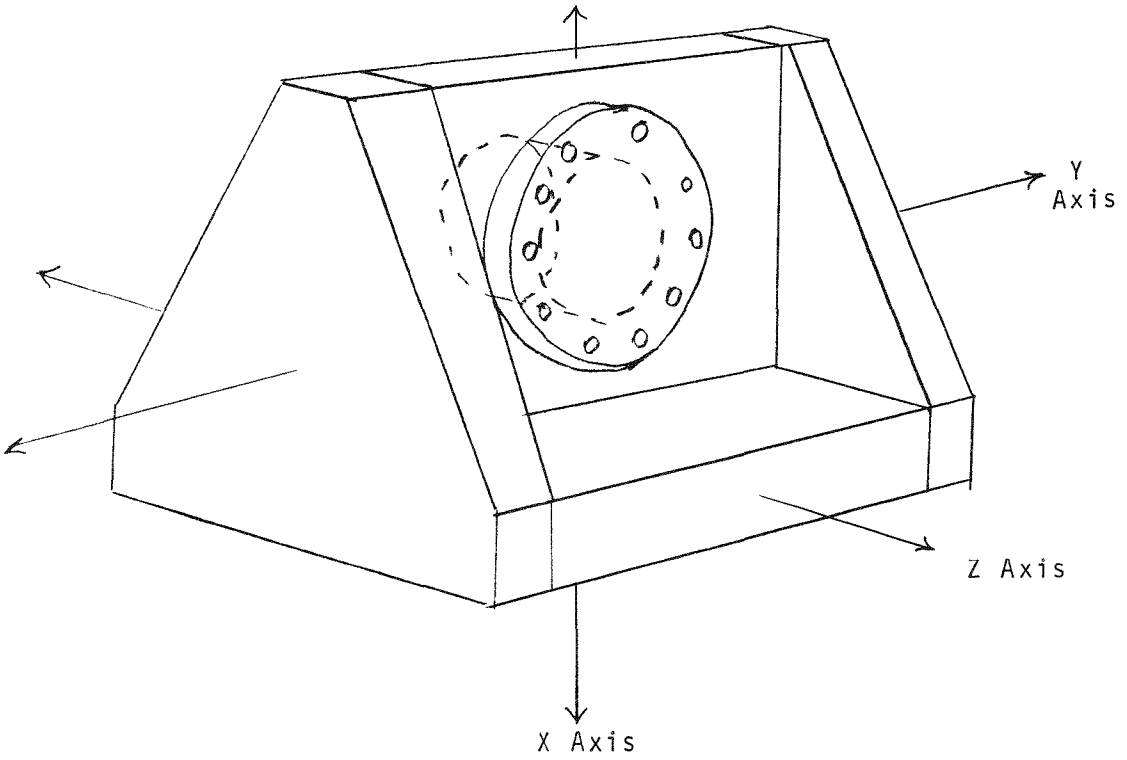

FIGURE NO 1

5 2 Device Testing

5 2 1 "Z" Axis

The generator was mounted to its holding fixture and this assembly was attached to the exciter in such a manner that the applied vibrations would be through and parallel to its Z Axis.

Vibration was applied as outlined in paragraph 3 for a period of 45 minutes, the time necessary to complete three cycles.

5. PROCEDURE AND RESULTS (Con't.)

During the second cycle on the sweep from 5 cps to 50 cps Graph No. 1 (3938-1) was plotted in db versus frequency, from the output of the control accelerometer. The generator appeared to function satisfactorily both during and at the completion of this test period.

5.2.2 "Y" Axis

The generator was mounted to its holding fixture and this assembly was attached to the exciter in such a manner that the applied vibrations would be through and parallel to its Y Axis.

Vibration was applied as outlined in paragraph 3 for a period of 45 minutes, the time necessary to complete three cycles.

During the second cycle on the sweep from 5 cps to 50 cps Graph No 2 (3938-1) was plotted in db versus frequency, from the output of the control accelerometer.

The generator appeared to function satisfactorily both during and at the completion of this test period.

5 2 3 "X" Axis

The generator was mounted to its holding fixture and this assembly was attached to the exciter in such a manner that the applied vibrations would be through and parallel to its X Axis.

5. PROCEDURE AND RESULTS (Con't.)

Vibration was applied as outlined in paragraph 3 for a period of 45 minutes, the time necessary to complete three cycles.

During the second cycle on the sweep from 5 cps to 50 cps Graph No. 3 (3938-1) was plotted in db versus frequency, from the output of the control accelerometer.

The generator appeared to function satisfactorily both during and at the completion of this test period.

Vibration testing on this generator is complete.

6 WITNESSING PERSONNEL

Mr J. Young, Mr. D. Messmer and Mr. D. Lindblad representing the 3 M Company witnessed this test.

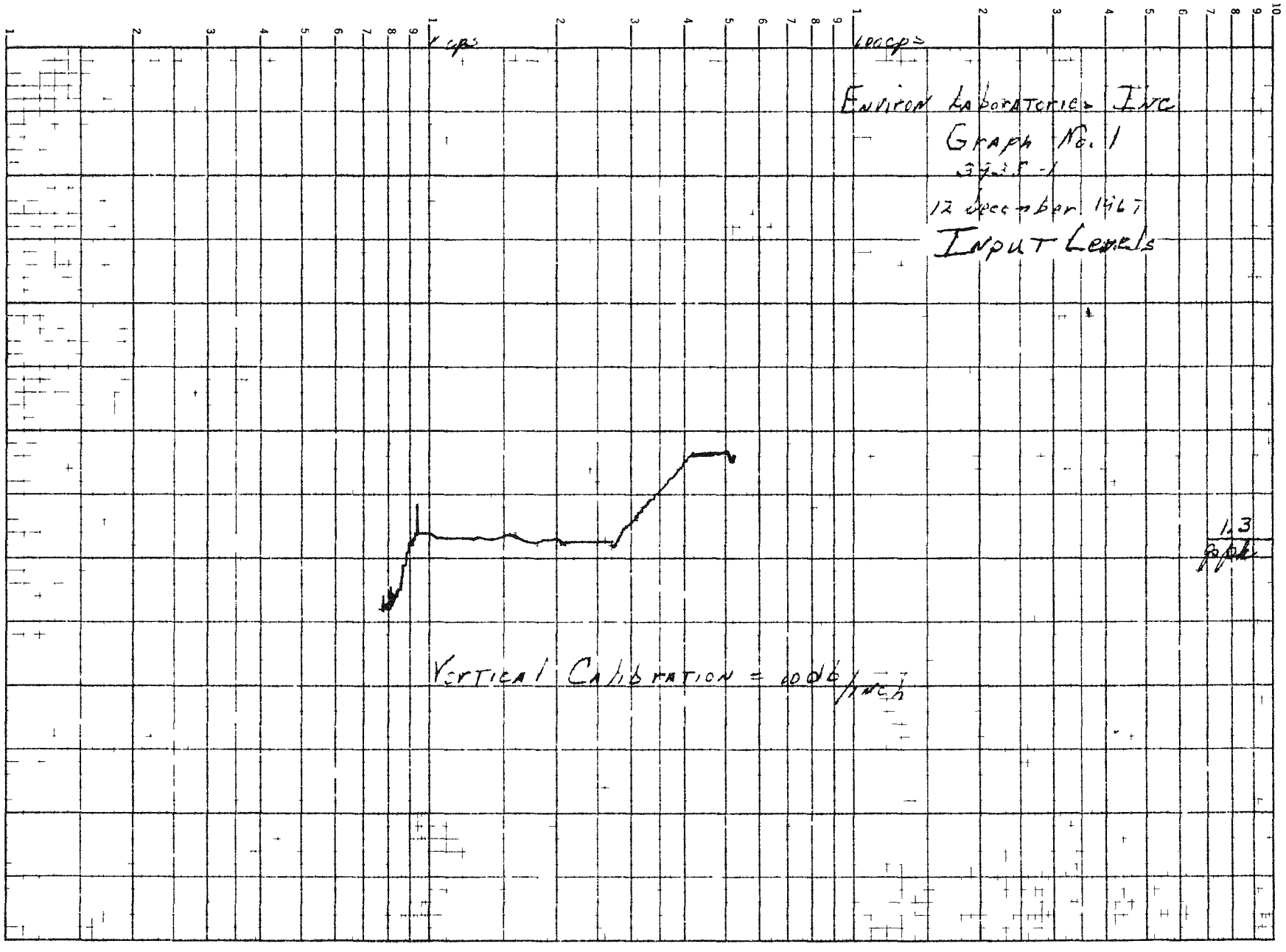
Environ Laboratories Inc
Graph No. 1
3-3-F-1
12 December 1967
Input Levels
1.3
Vertical Calibration = 0.006/inch

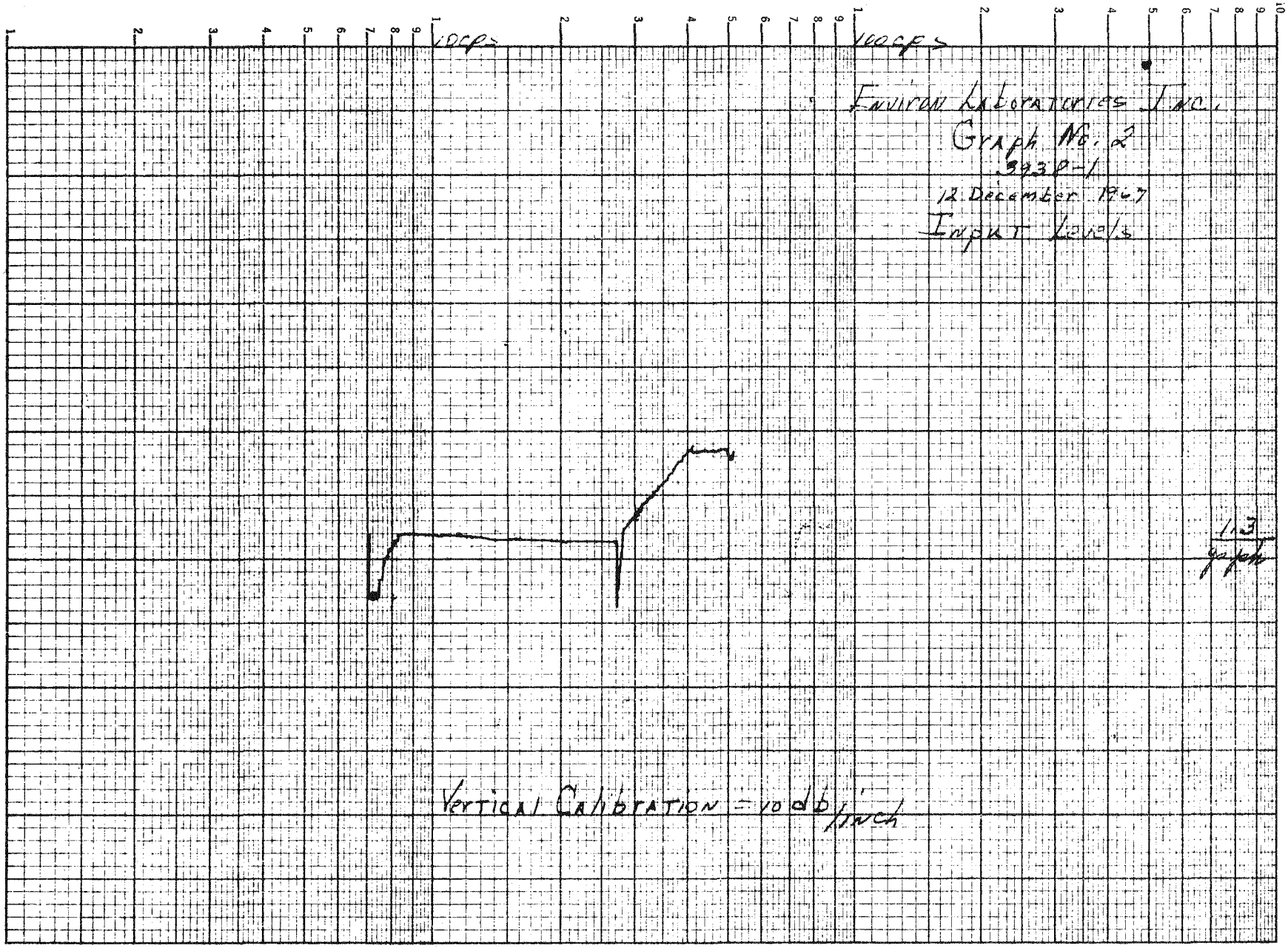
K+E SEMI-LOGARITHMIC 46 5492
3 CYCLES X 70 DIVISIONS MADE IN U.S.A.
KEUFFEL & ESSER CO.
100 cps
1000 cps
Environ Laboratories, Inc.
Graph No. 2
393P-1
12 December 1967
Input Level
1/3 octave
Vertical Calibration = 10 dB/inch

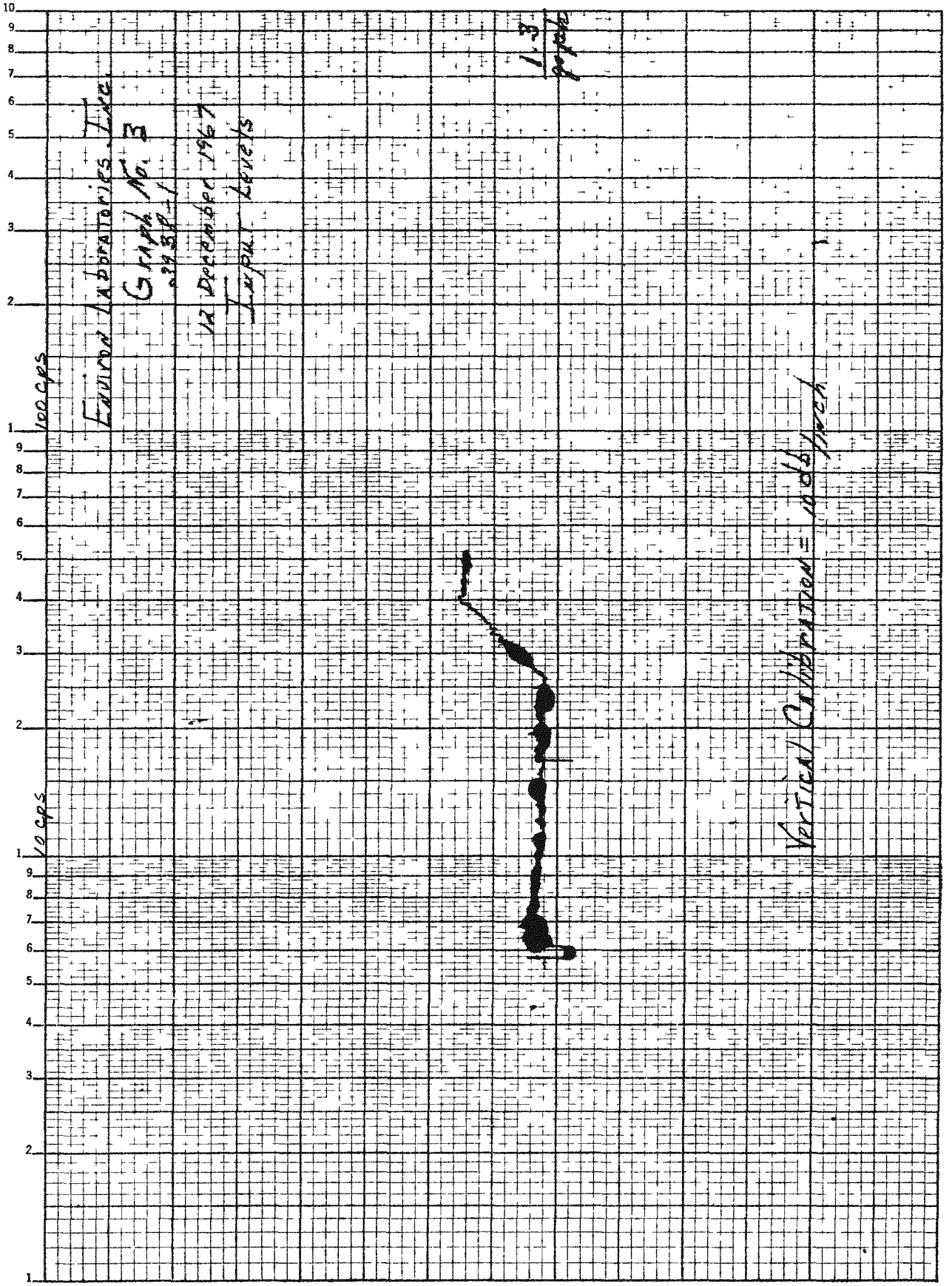
Environmental Laboratories, Inc.
Gamma Log No. 3
12 December 1967
Logged by L. Lewis
100 cps
10 cps
Vertical Calibrated = 10 ft/inch

Prepared for:

3 M COMPANY
2501 Walnut Street
Space Center - Building 551
St Paul, Minnesota 55113

Subject: SHOCK TEST

1 ABSTRACT

1.1 Object

To subject one Thermoelectric Generator, SNAP-21, Serial Number 10-D-5, to the Shock Test as requested by 3 M Company Purchase Order Number TC-03440

1.2 Conclusions

The Thermoelectric Generator, SNAP-21, Serial Number 10-D-5, satisfactorily met the requirements of the Shock Test as requested by 3 M Company Purchase Order Number TC-03440.

2. UNITS TESTED

One Thermoelectric Generator, SNAP-21, Serial Number 10-D-5, as submitted for testing by the 3 M Company of St. Paul, Minnesota.

3. TEST REQUESTED

Subject the test units to three sawtooth shocks, each having an amplitude of 6 G's and a duration of 6 milliseconds, in each direction of the three major axes (18 shocks).

The test unit shall be wired electrically and the output shall be monitored continuously throughout the test. All readings shall be recorded by 3 M Company personnel.

4 PROCEDURE AND RESULTS

4.1 Instrumentation

L.A.B. Corporation Pneumatic Shock Machine, Type 24-400, S/N 63402

Endevco Charge Amplifier, Model 2708

Tektronix Type 564 Oscilloscope

Tektronix Type 3A72 Vertical Preamp

Tektronix Type 2B67 Horizontal Preamp

Columbia Accelerometer, Model 300, S/N 633

Hewlett-Packard Oscilloscope Camera, Model 196A

Sanborn Recorder, Model 296, 2 Channel D.C.

Two Sanborn DC Coupling Preamps, Model 350-1300

Also associated monitoring equipment was supplied and operated by 3 M personnel.

4.2 Procedure

Weights equivalent to the combined weight of the test unit and fixture were attached to the shock machine table. Trial drops were conducted to obtain the desired shock level of 6 G's with a duration of 6 milliseconds. The test unit was then attached to the shock machine table, and in an operating condition, subjected to three shocks in each direction of the three major axes, for a total of 18 shocks.

The test unit was monitored continuously throughout the entire shock test by 3 M Company personnel. All the output data was recorded and retained by 3 M Company. No damage

4 PROCEDURE AND RESULTS (Con't)

to the test unit was reported by 3 M Company personnel, see Table I, Page 5, for results of each shock pulse. Pictures of the shock pulse waveforms are included on page 6.

Axes orientation was as shown on page 4.

Upon completion of the Shock Test, the unit was returned to 3 M Company for further evaluation

FIGURE I

SNAP 21

T/E GENERATOR MODEL 10-D-5

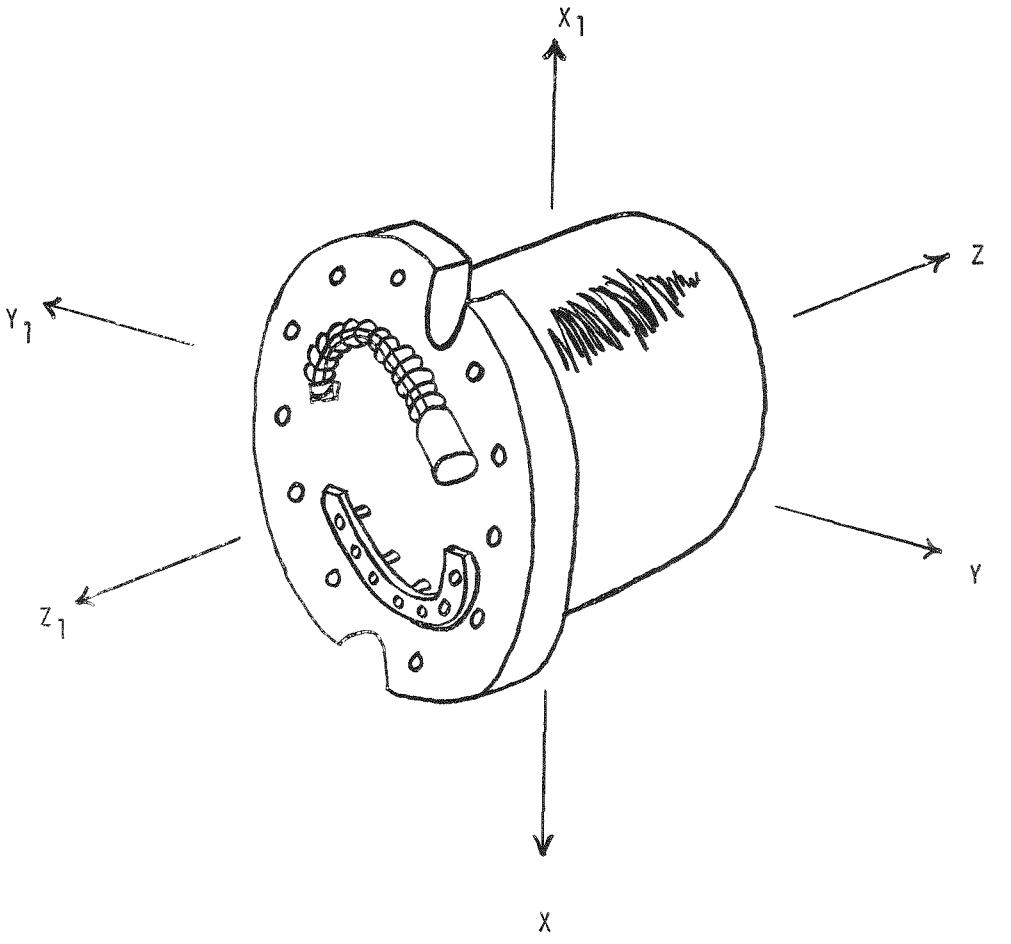

Orientation of Axes

TABLE I

SNAP-21 THERMOELECTRIC GENERATOR 10-D-5

RESULTS OF SHOCK TEST

AXIS	DROP NO.	"G" LEVEL	DURATION	VISUAL RESULTS
Z	1	6	6 ms.	Satisfactory
	2	6	6 ms.	"
	3	6	6 ms.	"
Z_1	1	6	6 ms	"
	2	6	6 ms.	"
	3	6	6 ms.	"
Y	1	6	6 ms.	"
	2	5.5	6 m.s	"
	3	5.5	6 ms.	"
Y_1	1	6.0	6 ms.	"
	2	5.5	6 ms	"
	3	6.0	6 ms.	"
X	1	5 0	6 ms.	"
	2	6.0	6 ms.	"
	3	7.0	6 ms.	"
X_1	1	6 0	6 ms.	"
	2	7.0	6 ms.	"
	3	7.0	6 ms.	"

SHOCK WAVEFORMS

5ms/cm Horizontal, 2.5 g's/cm Vertical

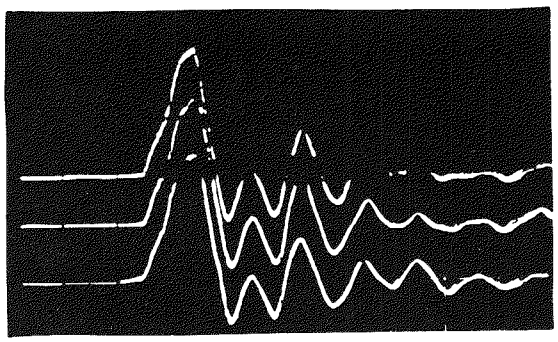

Z AXIS

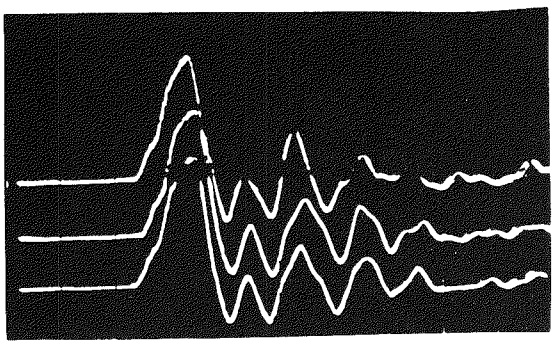

Z_1 AXIS

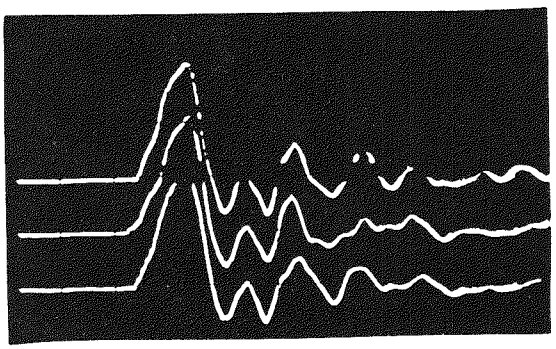

Y AXIS

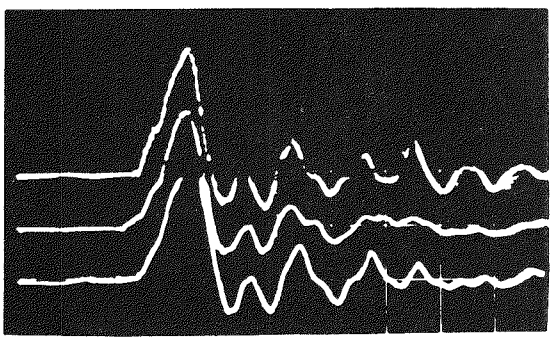

Y_1 AXIS

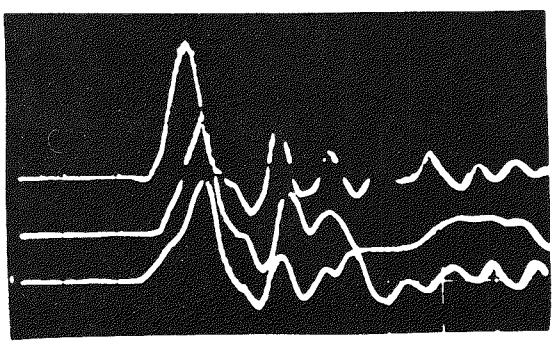

X AXIS

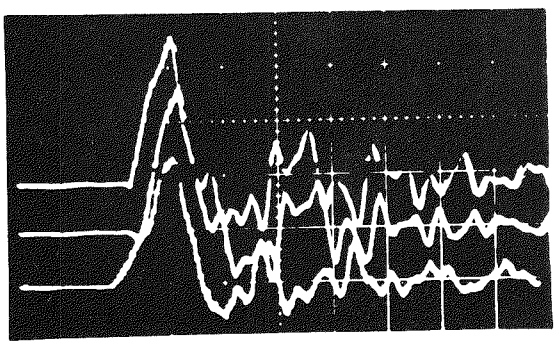

X_1 AXIS